

# Electron Interactions With Cl<sub>2</sub>

L. G. Christophorou<sup>a)</sup> and J. K. Olthoff

Electricity Division, Electronics and Electrical Engineering Laboratory, National Institute of Standards and Technology,  
Gaithersburg, Maryland 20899-8113

Received December 1, 1998; revised manuscript received February 8, 1999

Low-energy electron interactions with the Cl<sub>2</sub> molecule are reviewed. Information is synthesized and assessed on the cross sections for total electron scattering, total rotational excitation, total elastic electron scattering, momentum transfer, total vibrational excitation, electronic excitation, total dissociation into neutrals, total ionization, total electron attachment, and ion-pair formation. Similar data on the density-reduced ionization, density-reduced electron attachment, density-reduced effective ionization, electron transport coefficients, and electron attachment rate constant are also synthesized and critically evaluated. Cross sections are suggested for total electron scattering, total elastic electron scattering, total ionization, dissociation into neutrals, electron attachment, and ion-pair formation. A cross section is derived for the total vibrational excitation cross section via low-lying negative ion resonances. Data are suggested for the coefficients for electron attachment, ionization, and effective ionization, and for the rate constant for electron attachment. While progress has been made regarding our knowledge on electron-chlorine interactions at low energies (< 100 eV), there is still a need for: (i) improvement in the uncertainties of all suggested cross sections; (ii) measurement of the cross sections for momentum transfer, vibrational excitation, electronic excitation, and dissociative ionization; and (iii) accurate measurement of the electron transport coefficients in pure Cl<sub>2</sub> and in mixtures with rare gases. Also provided in this paper is pertinent information on the primary Cl<sub>2</sub> discharge byproducts Cl<sub>2</sub><sup>+</sup>, Cl<sub>2</sub><sup>-</sup>, Cl, Cl<sup>+</sup>, and Cl<sup>-</sup>. © 1999 American Institute of Physics and American Chemical Society. [S0047-2689(99)00401-8]

Key words: chlorine; Cl<sub>2</sub>; cross section; electron attachment; electron collisions; electron scattering; electron transport; ionization.

## Contents

1. Introduction.....	133	3.5.2. Total Vibrational Excitation Cross Section, $\sigma_{\text{vib,t}}(\epsilon)$ .....	147
2. Electronic and Molecular Structure.....	135	3.5.3. Electronic Excitation Cross Sections, $\sigma_{\text{elec}}(\epsilon)$ .....	147
2.1. Cl <sub>2</sub> .....	135	4. Electron Impact Ionization for Cl <sub>2</sub> .....	148
2.2. Cl <sub>2</sub> <sup>+</sup> .....	139	4.1. Total Ionization Cross Section, $\sigma_{\text{it}}(\epsilon)$ .....	148
2.3. Cl <sub>2</sub> <sup>-</sup> .....	139	4.2. Density-Reduced Electron-Impact Ionization Coefficient, $\alpha/N(E/N)$ .....	150
3. Electron Scattering for Cl <sub>2</sub> .....	140	5. Total Cross Section for Electron-Impact Dissociation into Neutral Fragments, $\sigma_{\text{diss,neut,t}}(\epsilon)$ for Cl <sub>2</sub> .....	151
3.1. Total Electron Scattering Cross Section, $\sigma_{\text{sc,t}}(\epsilon)$ .....	140	6. Electron Attachment to Cl <sub>2</sub> .....	151
3.2. Total Rotational Electron Scattering Cross Section, $\sigma_{\text{rot,t}}(\epsilon)$ .....	141	6.1. Total Dissociative Electron Attachment Cross Section, $\sigma_{\text{da,t}}(\epsilon)$ .....	152
3.3. Total Elastic Electron Scattering Cross Section, $\sigma_{\text{e,t}}(\epsilon)$ .....	143	6.2. Total Electron Attachment Rate Constant as a Function of the Density-Reduced Electric Field $E/N$ , $k_{\text{a,t}}(E/N)$ , and the Mean Electron Energy $\langle\epsilon\rangle$ , $k_{\text{a,t}}(\langle\epsilon\rangle)$ .....	153
3.4. Momentum Transfer Cross Section, $\sigma_{\text{m}}(\epsilon)$ ...	143	6.2.1. $k_{\text{a,t}}(E/N)$ in N <sub>2</sub> .....	153
3.5. Inelastic Electron Scattering Cross Section, $\sigma_{\text{inel}}(\epsilon)$ .....	145	6.2.2. $k_{\text{a,t}}(\langle\epsilon\rangle)$ .....	154
3.5.1. Rotational Excitation Cross Section, $\sigma_{\text{rot}}(\epsilon)$ .....	145	6.2.3. Thermal value, $(k_{\text{a,t}})_{\text{th}}$ , of the Total Electron Attachment Rate Constant....	154

<sup>a)</sup>Electronic mail: loucas.christophorou@nist.gov

©1999 by the U.S. Secretary of Commerce on behalf of the United States.  
All rights reserved. This copyright is assigned to the American Institute of  
Physics and the American Chemical Society.  
Reprints available from ACS; see Reprints List at back of issue.

6.2.4. Effect of Temperature on the Electron Attachment Rate Constant, $k_{a,t}(\langle \varepsilon \rangle, T)$ .....	154	4. Dissociation energy, vibrational energy, equilibrium internuclear separation, spin-orbit splitting, electron affinity, energy position of negative ion states, ionization threshold energy, dissociative ionization threshold energy, energy threshold for double ionization, and energy threshold for ion-pair formation of $\text{Cl}_2$ ....	138
6.3. Density-Reduced Electron Attachment Coefficient, $\eta/N(E/N)$ .....	155	5. Comparison of the energies of the $4s\sigma_g$ , $3\Pi_g$ , $4s\sigma_g$ , $1\Pi_g$ , $2^3\Pi(1u)$ , $2^1\Pi_u$ , $2^1\Sigma_u^+$ , and $1\Pi_g(?)$ states of $\text{Cl}_2$ .....	140
6.4. Density-Reduced Effective Ionization Coefficient, $(\alpha - \eta)/N(E/N)$ .....	155	6. Transitions observed by Stubbs <i>et al.</i> in Ref. 84 in a high-resolution energy-loss experiment below the second ionization $\text{Cl}_2^+$ ( $1\Pi_u$ ) onset.....	141
6.5. Cross Section for Ion-Pair Formation, $\sigma_{ip}(\varepsilon)$ .....	156	7. Some physical parameters for $\text{Cl}_2^-$ .....	142
6.6. Negative Ions in $\text{Cl}_2$ Discharges.....	156	8. Some parameters for $\text{Cl}_2^+$ .....	143
7. Electron Transport for $\text{Cl}_2$ .....	157	9. Recommended total electron scattering cross section, $\sigma_{sc,t}(\varepsilon)$ , for $\text{Cl}_2$ .....	143
7.1. Electron Drift Velocity, $w$ .....	157	10. Differential rotational excitation cross sections for electron scattering from $\text{Cl}_2$ .....	144
7.2. Lateral Electron Diffusion Coefficient to Electron Mobility Ratio, $D_T/\mu$ .....	157	11. Suggested total elastic electron scattering cross section, $\sigma_{e,t}(\varepsilon)$ , for $\text{Cl}_2$ .....	146
8. Optical Emission from $\text{Cl}_2$ Gas Discharges.....	157	12. Suggested total ionization cross section, $\sigma_{i,t}(\varepsilon)$ , for $\text{Cl}_2$ .....	149
9. Suggested Cross Sections and Coefficients for $\text{Cl}_2$ .....	158	13. Suggested density-reduced electron-impact ionization coefficient, $\alpha/N(E/N)$ , for $\text{Cl}_2$ .....	150
10. Data Needs for $\text{Cl}_2$ .....	158	14. Total cross section for electron-impact dissociation into neutral fragments, $\sigma_{diss,neut,t}(\varepsilon)$ , for $\text{Cl}_2$ .....	150
11. Electron Collision Data for Cl and $\text{Cl}^+$ .....	158	15. Negative ion states of $\text{Cl}_2$ .....	151
11.1. Cl.....	158	16. Suggested total dissociative electron attachment cross section, $\sigma_{da,t}(\varepsilon)$ , for $\text{Cl}_2$ .....	153
11.1.1. Total Electron Scattering Cross Section, $\sigma_{sc,t,Cl}(\varepsilon)$ .....	159	17. Suggested total electron attachment rate constant, $k_{a,t}(\langle \varepsilon \rangle)$ ( $T = 298\text{ K}$ ), for $\text{Cl}_2$ .....	154
11.1.2. Momentum Transfer Cross Section, $\sigma_{m,Cl}(\varepsilon)$ .....	159	18. Thermal values, $(k_{a,t})_{th}$ , of the total electron attachment rate constant for $\text{Cl}_2$ near room temperature.....	154
11.1.3. Total Elastic Electron Scattering Cross Section, $\sigma_{e,t,Cl}(\varepsilon)$ .....	159	19. Variation of $(k_{a,t})_{th}$ of $\text{Cl}_2$ with temperature.....	155
11.1.4. Electron-Impact Excitation Cross Section, $\sigma_{exc,Cl}(\varepsilon)$ .....	160	20. Suggested values for the density-reduced electron attachment coefficient, $\eta/N(E/N)$ , for $\text{Cl}_2$ .....	155
11.1.5. Electron-Impact Single-Ionization Cross Section, $\sigma_{i,Cl}(\varepsilon)$ .....	160	21. Suggested values of the density-reduced effective ionization coefficient, $(\alpha - \eta)/N(E/N)$ , for $\text{Cl}_2$ .....	156
11.1.6. Radiative Attachment.....	161	22. Suggested cross section for negative ion-positive ion pair production, $\sigma_{ip}(\varepsilon)$ , in $\text{Cl}_2$ between 12 and 100 eV.....	156
11.2. $\text{Cl}^+$ .....	161	23. Ionization energy of Cl ( $^2P_{3/2}$ ) for the production of $\text{Cl}^+$ ( $^3P_{2,1,0}$ ), $\text{Cl}^+$ ( $^1D_2$ ), and $\text{Cl}^+$ ( $^1S_0$ ).....	158
12. Electron Detachment, Electron Transfer, and Recombination and Diffusion Processes.....	161	24. Photoionization cross section, $\sigma_{pi,Cl}(\lambda)$ , of the Cl atom.....	158
12.1. Electron Detachment.....	161	25. Cross section, $\sigma_{i,Cl}(\varepsilon)$ , for single ionization of Cl by electron impact.....	160
12.1.1. Photodetachment (Photodetachment and Photodissociation) of $\text{Cl}_2^-$ .....	161	26. Photodestruction cross section, $\sigma_{pdest,Cl_2^-}(\lambda)$ , for $\text{Cl}_2^-$ .....	162
12.1.2. Electron-Induced and Collisional Detachment of $\text{Cl}_2^-$ .....	162	27. Associative detachment thermal rate constants involving $\text{Cl}^-$ .....	163
12.1.3. Photodetachment of $\text{Cl}^-$ .....	162	28. Energy threshold for the detachment of $\text{Cl}^-$ in	
12.1.4. Collisional Detachment of $\text{Cl}^-$ .....	163		
12.2. Electron Transfer.....	164		
12.3. Recombination and Diffusion Processes...	165		
12.3.1. Recombination of $\text{Cl}_2^+$ and $\text{Cl}^-$ ....	165		
12.3.2. Recombination of Cl.....	165		
12.3.3. Diffusion of Cl and $\text{Cl}^-$ in Gases..	166		
13. Summary for Other Species and Processes.....	166		
14. Acknowledgments.....	166		
15. References.....	167		

### List of Tables

1. Definition of symbols.....	134
2. Vertical electronic energies (MRD-CI values) from the ground state of $\text{Cl}_2$ to various excited states as calculated by Peyerimhoff and Buenker.....	137
3. Recommended total photoabsorption cross section, $\sigma_{pa,t}(\lambda)$ , for $\text{Cl}_2$ .....	137

collisions with various target gases. .... 164

### List of Figures

1. Composite potential-energy diagrams for most of the electronic states of the Cl <sub>2</sub> molecule as calculated by Peyerimhoff and Buenker. ....	136
2. Total photoabsorption cross section as a function of photon wavelength, $\sigma_{\text{pa,t}}(\lambda)$ , for Cl <sub>2</sub> . ....	137
3. Partial photoionization cross sections as a function of photon wavelength, $\sigma_{\text{pi,partial}}(\lambda)$ , for the production of the positive ions Cl <sub>2</sub> <sup>+</sup> , Cl <sup>+</sup> , and Cl <sub>2</sub> <sup>++</sup> from Cl <sub>2</sub> . ....	137
4. Threshold-electron excitation spectrum and electron energy-loss spectrum of Cl <sub>2</sub> . ....	139
5. Potential-energy curves for the lowest negative ion states of Cl <sub>2</sub> <sup>-</sup> . ....	142
6. Total electron scattering cross section, $\sigma_{\text{sc,t}}(\epsilon)$ , for Cl <sub>2</sub> . ....	143
7. Total cross section for rotational scattering, $\sigma_{\text{rot,t}}(\epsilon)$ , for Cl <sub>2</sub> . ....	145
8. Integrated (over angle) excitation cross sections, $\sigma_{\text{rot,t} \rightarrow 0}(\epsilon)$ , for Cl <sub>2</sub> . ....	145
9. Total elastic electron scattering cross section, $\sigma_{\text{e,t}}(\epsilon)$ , for Cl <sub>2</sub> . ....	146
10. Calculated momentum transfer cross sections, $\sigma_{\text{m}}(\epsilon)$ , for Cl <sub>2</sub> . ....	146
11. Comparison of experimental and calculated rotationally summed differential electron scattering cross sections $d^2\sigma_{\text{rot,sum}}/d\Omega d\epsilon$ , for Cl <sub>2</sub> . ....	146
12. Total vibrational excitation cross section, $\sigma_{\text{vib,t}}(\epsilon)$ , for Cl <sub>2</sub> . ....	147
13. Comparison of calculated cross sections for electronic excitation, $\sigma_{\text{elec}}(\epsilon)$ , of Cl <sub>2</sub> . ....	148
14. Electron-impact total ionization cross section, $\sigma_{\text{t,t}}(\epsilon)$ , for Cl <sub>2</sub> . ....	149
15. Density-reduced electron-impact ionization coefficient, $\alpha/N(E/N)$ , for Cl <sub>2</sub> . ....	150
16. Total cross section for electron-impact dissociation into neutral fragments, $\sigma_{\text{dis,neu,t}}(\epsilon)$ , for Cl <sub>2</sub> . ....	150
17. Total dissociative electron attachment, $\sigma_{\text{da,t}}(\epsilon)$ , for Cl <sub>2</sub> . ....	152
18. Total electron attachment rate constant as a function of $E/N$ , $k_{\text{a,t}}(E/N)$ , for Cl <sub>2</sub> ( $T \approx 298-300$ K). ....	153
19. Total electron attachment rate constant as a function of the mean electron energy, $k_{\text{a,t}}(\langle \epsilon \rangle)$ , for Cl <sub>2</sub> ( $T \approx 298$ K). ....	153
20. Variation of $k_{\text{a,t}}(\langle \epsilon \rangle)$ of Cl <sub>2</sub> with temperature. ....	155
21. Density-reduced electron attachment coefficient, $\eta/N(E/N)$ , for Cl <sub>2</sub> . ....	155
22. Density-reduced effective ionization coefficient, $(\alpha - \eta)/N(E/N)$ , for Cl <sub>2</sub> . ....	156
23. Cross section for ion-pair formation, $\sigma_{\text{ip}}(\epsilon)$ , for Cl <sub>2</sub> . ....	156
24. Electron drift velocity and lateral electron diffusion coefficient for Cl <sub>2</sub> . ....	157

25. Recommended and suggested cross sections for Cl <sub>2</sub> . ....	157
26. Photoionization cross section as a function of wavelength, $\sigma_{\text{pi,Cl}}(\lambda)$ , for atomic chlorine. ....	159
27. Momentum transfer cross section, $\sigma_{\text{m,Cl}}(\epsilon)$ , for atomic chlorine. ....	159
28. Calculated total elastic electron scattering cross sections, $\sigma_{\text{e,t,Cl}}(\epsilon)$ , for atomic chlorine. ....	159
29. Calculated cross sections for electron-impact excitation of the 4s, 5s, 6s, 4p, 5p, 3d, 4d, and 5d states of the chlorine atom from the ground state 3p( <sup>2</sup> P). ....	160
30. Electron-impact single-ionization cross section, $\sigma_{\text{i,Cl}}(\epsilon)$ , for the Cl atom. ....	160
31. Cross section, $\sigma_{\text{i,Cl}^+}(\epsilon)$ , for single ionization of Cl <sup>+</sup> by electron impact. ....	161
32. Cross section for photodestruction of Cl <sub>2</sub> as a function of photon wavelength, $\sigma_{\text{pdest,Cl}_2}(\lambda)$ . ....	161
33. Photodetachment cross section for Cl <sup>-</sup> , $\sigma_{\text{pd,Cl}}(\lambda)$ , as a function of photon wavelength, $\lambda$ . ....	163
34. Collisional detachment cross sections, $\sigma_{\text{cd,Cl}}(\mathcal{E})$ , as a function of the relative energy of the reactants, $\mathcal{E}$ , involving Cl <sup>-</sup> and various molecular targets. ....	165
35. Cross section, $\sigma_{\text{ct,Cl}^-}(\mathcal{E})$ , for charge transfer as a function of the relative energy of the reactants, $\mathcal{E}$ , in collisions of Cl <sup>-</sup> with Cl <sub>2</sub> . ....	166
36. The product, $D_{\text{L}}N(E/N)$ , of the longitudinal diffusion coefficient $D_{\text{L}}$ and the neutral gas number density $N$ as a function of $E/N$ for Cl <sup>-</sup> in Ne, Ar, Kr, Xe, and N <sub>2</sub> . ....	166

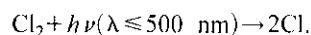
## 1. Introduction

Molecular chlorine (Cl<sub>2</sub>) is a plasma processing gas (e.g., see Refs. 1-24). It is used in plasma etching of semiconductors where the Cl atoms produced in a gas discharge efficiently etch a silicon surface. The dominant primary electron interaction processes are taken to be single-step electron-impact ionization of Cl<sub>2</sub> and Cl, dissociation of Cl<sub>2</sub> into neutrals, and dissociative attachment to Cl<sub>2</sub>.<sup>1,10,13,17</sup> The basic species involved in Cl<sub>2</sub> plasmas, then, are the three molecular species: Cl<sub>2</sub>, Cl<sub>2</sub><sup>-</sup>, and Cl<sub>2</sub><sup>+</sup>, and the three atomic species: Cl, Cl<sup>-</sup>, and Cl<sup>+</sup>. Although recent work on the interactions of Cl<sub>2</sub> with slow electrons is largely motivated by plasma etching technology, considerable work on electron interactions with the Cl<sub>2</sub> molecule was done in the 1970s and the 1980s motivated by gas ultraviolet (UV) laser applications.<sup>25-31</sup> In this latter application the fundamental process of interest is dissociative electron attachment producing halogen atomic negative ions (Cl<sup>-</sup>) which efficiently recombine with the rare-gas positive ions<sup>29,30</sup> to form the lasing species (e.g., ArI<sup>\*</sup>, KrI<sup>\*</sup>, and XeCl<sup>\*</sup> excimers) in rare-gas halide lasers.<sup>27,28</sup>

Molecular chlorine is also of atmospheric and environmental interest.<sup>32</sup> It is a potential atmospheric reservoir of chlorine atoms<sup>33</sup> which are released photolytically.

TABLE I. Definition of symbols

Symbol	Definition	Common scale and units
$\sigma_{\text{pa},i}(\lambda)$	Total photoabsorption cross section	$10^{-20} \text{ cm}^2; 10^{-24} \text{ m}^2$
$\sigma_{\text{pi},i}(\lambda)$	Total photoionization cross section	$10^{-20} \text{ cm}^2; 10^{-24} \text{ m}^2$
$\sigma_{\text{pi},\text{partial}}(\lambda)$	Partial photoionization cross section	$10^{-20} \text{ cm}^2; 10^{-24} \text{ m}^2$
$\sigma_{\text{sc},i}(\epsilon)$	Total electron scattering cross section	$10^{-16} \text{ cm}^2; 10^{-20} \text{ m}^2$
$\sigma_{\text{rot},i}(\epsilon)$	Total rotational electron scattering cross section	$10^{-16} \text{ cm}^2; 10^{-20} \text{ m}^2$
$\sigma_{\text{rot},j-0}(\epsilon)$	Cross section for rotational excitation of the $j$ rotational state integrated over angle	$10^{-16} \text{ cm}^2; 10^{-20} \text{ m}^2$
$\sigma_{\text{rot,sum}}(\epsilon)$	Rotationally summed electron scattering cross section	$10^{-16} \text{ cm}^2 \text{ sr}^{-1}$
$d^2\sigma_{\text{rot,sum}}/d\Omega d\epsilon$	Rotationally summed differential electron scattering cross section	$10^{-16} \text{ cm}^2 \text{ sr}^{-1} \text{ eV}^{-1}$
$\sigma_{\text{e},i}(\epsilon)$	Total elastic electron scattering cross section	$10^{-16} \text{ cm}^2; 10^{-20} \text{ m}^2$
$\sigma_{\text{m},i}(\epsilon)$	Momentum transfer cross section (elastic)	$10^{-16} \text{ cm}^2; 10^{-20} \text{ m}^2$
$\sigma_{\text{vib},i}(\epsilon)$	Total vibrational excitation cross section	$10^{-16} \text{ cm}^2; 10^{-20} \text{ m}^2$
$\sigma_{\text{vib,indir}}(\epsilon)$	Total indirect vibrational excitation cross section	$10^{-16} \text{ cm}^2; 10^{-20} \text{ m}^2$
$\sigma_{\text{elec},i}(\epsilon)$	Electronic excitation cross section	$10^{-16} \text{ cm}^2; 10^{-20} \text{ m}^2$
$\sigma_{\text{i},i}(\epsilon)$	Total ionization cross section	$10^{-16} \text{ cm}^2; 10^{-20} \text{ m}^2$
$\sigma_{\text{diss},i}(\epsilon)$	Total dissociation cross section	$10^{-16} \text{ cm}^2; 10^{-20} \text{ m}^2$
$\sigma_{\text{diss,neu},i}(\epsilon)$	Total cross section for electron impact dissociation into neutrals	$10^{-16} \text{ cm}^2; 10^{-20} \text{ m}^2$
$\sigma_{\text{a},i}(\epsilon)$	Total electron attachment cross section	$10^{-16} \text{ cm}^2; 10^{-20} \text{ m}^2$
$\sigma_{\text{da},i}(\epsilon)$	Total dissociative electron attachment cross section	$10^{-16} \text{ cm}^2; 10^{-20} \text{ m}^2$
$\sigma_{\text{ip}}(\epsilon)$	Cross section for ion-pair formation	$10^{-18} \text{ cm}^2; 10^{-22} \text{ m}^2$
$\sigma_{\text{pdest},\text{Cl}_2}(\lambda)$	Photodestruction cross section for $\text{Cl}_2$	$10^{-18} \text{ cm}^2; 10^{-22} \text{ m}^2$
$\sigma_{\text{pi},\text{Cl}}(\lambda)$	Photoionization cross section of Cl	$10^{-18} \text{ cm}^2; 10^{-22} \text{ m}^2$
$\sigma_{\text{sc},\text{Cl}}(\epsilon)$	Total electron scattering cross section for Cl	$10^{-16} \text{ cm}^2; 10^{-20} \text{ m}^2$
$\sigma_{\text{e},\text{Cl}}(\epsilon)$	Total elastic electron scattering cross section for Cl	$10^{-16} \text{ cm}^2; 10^{-20} \text{ m}^2$
$\sigma_{\text{m},\text{Cl}}(\epsilon)$	Momentum transfer cross section for Cl	$10^{-16} \text{ cm}^2; 10^{-20} \text{ m}^2$
$\sigma_{\text{exc},\text{Cl}}(\epsilon)$	Total electron-impact excitation cross section of Cl	$10^{-16} \text{ cm}^2; 10^{-20} \text{ m}^2$
$\sigma_{\text{i},\text{Cl}}(\epsilon)$	Total electron-impact ionization cross section for Cl	$10^{-16} \text{ cm}^2; 10^{-20} \text{ m}^2$
$\sigma_{\text{i},\text{Cl}}(\epsilon)$	Electron-impact single ionization cross section for Cl	$10^{-16} \text{ cm}^2; 10^{-20} \text{ m}^2$
$\sigma_{\text{pd},\text{Cl}}(\lambda)$	Photodetachment cross section for $\text{Cl}^-$	$10^{-18} \text{ cm}^2; 10^{-22} \text{ m}^2$
$\sigma_{\text{cd},\text{Cl}}(\epsilon)$	Collisional detachment cross section involving Cl	$10^{-16} \text{ cm}^2; 10^{-20} \text{ m}^2$
$\sigma_{\text{ct},\text{Cl}}(\epsilon)$	Cross section for charge transfer in collisions involving Cl	$10^{-16} \text{ cm}^2; 10^{-20} \text{ m}^2$
$\sigma_{\text{i},\text{Cl}^+}(\epsilon)$	Cross section for single ionization of $\text{Cl}^+$	$10^{-16} \text{ cm}^2; 10^{-20} \text{ m}^2$
$\alpha/N$	Density-reduced ionization coefficient	$10^{22} \text{ m}^2$
$(\alpha - \eta)/N$	Density-reduced effective ionization coefficient	$10^{22} \text{ m}^2$
$\eta/N$	Density-reduced electron attachment coefficient	$10^{-22} \text{ m}^2$
$k_{\text{a},\text{t}}$	Total electron attachment rate constant	$10^{-10} \text{ cm}^3 \text{ s}^{-1}$
$(k_{\text{a},\text{t}})_{\text{th}}$	Thermal electron attachment rate constant	$10^{-10} \text{ cm}^3 \text{ s}^{-1}$
$w$	Electron drift velocity	$10^6 \text{ cm s}^{-1}$
$D_T/\mu$	Transverse electron diffusion coefficient to electron mobility ratio	V



In this paper a number of collision cross sections, coefficients, and rate constants are used to quantify the various processes which result from collisions of low-energy (mostly below about 100 eV) electrons with the  $\text{Cl}_2$  molecule. These are identified in Table I along with the corresponding symbols and units. The procedure for assessing and recommending data followed in this paper is the same as in the previous five papers in this series.<sup>34-38</sup> As will be discussed throughout this paper, few of the available data sufficiently meet the criteria to be "recommended." This demonstrates the need for additional data for this molecule. We have, however, "suggested" the best available data for each collision process.

Since the  $\text{Cl}_2$  molecule is one of the simplest reactive gases used in plasma processing (often in mixtures with Ar), we consider it desirable from the point of view of this application to also provide relevant information on the most likely discharge byproducts, namely  $\text{Cl}_2^-$ ,  $\text{Cl}_2^+$ , Cl,  $\text{Cl}^-$ , and  $\text{Cl}^+$ . In this way, one may have more complete information about the key species and processes. Therefore, while the emphasis in this paper is on low-energy electron interactions with the neutral  $\text{Cl}_2$  molecule, pertinent information is also provided for the  $\text{Cl}_2^-$  and  $\text{Cl}_2^+$  molecular ions, and for the atomic species Cl,  $\text{Cl}^-$ , and  $\text{Cl}^+$ .

An early attempt to critically evaluate low-energy electron-impact cross section data for  $\text{Cl}_2$  was made by Morgan.<sup>31</sup> In addition, a number of investigators have used

Boltzmann codes and electron transport data to calculate cross sections and rate coefficients for some electron collision processes in Cl<sub>2</sub>.<sup>1,10,39-41</sup> The value of these results is questionable however, partly because of the limited measurements on electron transport parameters upon which they are based, and because of the model dependent nature of the calculated cross sections. The results of two such calculations by Rogoff *et al.*<sup>1</sup> and Pinhão and Chouki<sup>40</sup> are compared with other data in later sections of this paper.

## 2. Electronic and Molecular Structure

### 2.1. Cl<sub>2</sub>

The electronic structure of the outermost (valence) shell of the Cl<sub>2</sub> molecule in its ground electronic state<sup>42-44</sup> is:  $\dots(\sigma_g 3p)^2, (\pi_u 3p)^4, (\pi_g 3p)^4, (\sigma_u 3p)^0$  and has  $^1\Sigma_g^+$  symmetry. The first four excited electronic states of Cl<sub>2</sub> listed by Huber and Herzberg<sup>45</sup> are  $A' ^3\Pi_{2u}, A' ^3\Pi_{1u}, B' ^3\Pi_{0u},$  and  $C' ^1\Pi_u$ . A number of theoretical and experimental studies have located many other excited electronic states (see below).

There are three types of sources of information of interest to the present study regarding the electronic structure of the chlorine molecule: calculations, photoabsorption and photoelectron studies, and electron energy-loss investigations. Although our interest is focused on the third type of information, basic information provided by the other two types of investigations is included in the paper as complementary.

The most useful theoretical work concerning the electronic states of chlorine are the *ab initio* calculations of Peyerimhoff and Buenker.<sup>46</sup> These workers calculated potential energy curves for the ground and excited electronic states of the chlorine molecule and for its positive and negative ions using the multireference single and double excitation with configuration interaction (MRD-CI) method. They considered all states which correlate with the lowest atomic limit  $[\text{Cl}(^2P_u) + \text{Cl}(^2P_u)]$  and many others which go into ionic  $\text{Cl}^+ + \text{Cl}^-$  or Rydberg  $\text{Cl}^* + \text{Cl}$  asymptotes. All singlet states which correlate with the ground atomic products were found to be repulsive. Among the triplet states of Cl<sub>2</sub> which dissociate into the ground state atoms only the  $^3\Pi_u$  state is not repulsive. The potential energy curves calculated by Peyerimhoff and Buenker<sup>46</sup> are reproduced in Fig. 1. The potential-energy curves shown in the figure are for the electronic states of Cl<sub>2</sub> which dissociate into the lowest atomic limit  $[\text{Cl}(^2P_u) + \text{Cl}(^2P_u)]$ . In Fig. 2 are also shown the potential-energy curves for the lowest electronic states of Cl<sub>2</sub><sup>+</sup> with various asymptotic limits and a potential-energy curve for the ground state of Cl<sub>2</sub><sup>-</sup> for the asymptotic limit  $\text{Cl}(^2P_u) + \text{Cl}^-(^1S_g)$ . As will be seen from subsequent discussions in this paper, the potential-energy curves for Cl<sub>2</sub>, Cl<sub>2</sub><sup>-</sup>, and Cl<sub>2</sub><sup>+</sup> in Fig. 1 are most helpful in understanding the low-energy electron interaction processes with the Cl<sub>2</sub> molecule. Peyerimhoff and Buenker calculated for the dissociation energy  $D_0$ , the vertical ionization energy, and the electron affinity of Cl<sub>2</sub>, respectively, the values 2.455, 11.48, and 2.38 eV. These values are in good agreement with experimental

values discussed later in this paper. The estimated electronic-state energies (MRD-CI values) are listed in Table 2.

There have been many photoabsorption and photoionization studies,<sup>33,45,47-66</sup> as well as a number of photoelectron studies<sup>67-73</sup> of Cl<sub>2</sub>. The data on the total photoabsorption cross section,  $\sigma_{\text{pa,t}}(\lambda)$ , of Cl<sub>2</sub> have been discussed and summarized by a number of groups (e.g., Gallagher *et al.*,<sup>64</sup> Maric *et al.*,<sup>33</sup> and Hubinger and Nee<sup>66</sup>). In Fig. 2 are plotted the measurements of  $\sigma_{\text{pa,t}}(\lambda)$  of a number of investigators<sup>33,49,51,57,59,62,63,65,66</sup> in the wavelength range 15.5–550 nm. Between 250 and ~500 nm the agreement among the various measurements is good. A least squares fit to the data in this wavelength region is shown in Fig. 2 by the solid line. Data taken off this line are given in Table 3 as our recommended values for the  $\sigma_{\text{pa,t}}(\lambda)$  of Cl<sub>2</sub> in this wavelength range. The extensive measurements of Samson and Angel<sup>63</sup> cover the wavelength range 15.5–103.8 nm and are recommended for this energy range (Table 3). The measurements of Samson and Angel of the total photoionization cross section  $\sigma_{\text{pi,t}}(\lambda)$  show that  $\sigma_{\text{pi,t}}(\lambda)$  is equal to the total photoabsorption cross section  $\sigma_{\text{pa,t}}(\lambda)$  except in the wavelength range 82.5–77.0 nm where it is up to 10% lower, depending on the value of the wavelength. The decrease of the photoionization efficiency to values below 1.0 in this wavelength range has been attributed to photoabsorption processes leading to the production of neutrals.<sup>63</sup>

Measurements have also been made by Samson and Angel<sup>63</sup> of the partial photoionization cross section,  $\sigma_{\text{pi,partial}}(\lambda)$ , for the production of Cl<sub>2</sub><sup>+</sup> and Cl<sup>+</sup> by photon impact on Cl<sub>2</sub>. These are shown in Fig. 3. In Fig. 3 are also plotted the results of Samson and Angel for the production of Cl<sub>2</sub><sup>+</sup> by photon impact on Cl<sub>2</sub>. The data in Fig. 3 show that for photon wavelengths down to ~80.0 nm, the cross section for the production of the Cl<sub>2</sub><sup>+</sup> ion is about equal to the total, that is, it far exceeds the cross section for the production of the Cl<sup>+</sup> ion (dissociative photoionization has a much lower probability than nondissociative photoionization). At progressively shorter wavelengths, dissociative photoionization becomes more probable. The cross section for double electron ejection is negligible down to about 40 nm. Carlson *et al.*<sup>71</sup> and Gallagher *et al.*<sup>64</sup> have published measurements of the production of Cl<sub>2</sub><sup>+</sup> in the ionic states  $(2\pi_g^{-1})X^2\Pi_g, (2\pi_u^{-1})A^2\Pi_u,$  and  $(5\sigma_g^{-1})B^2\Sigma_g$  by photon impact on Cl<sub>2</sub>.

Data on photoionization energetics are given in Table 4 where they are compared with data obtained using other methods. For further spectroscopic investigations of the electronic structure of the chlorine molecule see Lee and Walsh,<sup>54</sup> Iczkowski *et al.*,<sup>55</sup> Douglas *et al.*,<sup>56</sup> Frost *et al.*,<sup>67</sup> Bondybey and Fletcher,<sup>81</sup> Huber and Herzberg,<sup>45</sup> Douglas,<sup>61</sup> Moeller *et al.*,<sup>82</sup> Burkholder and Bair,<sup>62</sup> McLoughlin *et al.*,<sup>83</sup> Lonkhuyzen and de Lange,<sup>72</sup> and Frost *et al.*<sup>77</sup>

There have been three major electron-impact studies of the electronic structure of Cl<sub>2</sub>: the threshold-electron excitation study of Jureta *et al.*<sup>43</sup> which covered the excitation energy range up to 11.5 eV, the electron energy-loss study of Spence *et al.*<sup>44</sup> which covered the energy-loss range 5.5–14.5 eV, and the electron energy-loss study of Stubbs *et al.*<sup>84</sup>

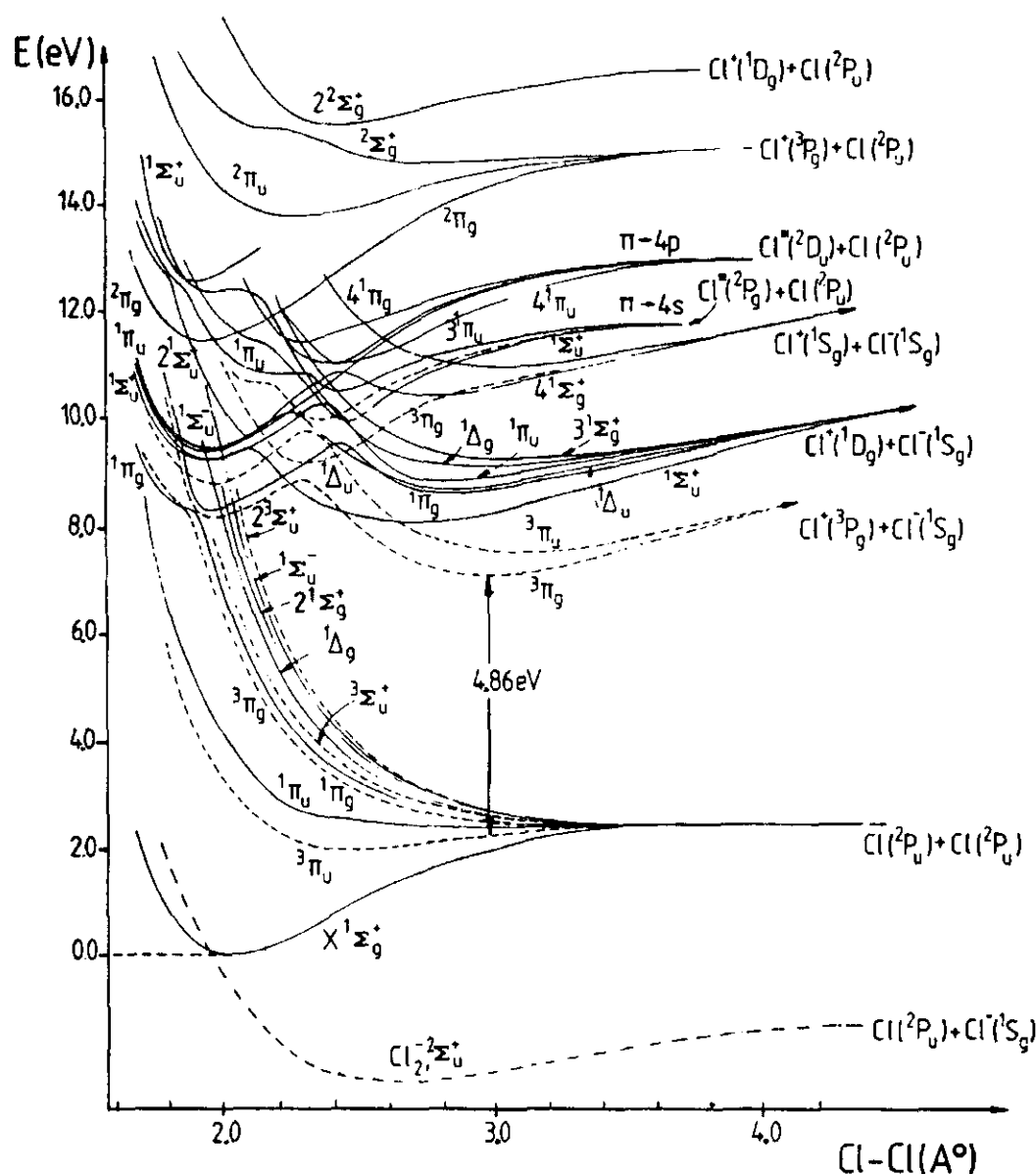


FIG. 1. Composite potential-energy diagrams for most of the electronic states of the  $\text{Cl}_2$  molecule as calculated by Peyerimhoff and Buenker (Ref. 46)

which covered the electron energy-loss range up to 14.252 eV. Threshold-electron excitation methods are best suited for locating optically forbidden states, while electron energy-loss spectra using sufficiently energetic electrons give spectra similar to photoabsorption. Figure 4(a) shows the threshold-electron excitation spectrum of  $\text{Cl}_2$  obtained by Jureta *et al.*<sup>43</sup> in the region of Rydberg excitation between about 7.5 and 11.5 eV, and Fig. 4(b) shows an electron energy-loss (in the range 5.5–11.5 eV) spectrum of  $\text{Cl}_2$  obtained by Spence *et al.*<sup>44</sup> at a scattering angle of  $3^\circ$  using 200 eV incident energy electrons. The threshold-electron excitation technique of Jureta *et al.* had an energy resolution [full-width-at-half-maximum (FWHM)] of about 35 meV and the energy-loss experiment of Spence *et al.* had an energy resolution of 50–60 meV. As expected, the spectra they

obtained at small scattering angles [Fig. 4(b)] differ from the threshold-electron excitation spectra and correspond closely to the photoabsorption spectra. The most prominent features of the energy-loss spectra arise from excitation of optically allowed Rydberg states. Larger-angle scattering data showed additional structures due to excitation of optically forbidden states. The spectra also showed the presence of hot bands. Such observation of hot bands in electron scattering spectra is unusual, but because the ground-state vibrational spacing of  $\text{Cl}_2$  is small (0.0694 eV) and the Franck–Condon overlaps are particularly favorable, such structures become relatively strong for some electronic transitions. Stubbs *et al.*<sup>84</sup> had a better electron beam energy resolution (FWHM  $\approx 18$  meV) than the other two studies. This allowed them to obtain highly resolved electron energy-loss spectra up to

TABLE 2. Vertical electronic energies (MRD-CI values) from the ground state of Cl<sub>2</sub> to various excited states as calculated by Peyerimhoff and Buenker (Ref. 46)

State/Excitation	Vertical energy (eV)
X <sup>1</sup> Σ <sub>g</sub> <sup>+</sup>	0.00
1 <sup>3</sup> Π <sub>u</sub> π <sub>g</sub> → σ <sub>u</sub>	3.24
1 <sup>1</sup> Π <sub>u</sub> π <sub>g</sub> → σ <sub>u</sub>	4.04
1 <sup>3</sup> Π <sub>g</sub> π <sub>u</sub> → σ <sub>u</sub>	6.23
1 <sup>1</sup> Π <sub>g</sub> π <sub>u</sub> → σ <sub>u</sub>	6.86
1 <sup>3</sup> Σ <sub>u</sub> <sup>+</sup> σ <sub>g</sub> → σ <sub>u</sub>	6.80
1 <sup>1</sup> Δ <sub>g</sub> π <sub>g</sub> <sup>2</sup> → σ <sub>u</sub> <sup>2</sup>	8.25
2 <sup>3</sup> Π <sub>g</sub> π <sub>g</sub> → 4s	8.34
2 <sup>1</sup> Π <sub>g</sub> π <sub>g</sub> → 4s	8.38
1 <sup>1</sup> Δ <sub>g</sub> π <sub>g</sub> <sup>2</sup> → σ <sub>u</sub> <sup>2</sup>	8.25
2 <sup>1</sup> Σ <sub>g</sub> <sup>+</sup> π <sub>g</sub> <sup>2</sup> → σ <sub>u</sub> <sup>2</sup>	8.35
2 <sup>3</sup> Π <sub>u</sub> π <sub>g</sub> → 4pσ	8.80
2 <sup>1</sup> Π <sub>u</sub> π <sub>g</sub> → 4pσ	9.22
1 <sup>1</sup> Σ <sub>u</sub> <sup>+</sup> π <sub>g</sub> → 4pπ	9.32
1 <sup>1</sup> Σ <sub>u</sub> <sup>+</sup> π <sub>g</sub> → 4pπ	9.58
1 <sup>1</sup> Δ <sub>u</sub> π <sub>g</sub> → 4pπ	9.62
2 <sup>1</sup> Σ <sub>u</sub> <sup>+</sup> π <sub>u</sub> π <sub>g</sub> → σ <sub>u</sub> <sup>2</sup>	9.67
2 <sup>3</sup> Σ <sub>u</sub> <sup>+</sup> π <sub>u</sub> π <sub>g</sub> → σ <sub>u</sub> <sup>2</sup>	9.75
1 <sup>1</sup> Δ <sub>g</sub> π <sub>g</sub> → 4dπ	9.92
1 <sup>1</sup> Π <sub>g</sub> π <sub>g</sub> → 4dσ	10.01
1 <sup>1</sup> Π <sub>g</sub> π <sub>g</sub> → 4dδ	10.10
2 <sup>1</sup> Σ <sub>u</sub> <sup>+</sup> σ <sub>g</sub> → σ <sub>u</sub> ; π <sub>g</sub> → 4pπ	10.34
3 <sup>3</sup> Π <sub>u</sub> π <sub>u</sub> → 4s	11.33
3 <sup>1</sup> Π <sub>u</sub> π <sub>u</sub> → 4s	11.51
1 <sup>1</sup> Π <sub>u</sub> π <sub>u</sub> → 4dδ	12.74

14.252 eV, using electrons with incident energy between 10 and 120 eV. These incident energies are lower than that (200 eV) used by Spence *et al.*

The strongest structures in the energy-loss spectrum of chlorine lie between 9 and 10 eV under all scattering conditions. They primarily consist of two vibrational series comprising transitions that are allowed by electric-dipole selection rules and have been previously reported in both

TABLE 3. Recommended total photoabsorption cross section, σ<sub>pa,t</sub>(λ), for Cl<sub>2</sub>. Data of Samson and Angel (Ref. 63) in the wavelength range of 16–103.8 nm, and data taken off the solid line in Fig. 2 between 250 and 500 nm

Wavelength (nm)	σ <sub>pa,t</sub> (λ) (10 <sup>-24</sup> m <sup>2</sup> )	Wavelength (nm)	σ <sub>pa,t</sub> (λ) (10 <sup>-24</sup> m <sup>2</sup> )
16.0	255	320	23.7
20.0	260	330	25.6
30.0	186	340	23.6
40.0	1480	350	19.1
50.0	4220	360	13.3
60.0	6300	370	8.41
70.0	7180	380	5.10
80.0	7480	390	3.06
85.0	9040	400	1.92
92.4	9803	410	1.39
103.8	4384	420	1.02
		430	0.77
		440	0.56
		450	0.39
		460	0.26
		470	0.17
		480	0.11
		490	0.071
		500	0.046

photoabsorption and electron impact studies. In Table 5 are listed the energy positions of the energy-loss peaks observed in the electron impact studies of Spence *et al.*<sup>44</sup> and Jureta *et al.*<sup>43</sup> For comparison, photoabsorption data from Moeller *et al.*<sup>82</sup> are also shown along with possible identification of the states responsible for the observed energy losses. A comparison of the values of the energies of the various states as determined from the energy-loss spectra and from the threshold-electron excitation spectra shows excellent agreement (Table 5). The higher-energy resolution in the study of Stubbs *et al.*<sup>84</sup> allowed detection of more transitions than in the other two studies. These are listed in Table 6.

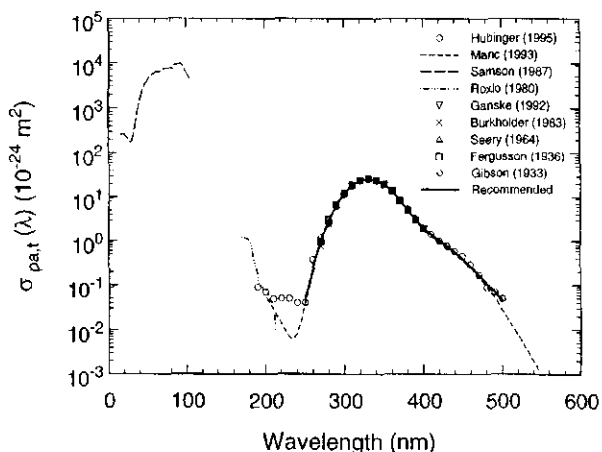


FIG. 2. Total photoabsorption cross section as a function of photon wavelength, σ<sub>pa,t</sub>(λ), for Cl<sub>2</sub>: (—) Ref. 63; (---) Ref. 59; (○) Ref. 66; (- - -) Ref. 33; (▽) Ref. 65; (×) Ref. 62; (△) Ref. 57; (□) Ref. 51; (◇) Ref. 49; (—) recommended.

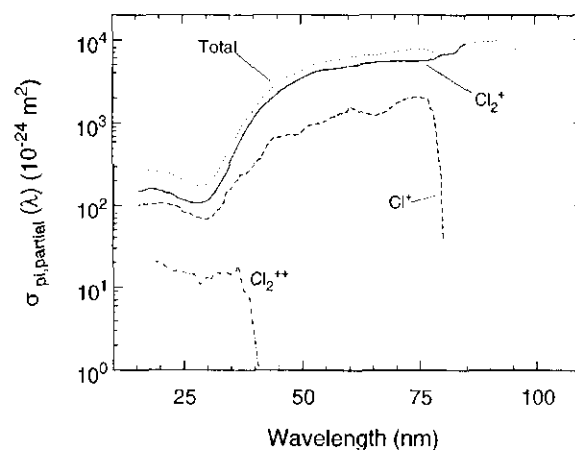


FIG. 3. Partial photoionization cross sections as a function of photon wavelength, σ<sub>pi,partial</sub>(λ), for the production of the positive ions Cl<sub>2</sub><sup>+</sup>, Cl<sup>+</sup>, and Cl<sub>2</sub><sup>++</sup> from Cl<sub>2</sub> (data of Samson and Angel, Ref. 63): (—) Cl<sub>2</sub><sup>+</sup>; (---) Cl<sup>+</sup>; (---) Cl<sub>2</sub><sup>++</sup>; (---) total.

TABLE 4. Dissociation energy, vibrational energy, equilibrium internuclear separation, spin-orbit splitting, electron affinity, energy position of negative ion states, ionization threshold energy, dissociative ionization threshold energy, energy threshold for double ionization, and energy threshold for ion-pair formation of  $\text{Cl}_2$ 

Physical quantity	Value/Method/Reference
Dissociation energy $\text{Cl}_2 (X^1\Sigma_g^+)$ (eV)	$D_0 = 2.4793$ , (45) $D_0 = 2.4794$ , (56) $D_e = 2.5139$ , (56)
Vibrational energy (eV)	0.0694, (45), (56)
Equilibrium internuclear separation (Å)	1.9879, (45) 1.9878, (56)
Spin-orbit splitting (eV)	$0.080 \pm 0.002$ [for the $(1\pi_g)^{-1}$ state], (68)
Electron affinity (eV)	2.45, <sup>a</sup> (74)
Energy position of negative ion states (eV)	See Table 15 in Sect. 6
Ionization threshold energy (eV)	
$\text{Cl}_2^+ (X^2\Pi_{g,3/2})$	<i>Adiabatic</i> 11.50 (photoelectron), (45) $11.48 \pm 0.01$ (photoionization), (53) 11.49 <sup>b</sup> (photoelectron) ( $^2\Pi_g$ ), (69) 11.48 (photoelectron), (72) $11.480 \pm 0.005$ eV, (75) 11.50 (photoelectron) ( $^2\Pi_g$ ), (67) 11.5 (photoelectron), (70) $11.51 \pm 0.01$ (photoelectron), (68) <i>Vertical</i> $11.48 \pm 0.01$ (electron impact), (76) 11.559 (photoelectron), (72) $11.59 \pm 0.01$ (photoelectron), (68)
$\text{Cl}_2^+ (^2\Pi_{g,1/2})$	11.56, (75) 11.63 (vertical, electron momentum spectroscopy, $2\pi_g$ ), (77) $\sim 11.6$ (electron impact), (76)
$\text{Cl}_2^+ (^2\Pi_{u,3/2})$	$\sim 11.8$ (electron impact), (76) 11.80 (electron impact), (78) $11.80 \pm 0.1$ (electron impact), (79)
$\text{Cl}_2^+ (^2\Pi_{u,1/2})$	$\sim 11.9$ (electron impact), (76)
$\text{Cl}_2^+ (^2\Pi_u)$	<i>Adiabatic</i> $13.96 \pm 0.02$ (photoelectron), (68) 14.0 (photoelectron), (70) 14.0 <sup>c</sup> (photoelectron), (69) 14.04 (photoelectron, $^2\Pi_{u,3/2}$ ), (72) 14.11 (photoelectron), (67) <i>Vertical</i> 14.33 (photoelectron), (70) 14.39 (photoelectron) ( $^2\Pi_{u,3/2}$ ), (72) $14.40 \pm 0.02$ (photoelectron), (68) 14.43 <sup>d</sup> (photoelectron), (69) 14.41 (electron momentum spectroscopy, $2\pi_u$ ), (77)
$\text{Cl}_2^+ (^2\Sigma_g^+)$	<i>Adiabatic</i> $15.72 \pm 0.02$ (photoelectron), (68) 15.70 <sup>c</sup> (photoelectron), (72) 15.8 (photoelectron), (70) 15.8 <sup>c</sup> (photoelectron), (69) <i>Vertical</i> $14.09 \pm 0.03$ (electron impact), (76) 15.94 (photoelectron), (67) 16.082 (photoelectron), (72) $16.08 \pm 0.02$ (photoelectron), (68) 16 (photoelectron), (70) 16.10 <sup>d</sup> (photoelectron), (69) 16.18 (electron momentum spectroscopy, $5\sigma_g$ ), (77)



TABLE 4. Dissociation energy, vibrational energy, equilibrium internuclear separation, spin-orbit splitting, electron affinity, energy position of negative ion states, ionization threshold energy, dissociative ionization threshold energy, energy threshold for double ionization, and energy threshold for ion-pair formation of Cl<sub>2</sub>. Continued

Physical quantity	Value/Method/Reference
Cl <sub>2</sub> ( <sup>2</sup> Σ <sub>u</sub> <sup>+</sup> )	<i>Vertical</i> 20.61 ± 0.06 (electron impact), (76) 21.8, 24.0 (electron momentum spectroscopy, 4σ <sub>u</sub> ), (77) 27.3 (electron momentum spectroscopy, 4σ <sub>g</sub> ), (77)
Dissociative ionization (Cl <sub>2</sub> + e → Cl <sup>+</sup> + Cl + 2e) threshold energy (eV)	15.45 (adiabatic), (70) 15.7 ± 0.3 (electron impact), (79)
Energy threshold for double ionization (eV)	30.5 (photoionization), (63) 31.13 [Cl <sub>2</sub> <sup>2+</sup> ( <i>X</i> <sup>3</sup> Σ <sub>g</sub> <sup>+</sup> , ν = 0), threshold photoelectron spectroscopy], (73)
Energy threshold for ion-pair (Cl <sub>2</sub> + e → Cl <sup>+</sup> + Cl <sup>-</sup> + e) formation (eV)	11.9 ± 0.2, (79), (80)

<sup>a</sup>Thirteen values are listed by Christodoulides *et al.* (Ref. 74). If we exclude the lowest three as too low and the highest one as too high, the average of the other nine values is 2.45 eV which is within the combined quoted uncertainty of the averaged values.

<sup>b</sup>0-0 band.

<sup>c</sup>Onset.

<sup>d</sup>Band maximum.

## 2.2. Cl<sub>2</sub><sup>-</sup>

The Cl<sub>2</sub><sup>-</sup> negative ion consisting of Cl (<sup>1</sup>S<sub>0</sub>) and Cl (<sup>2</sup>P<sub>3/2,1/2</sub>) has four electronic states. These states can be arranged<sup>80,85-90</sup> in order of increasing energy as: <sup>2</sup>Σ<sub>u</sub><sup>+</sup>, <sup>2</sup>Π<sub>g</sub>, <sup>2</sup>Π<sub>u</sub>, and <sup>2</sup>Σ<sub>g</sub><sup>+</sup>. In Fig. 5(a) are shown the potential-energy curves for these states as calculated by Gilbert and Wahl<sup>85</sup> in the molecular-orbital self-consistent-field (SCF) approximation. In Fig. 5(b) similar curves are shown for the negative ion states <sup>2</sup>Σ<sub>u</sub><sup>+</sup>, <sup>2</sup>Π<sub>g,1/2</sub>, and <sup>2</sup>Σ<sub>g</sub><sup>+</sup> as they have been determined by Lee *et al.*<sup>89</sup> using their photodissociation cross section measurements for Cl<sub>2</sub><sup>-</sup> and adjusted potential-energy curves for Cl<sub>2</sub><sup>-</sup> based on those calculated by Gilbert and Wahl.<sup>85</sup> The numerical values shown in Fig. 5(b) for the various quantities are those used by Lee *et al.*, and the designations *a*<sub>1</sub> and *a*<sub>2</sub> refer, respectively, to the Cl (<sup>2</sup>P<sub>3/2</sub>) and Cl (<sup>2</sup>P<sub>1/2</sub>) asymptotic limits. Data for a number of physical parameters of the Cl<sub>2</sub><sup>-</sup> ion are given in Table 7.

## 2.3. Cl<sub>2</sub><sup>+</sup>

Photoelectron studies have shown<sup>70</sup> that the known states of the Cl<sub>2</sub><sup>+</sup> ion correspond to the ejection of one electron from one of the occupied orbitals of the outer orbital structure of the Cl<sub>2</sub> molecule [(σ<sub>g</sub>)<sup>2</sup>, (π<sub>u</sub>)<sup>4</sup>, (π<sub>g</sub>)<sup>4</sup>]. The <sup>2</sup>Σ<sub>g</sub><sup>+</sup> state of Cl<sub>2</sub><sup>+</sup> lies above the first dissociation limit (Ref. 70; Table 4). Optical emission from the excited *A* <sup>2</sup>Π<sub>u</sub> state of Cl<sub>2</sub><sup>+</sup> to the ground state *X*<sup>2</sup>Π<sub>g</sub> of Cl<sub>2</sub><sup>+</sup> is known,<sup>70</sup> but emission from the <sup>2</sup>Σ<sub>g</sub><sup>+</sup> state to the *A* <sup>2</sup>Π<sub>u</sub> state, although allowed by the selection rules, has not been observed, possibly because the <sup>2</sup>Σ<sub>g</sub><sup>+</sup> state is entirely predissociated.<sup>70</sup> The photodissociation spectra<sup>83</sup> of Cl<sub>2</sub><sup>+</sup> obtained in the range 1.80–2.55 eV showed vibrational structure indicating that the

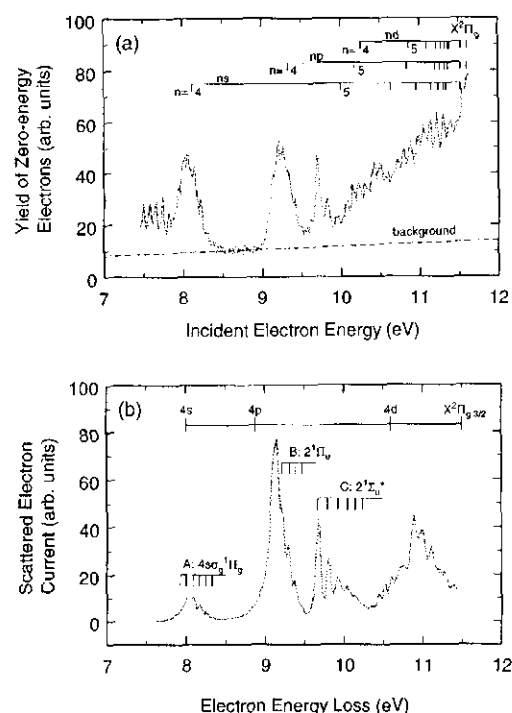


FIG. 4. (a) Threshold-electron excitation spectrum of Cl<sub>2</sub>. Here the electron energy is varied and the excitation spectrum reflects the relative probability of electrons having energy from about 7.5 eV to about 11.5 eV to lose all their energy in a collision with a Cl<sub>2</sub> molecule. The experiment detects only the "zero-energy electrons" (data of Jurca *et al.*, Ref. 43). (b) Electron energy-loss spectrum from Ref. 44 of Cl<sub>2</sub> between 7.5 and 11.5 eV using 200 eV incident electrons and a scattering angle of 3°. The scale above the spectrum shows the expected locations of Rydberg states due to excitations of a π<sub>g</sub>3p electron to 4s, 4p, and 4d orbitals.

TABLE 5. Comparison of the energies of the  $4s\sigma_g^2\pi_g$ ,  $4s\sigma_g^2\Pi_g$ ,  $2^3\Pi(1u)$ ,  $2^1\Pi_u$ ,  $2^1\Sigma_u^-$ , and  $^1\Pi_g(?)$  states of  $\text{Cl}_2$ . (The electronic configuration and term symbol are as given by Spence *et al.* in Ref. 44.)

Name/ Assignment	Vibrational level	Energy (eV) Energy-loss experiment (Ref. 44)	Energy (eV) Threshold-electron excitation experiment (Ref. 43)	Energy (eV) Photoabsorption experiments <sup>a</sup> (Ref. 82)
$4s\sigma_g^2\pi_g$	hot band		(7.83) <sup>b</sup>	
	$\nu=0$		7.91	
	$\nu=1$		7.99	
	$\nu=2$		(8.07)	
	$\nu=3$		(8.15)	
$4s\sigma_g^2\Pi_g$	hot band		(7.87)	
	$\nu=0$	7.939	(7.95)	
	$\nu=1$	8.019	8.03	
	$\nu=2$	8.101	8.11	
	$\nu=3$	8.186	8.19	
	$\nu=4$	8.270	8.27	
$2^3\Pi(1u)$	$\nu=0$		9.130	9.116
	$\nu=1$		9.190	9.193
$2^1\Pi_u$	$\nu=0$	9.225	9.250	9.230
	$\nu=1$	9.305	9.320	9.307
	$\nu=2$	9.381	9.395	9.384
	$\nu=3$	9.455	9.465	9.459
	$\nu=4$		9.530	9.534
$2^1\Sigma_u^-$	hot band		(9.620)	
	$\nu=0$	9.682	9.695 <sup>c</sup>	9.688
	$\nu=1$	9.815	9.815 <sup>c</sup>	9.807
	$\nu=2$	9.938	9.930 <sup>c</sup>	9.928
	$\nu=3$	10.046		10.028
$^1\Pi_g(?)$		10.141		
		9.900		
		9.966		
		10.025		

<sup>a</sup>Other photoabsorption data can be found in Refs. 54, 55, and 61.<sup>b</sup>Numbers in parentheses represent unresolved components.<sup>c</sup>May be due to the presence of a nearby triplet state.

dissociation of these ions involves a predissociation mechanism. Data on low-lying ionic states of  $\text{Cl}_2^+$  derived from optical emission and photoelectron spectroscopy investigations are listed in Table 8.

### 3. Electron Scattering for $\text{Cl}_2$

#### 3.1. Total Electron Scattering Cross Section, $\sigma_{\text{sc,t}}(\epsilon)$

Up until very recently, the only data on the total electron scattering cross section,  $\sigma_{\text{sc,t}}(\epsilon)$ , for  $\text{Cl}_2$  were the 1937 measurements of Fisk<sup>91</sup> which are very large (Fig. 6). The absence of reliable experimental data on  $\sigma_{\text{sc,t}}(\epsilon)$ , coupled with the lack of calculations of this quantity, led to two very recent measurements<sup>92,93</sup> of  $\sigma_{\text{sc,t}}(\epsilon)$  for  $\text{Cl}_2$ . The measurements of Gulley *et al.*<sup>92</sup> covered the energy range 0.02–9.5 eV and those of Cooper *et al.*<sup>93</sup> the energy range 0.3–23 eV. They are plotted in Fig. 6 and are seen to be very much smaller than the old measurements of Fisk. The uncertainties are estimated to be  $\pm 20\%$  in the measurements of Cooper *et al.* and  $\pm 8\%$  in the measurements of Gulley *et al.* While

the shape of  $\sigma_{\text{sc,t}}(\epsilon)$  as determined by the two recent measurements is similar, the magnitude of  $\sigma_{\text{sc,t}}(\epsilon)$  as measured by Cooper *et al.* is systematically lower than that measured by Gulley *et al.* at all but the lowest energies (below  $\sim 0.7$  eV). The magnitude of the data of Gulley *et al.* is consistent with the total rotational excitation cross sections (see Sec. 3.2). Cooper *et al.*<sup>93</sup> pointed out that the lower values of their  $\sigma_{\text{sc,t}}(\epsilon)$  measurements may in part result from the fact that electrons scattered into small angles ( $\leq 2^\circ$ ) with little energy loss are detected as “unscattered” in their apparatus, and since the measurements of Gote and Ehrhardt<sup>94</sup> on rotational scattering from  $\text{Cl}_2$  showed (see Sec. 3.5.1) that forward scattering is appreciable, this may be a significant cause of error in determining the value of  $\sigma_{\text{sc,t}}(\epsilon)$ .

In the energy range covered by the two recent experimental studies, the  $\sigma_{\text{sc,t}}(\epsilon)$  for  $\text{Cl}_2$  has two distinct features: It shows a minimum around 0.4 eV and structure that can be attributed to resonance-enhanced electron scattering. In connection with the latter, the peaks at low energies in the Gulley *et al.*<sup>92</sup> data and the bump (or unresolved peak) in the Cooper *et al.*<sup>93</sup> data at 2.5 eV correspond to the energy po-

TABLE 6. Transitions observed by Stubbs *et al.* in Ref. 84 in a high-resolution energy-loss experiment below the second ionization Cl<sub>2</sub><sup>+</sup>(Π<sub>u</sub>) onset

Name/Assignment	Vibrational level (ν)	Excitation energy (eV)
(5sσ <sub>g</sub> ) <sup>1</sup> Π <sub>g</sub>	0	9.803 <sup>a</sup>
	1	9.886
	2	9.962
	3	10.037
	4	10.121
F	—	9.162 <sup>b</sup>
	—	9.602 <sup>b</sup>
	—	9.743 <sup>b</sup>
	—	10.693 <sup>b</sup>
G(8pσ <sub>u</sub> ) <sup>1</sup> Π <sub>u</sub>	1	11.272
	2	11.356
	3	11.435
	4	11.513
	5	11.593
	6	11.670
a	0	10.937 <sup>c</sup>
	1	11.029
	2	11.105
	3	11.193
	4	11.275
	5	11.358
	6	11.437
	7	11.500
H	—	10.162 <sup>b</sup>
	—	10.230
b	—	10.196 <sup>c</sup>
	—	10.278
i	—	10.764 <sup>b</sup>
	—	11.157 <sup>b</sup>
	—	11.251 <sup>b</sup>
c	—	10.711 <sup>c</sup>
J(4sσ <sub>g</sub> ) <sup>1</sup> Σ <sub>g</sub> <sup>+</sup>	0	12.565 <sup>b</sup>
	1	12.605
	2	12.655
	3	12.699
	4	12.742
	5	12.785
	6	12.834
	7	12.880
	8	12.926
	9	12.971
K	0	12.953 <sup>b</sup>
	1	13.005
	2	13.063
	3	13.112
	4	13.170
L(5sσ <sub>g</sub> ) <sup>1</sup> Σ <sub>g</sub> <sup>+</sup>	5	13.224
	0	13.290 <sup>b</sup>
	1	13.335
	2	13.380
	3	13.429
	4	13.466
	5	13.516
	6	13.559
	7	13.599

TABLE 6. Transitions observed by Stubbs *et al.* in Ref. 84 in a high-resolution energy-loss experiment below the second ionization Cl<sub>2</sub><sup>+</sup>(Π<sub>u</sub>) onset—Continued

Name/Assignment	Vibrational level (ν)	Excitation energy (eV)
M(6sσ <sub>g</sub> ) <sup>1</sup> Σ <sub>g</sub> <sup>+</sup>	0	13.631 <sup>b</sup>
	1	13.674
	2	13.715
	3	13.757
	4	13.803
	5	13.844
	6	13.884
	7	13.934
	8	13.977
	9	14.023
d	10	14.066
	0	11.835 <sup>c</sup>
	1	11.915
	2	11.984
	3	12.055
e	4	12.127
	0	12.113 <sup>c</sup>
	1	12.167
	2	12.215
f	3	12.264
	4	12.319
	—	12.353 <sup>c</sup>
	—	12.402
	—	12.459
	—	12.488

<sup>a</sup>Symmetry forbidden.<sup>b</sup>Allowed.<sup>c</sup>Spin forbidden.

sitions of the negative ion states identified in electron attachment studies near 0 and 2.5 eV (see Sec. 6.1 and Refs. 87, 95, and 96). Similarly, the strong peak near 7 eV (Fig. 6) corresponds to the negative ion state (see Sec. 6.1 and Refs. 87, 95, 96) at 5.5 eV overlapping with the lowest electron-excited Feshbach resonance of Cl<sub>2</sub> at 7.5 eV which has been identified by Spence<sup>97</sup> in an electron transmission experiment. The spacing of the peaks and inflections in the data of Gulley *et al.* at 0.09, 0.14, and 0.2 eV may be associated with indirect (resonance enhanced) vibrational excitation of Cl<sub>2</sub> via the near 0 eV negative ion state of Cl<sub>2</sub><sup>−</sup> (see discussion in subsequent sections).

In view of the fact that the data of Gulley *et al.*<sup>92</sup> exhibit lower uncertainty, superior electron energy resolution, a more extensive energy range, and consistency with rotational excitation cross section data,<sup>94</sup> we performed a least squares fit to the measurements of Gulley *et al.* which we extended to 23 eV using the shape of the Cooper *et al.* cross section between 9.5 and 23 eV. The solid line in Fig. 6 is a plot of this least-squares fit, and represents our recommended  $\sigma_{\text{sc,t}}(\epsilon)$  for Cl<sub>2</sub>. Values taken from this curve are listed in Table 9.

### 3.2. Total Rotational Electron Scattering Cross Section, $\sigma_{\text{rot,t}}(\epsilon)$

Recently Gote and Ehrhardt<sup>94</sup> measured the absolute differential cross sections for electron-impact rotational excita-

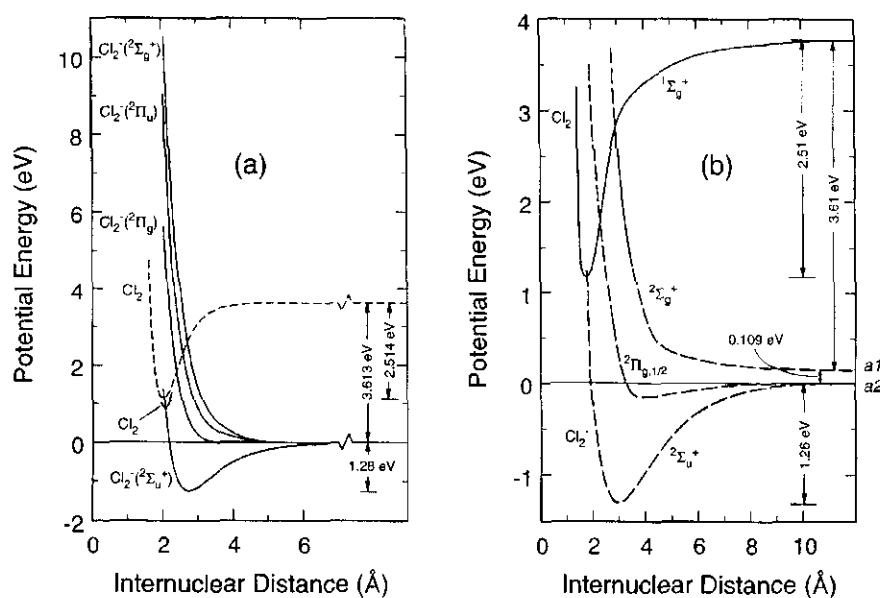


FIG. 5. (a) Potential-energy curves for the lowest four negative ion states ( $2\Sigma_g^+$ ,  $2\Pi_u$ ,  $2\Pi_g$ ,  $2\Sigma_u^+$ ) of  $\text{Cl}_2$  as calculated by Gilbert and Wahl in Ref. 85 using the molecular orbital self-consistent-field approximation. (The broken and solid curves for  $\text{Cl}_2$  are two different determinations by Gilbert and Wahl.) (b) Potential-energy curves for the states  $2\Sigma_g^+$ ,  $2\Pi_{u,1/2}$ , and  $2\Sigma_u^+$  of  $\text{Cl}_2^-$  determined by Lee *et al.* in Ref. 89 using their photodissociation cross section measurements for  $\text{Cl}_2$  and the potential-energy curves of Gilbert and Wahl in (a). The designations  $a1$  and  $a2$  represent, respectively, the asymptotic limits  $\text{Cl} ({}^2P_{3/2}) + \text{Cl}$  and  $\text{Cl} ({}^2P_{1/2}) + \text{Cl}$ .

tion of  $\text{Cl}_2$ . The measurements of Gote and Ehrhardt are listed in Table 10. These data allowed determination of the total cross section for rotational scattering (rotational elastic plus rotational inelastic) as a function of electron-impact energy,  $\sigma_{\text{rot},t}(\epsilon)$ . In Fig. 7 is plotted (open circles) the cross section  $\sigma_{\text{rot},t}(\epsilon)$  as determined (summed over all  $j$  values and all scattering angles) by Kutz and Meyer<sup>98</sup> from the data of

Gote and Ehrhardt (Table 10). Also plotted in Fig. 7 are the full-potential calculation results of Kutz and Meyer (solid circles) which extend over a much larger energy range. There is good agreement between theory and experiment in the overlapping energy range. It is interesting to observe that both the experimental measurements (Table 10) and the calculation<sup>98,99</sup> show a "rotational rainbow," i.e., a maxi-

TABLE 7. Some physical parameters for  $\text{Cl}_2$

Quantity	Value	Method/Reference
Dissociation energy, $D_e$	1.28 eV	Calculation, (85)
	1.24 eV	Calculation, (86)
Dissociation energy, $D_0$	1.26 eV	(45)
Equilibrium internuclear distance, $R_e$	2.65 Å	Calculation, (85)
	2.71 Å	Calculation, (86)
Fundamental vibrational frequency	0.0322 eV	Calculation, (85)
	0.0320 eV	Calculation, (86)
Transition energies <sup>a</sup>	3.46 eV ( $2\Sigma_g^+ \rightarrow 2\Sigma_u^+$ )	Calculation, (86)
	2.89 eV ( $2\Pi_u \rightarrow 2\Sigma_u^+$ )	
	1.78 eV ( $2\Pi_g \rightarrow 2\Sigma_u^+$ )	
Ionization energy of $\text{Cl}_2^b$	2.39 eV	(45)
Electron affinity of $\text{Cl}_2^b$	2.45 eV <sup>c</sup>	(74)
Negative ion states	~0.0 eV ( $2\Sigma_u^+$ )	From Table 15, Sec. 6
	2.5 eV ( $2\Pi_g$ )	
	5.5 eV ( $2\Pi_u$ )	
	7.5 eV ( $X^2\Pi_g$ )( $4s\sigma$ ) $^2[{}^2\Pi_{1/2,3/2}]$	

<sup>a</sup>At the ground state equilibrium bond length.

<sup>b</sup>These two quantities should be the same and have both adiabatic and vertical values. The vertical values normally exceed the adiabatic.

<sup>c</sup>Thirteen values are listed by Christodoulides *et al.* in Ref. 74. If we exclude the lowest three values listed in this reference as too low and the highest one as too high, the average of the remaining nine values is 2.45 eV. This value is within the combined quoted uncertainty of the values used in the averaging.

TABLE 8. Some parameters for Cl<sub>2</sub><sup>+</sup>

Parameter	Value	Reference
Equilibrium separation (Å)	1.890 ( <sup>2</sup> Π <sub>g,3/2</sub> )	72
Dissociation energy (eV)	3.99 ( <sup>2</sup> Π <sub>g</sub> )	67
	3.966 ( <sup>2</sup> Π <sub>g,3/2</sub> )	72
	3.876 ( <sup>2</sup> Π <sub>g,1/2</sub> )	72
	1.38 ( <sup>2</sup> Π <sub>u</sub> )	67
	1.41 ( <sup>2</sup> Π <sub>u,3/2</sub> )	72
	1.32 ( <sup>2</sup> Π <sub>u,1/2</sub> )	72
D <sub>0</sub>	3.95	45
Energy of fundamental vibration (eV)	0.08004 ( <sup>2</sup> Π <sub>g,3/2</sub> )	45
	~0.080 ( <sup>2</sup> Π <sub>g,3/2</sub> )	72
	0.07994 ( <sup>2</sup> Π <sub>g,1/2</sub> )	45
	~0.0459 ( <sup>2</sup> Π <sub>u,3/2</sub> )	72
	~0.0347 ( <sup>2</sup> Σ <sub>g</sub> <sup>+</sup> )	72
Energies to various ionic states (adiabatic/vertical) (eV)	See Table 4	

imum in the rotational excitation cross section at a relatively high  $\Delta j$ . The experimental and calculated values of  $\sigma_{\text{rot},l}(\epsilon)$  are compared in Fig. 7 with the suggested value of  $\sigma_{\text{sc},l}(\epsilon)$  (solid line in Fig. 6). From the figure it can be seen that  $\sigma_{\text{rot},l}(\epsilon)$  exceeds the total scattering cross section near 2 eV. This is physically impossible, but the discrepancy is well within the combined uncertainties of the two measurements. It is interesting to note the deep minimum shown by the calculated  $\sigma_{\text{rot},l}(\epsilon)$  that is also present in the measured  $\sigma_{\text{sc},l}(\epsilon)$ . Below this minimum the calculated values for  $\sigma_{\text{rot},l}(\epsilon)$  exceed the measured  $\sigma_{\text{sc},l}(\epsilon)$ .

In Fig. 8 are shown the various contributions to  $\sigma_{\text{rot},l}(\epsilon)$ , that is, the integrated (over angle) excitation cross sections,  $\sigma_{\text{rot},j=0}(\epsilon)$ , for  $j=0, 2, 4$ , and  $6$ . Clearly the rotationally elastic electron scattering channel ( $j=0$ ) dominates over all energies, especially below the minimum.

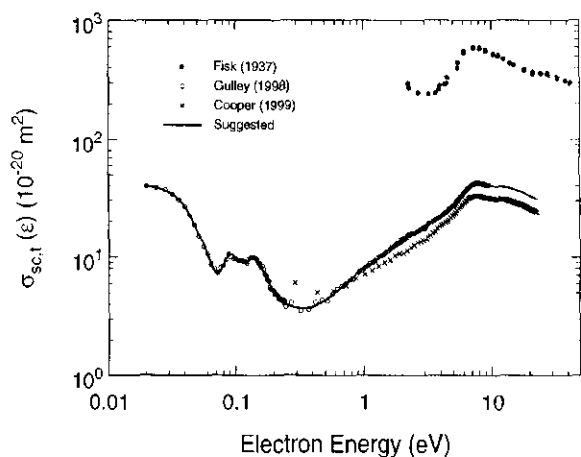


FIG. 6. Total electron scattering cross section,  $\sigma_{\text{sc},l}(\epsilon)$ , for Cl<sub>2</sub>: (●) Ref. 91; (○) Ref. 92; (×) Ref. 93; (—) recommended values.

TABLE 9. Recommended total electron scattering cross section,  $\sigma_{\text{sc},l}(\epsilon)$ , for Cl<sub>2</sub>

Electron energy (eV)	$\sigma_{\text{sc},l}(\epsilon)$ ( $10^{-20} \text{ m}^2$ )	Electron energy (eV)	$\sigma_{\text{sc},l}(\epsilon)$ ( $10^{-20} \text{ m}^2$ )
0.02	40.0	0.80	6.55
0.03	35.2	0.90	7.36
0.04	26.8	1.00	7.97
0.05	17.0	1.20	9.06
0.06	10.7	1.50	11.1
0.07	7.36	2.00	13.9
0.08	8.50	2.50	16.0
0.09	10.6	3.00	17.9
0.10	9.68	3.50	19.9
0.11	9.26	4.00	21.9
0.12	9.06	4.50	24.2
0.13	9.76	5.00	26.8
0.14	9.89	6.00	34.5
0.15	8.90	7.00	41.2
0.17	7.19	8.00	42.8
0.20	5.09	9.00	41.0
0.22	4.44	10.0	40.3
0.25	4.00	12.0	39.7
0.30	3.75	14.0	38.6
0.35	3.70	16.0	36.7
0.40	3.80	18.0	35.1
0.50	4.32	20.0	33.0
0.60	5.00	22.0	31.5
0.70	5.83	23.0	31.0

### 3.3. Total Elastic Electron Scattering Cross Section, $\sigma_{e,l}(\epsilon)$

There are no measurements of the total elastic electron scattering cross section,  $\sigma_{e,l}(\epsilon)$ , for Cl<sub>2</sub>. There have been, however, two calculations of this cross section, the old phase-shift calculation of Fisk,<sup>91</sup> and the more recent close-coupling calculation of Rescigno.<sup>100</sup> These results are shown in Fig. 9. The Fisk result is clearly unacceptable. We have also plotted in Fig. 9 the total rotational scattering cross section  $\sigma_{\text{rot},l}(\epsilon)$  as calculated by Kutz and Meyer.<sup>98</sup> Similarly, we have plotted the  $\sigma_{\text{rot},l}(\epsilon)$  determined by Kutz and Meyer from the measurements of Gote and Ehrhardt.<sup>94</sup> From an experimental perspective,  $\sigma_{\text{rot},l}(\epsilon)$  may be considered equivalent to  $\sigma_{e,l}(\epsilon)$  since  $\sigma_{\text{rot},l}(\epsilon)$  contains a large elastic component and the energy loss of rotational excitations is small ( $< 10^{-4}$  eV).<sup>98</sup> Clearly, the  $\sigma_{\text{rot},l}(\epsilon)$  based on the experimental data of Gote and Ehrhardt and the  $\sigma_{e,l}(\epsilon)$  calculated by Rescigno are similar in shape and comparable in magnitude over a large energy range. The solid line in Fig. 9 represents a fit to these two data sets, and values obtained from this fit are given in Table II as our suggested set of data for  $\sigma_{e,l}(\epsilon)$  for molecular chlorine.

### 3.4. Momentum Transfer Cross Section, $\sigma_m(\epsilon)$

There are no measurements of the momentum transfer cross section,  $\sigma_m(\epsilon)$ , for Cl<sub>2</sub>. The results of two Boltzmann-code analyses<sup>1,40</sup> are questionable, in part because they were hindered by the lack of accurate electron transport coefficient measurements. The two Boltzmann analyses used the early

TABLE 10. Differential rotational excitation cross sections for electron scattering from Cl<sub>2</sub> from Ref. 94. The rotationally summed cross sections,  $\sigma_{\text{rot,sum}}(\epsilon)$ , (in units of  $10^{-16} \text{ cm}^2 \text{ sr}^{-1}$ ) are also listed. The partial cross sections are listed as the percentage of their relative contribution to  $\sigma_{\text{rot,sum}}(\epsilon)$ 

Scattering angle	10°	20°	30°	40°	50°	60°	70°	80°	90°	100°	110°	120°	130°	140°	150°	160°
2 eV																
$j_i=0$	53.1	63.7	97.0	98.2	100	100	100	90.7	86.5	77.9	49.6	31.5	17.3	18.6	34.6	43.7
$j_i=2$	40.7	31.0	<1	<1	<1	<1	<1	4.1	12.1	17.6	50.4	67.6	82.7	70.8	65.3	54.9
$j_i=4$	6.1	3.4	<1	<1	<1	<1	<1	1.6	<1	4.2	<1	<1	<1	6.3	<1	<1
$j_i=6$	<1	<1	<1	<1	<1	<1	<1	3.5	<1	<1	<1	<1	<1	4.2	<1	<1
$j_i=8$	<1	<1	<1	1.8	<1	<1	<1	<1	1.4	<1	<1	<1	<1	<1	<1	<1
$\sigma_{\text{rot,sum}}(\epsilon)$	1.59	1.13	0.86	1.02	1.32	1.53	1.62	1.58	1.45	1.29	1.03	0.72	0.54	0.51	0.60	0.74
5 eV																
$j_i=0$	100	90.1	73.1	67.2	79.6	74.1	68.4	33.1	19.6	4.2	32.3	28.4	42.4	55.5	56.5	52.5
$j_i=2$	<1	6.1	24.6	32.8	14.3	14.4	17.0	55.0	68.5	74.7	64.2	70.3	40.9	36.3	24.4	31.6
$j_i=4$	<1	3.4	2.3	<1	3.7	9.0	7.9	11.4	7.7	21.1	<1	<1	13.2	6.7	16.8	15.8
$j_i=6$	<1	<1	<1	<1	<1	2.5	4.8	<1	4.1	<1	1.1	<1	2.1	1.5	2.4	<1
$j_i=8$	<1	<1	<1	<1	<1	<1	2.0	<1	<1	<1	1.1	<1	1.4	<1	<1	<1
$\sigma_{\text{rot,sum}}(\epsilon)$	5.82	4.58	3.35	2.98	2.54	2.02	1.72	1.51	1.38	1.18	1.12	1.20	1.15	1.16	1.23	1.29
10 eV																
$j_i=0$	97.1	100	97.3	76.3	72.2	43.7	31.8	29.2	27.3	18.3	<1	18.0	16.4	11.2	11.7	1.3
$j_i=2$	2.8	<1	<1	10.6	27.3	45.0	45.3	55.6	40.4	57.7	73.3	62.5	44.7	65.5	47.9	55.5
$j_i=4$	<1	<1	1.5	6.3	<1	<1	12.1	5.3	26.4	18.5	21.6	7.6	28.6	20.4	39.2	41.0
$j_i=6$	<1	<1	<1	6.1	<1	3.8	9.1	8.4	3.4	1.4	<1	7.2	6.7	<1	<1	<1
$j_i=8$	<1	<1	<1	<1	<1	5.8	<1	1.2	<1	1.4	<1	3.2	<1	1.1	<1	<1
$\sigma_{\text{rot,sum}}(\epsilon)$	21.28	14.39	7.49	4.62	1.74	1.41	1.08	0.96	0.84	0.86	0.87	0.98	1.08	1.57	2.06	3.12
20 eV																
$j_i=0$	100	94.9	79.2	83.9	58.1	39.0	80.4	62.6	28.8	14.5	24.0	15.0	18.9	11.0	12.6	<1
$j_i=2$	<1	<1	20.8	5.5	35.2	35.9	8.6	17.1	45.1	43.0	35.2	19.6	24.9	31.8	12.8	17.1
$j_i=4$	<1	1.4	<1	7.8	3.7	16.4	7.0	13.4	26.1	33.5	38.5	55.7	39.5	57.2	51.0	62.3
$j_i=6$	<1	2.3	<1	2.7	3.0	5.8	4.0	2.7	<1	5.2	2.2	9.7	13.6	<1	17.5	16.3
$j_i=8$	<1	1.2	<1	<1	<1	3.1	<1	4.2	<1	3.8	<1	<1	3.1	<1	6.1	4.3
$\sigma_{\text{rot,sum}}(\epsilon)$	31.61	19.32	9.41	3.97	1.83	1.32	0.96	0.75	0.80	0.89	0.89	0.83	0.65	0.55	0.57	0.89
30 eV																
$j_i=0$	99.8	87.3	68.1	30.6	25.2	<1	<1	<1	<1	<1	<1	<1	2.1	<1	6.6	2.8
$j_i=2$	<1	12.2	24.1	69.4	51.5	83.0	68.7	54.3	32.1	26.1	17.1	12.4	16.2	11.1	15.5	4.5
$j_i=4$	<1	<1	6.1	<1	18.2	10.6	25.8	41.1	52.5	69.1	58.1	58.2	48.5	51.5	51.7	70.9
$j_i=6$	<1	<1	1.7	<1	<1	6.4	3.2	<1	13.9	3.9	23.9	28.3	29.6	34.4	22.6	21.8
$j_i=8$	<1	<1	<1	<1	<1	<1	<1	<1	1.4	<1	<1	<1	<1	<1	<1	<1
$\sigma_{\text{rot,sum}}(\epsilon)$	31.84	15.90	5.86	2.26	1.18	0.69	0.41	0.43	0.62	0.71	0.59	0.39	0.22	0.11	0.11	0.20
50 eV																
$j_i=0$	95.2	84.6	50.8	3.6	16.7	13.5	<1	8.7	<1	3.6	2.5	5.8	<1	10.5	8.6	4.9
$j_i=2$	3.3	11.9	31.4	81.4	69.7	69.3	46.9	21.8	15.8	10.0	15.3	13.3	17.3	12.0	10.1	8.8
$j_i=4$	1.4	3.5	14.4	12.3	13.6	<1	35.5	54.6	52.8	61.7	53.7	43.7	48.6	31.4	22.9	28.4
$j_i=6$	<1	<1	3.3	2.8	<1	13.2	4.7	11.0	28.1	21.3	27.4	36.2	32.2	29.8	28.2	35.3
$j_i=8$	<1	<1	<1	<1	<1	<1	1.3	<1	3.1	3.4	<1	<1	<1	15.4	21.5	22.5
$\sigma_{\text{rot,sum}}(\epsilon)$	28.72	8.61	2.41	1.01	0.51	0.20	0.16	0.30	0.44	0.49	0.44	0.29	0.18	0.15	0.33	0.69
100 eV																
$j_i=0$	99.6	76.3	17.5	15.7	20.5	26.5	<1	8.1	6.3	7.0	<1	13.9	6.0	<1	<1	<1
$j_i=2$	<1	23.5	72.1	55.4	50.4	31.8	19.1	23.8	15.3	14.3	7.1	18.4	6.7	5.3	<1	<1
$j_i=4$	<1	<1	7.0	23.8	29.1	22.7	50.6	39.1	45.2	34.9	30.6	15.9	7.6	17.1	7.0	3.0
$j_i=6$	<1	<1	3.4	5.1	<1	10.3	24.4	24.0	30.2	29.9	37.7	12.3	23.5	31.3	34.5	30.6
$j_i=8$	<1	<1	<1	<1	<1	6.5	5.7	3.2	1.9	11.5	20.1	19.8	30.2	33.0	42.0	41.9
$j_i=10$	<1	<1	<1	<1	<1	1.7	<1	<1	<1	<1	4.2	18.1	20.6	12.9	16.2	24.0
$j_i=12$	<1	<1	<1	<1	<1	<1	<1	<1	<1	<1	<1	1.7	4.4	<1	<1	<1
$\sigma_{\text{rot,sum}}(\epsilon)$	15.70	3.50	0.91	0.42	0.19	0.13	0.15	0.20	0.19	0.15	0.08	0.04	0.07	0.15	0.59	0.91

TABLE 10. Differential rotational excitation cross sections for electron scattering from Cl<sub>2</sub> from Ref. 94. The rotationally summed cross sections,  $\sigma_{\text{rot,sum}}(\epsilon)$ , (in units of  $10^{-16} \text{ cm}^2 \text{ sr}^{-1}$ ) are also listed. The partial cross sections are listed as the percentage of their relative contribution to  $\sigma_{\text{rot,sum}}(\epsilon)$  —Continued

Scattering angle	10°	20°	30°	40°	50°	60°	70°	80°	90°	100°	110°	120°	130°	140°	150°	160°
200 eV																
$j_i=0$	9.4	14.9	24.3	13.7	<1	3.6	<1	6.3	<1	<1	<1	<1	<1	<1	<1	<1
$j_i=2$	5.6	85.1	52.0	30.9	19.0	12.2	2.0	6.7	<1	13.0	<1	<1	<1	<1	<1	<1
$j_i=4$	<1	<1	21.6	42.5	39.3	25.5	23.9	28.5	33.1	6.2	<1	1.1	<1	<1	<1	<1
$j_i=6$	<1	<1	1.1	8.9	34.2	39.7	42.5	34.3	47.6	11.3	32.5	23.7	5.3	<1	2.6	<1
$j_i=8$	<1	<1	<1	1.7	6.9	17.6	28.6	14.2	13.3	23.9	33.6	31.1	21.0	20.1	17.5	15.7
$j_i=10$	<1	<1	<1	<1	<1	<1	1.4	7.2	3.6	24.8	20.4	30.9	29.7	28.2	25.1	25.0
$j_i=12$	<1	<1	<1	<1	<1	<1	<1	2.4	<1	13.0	13.2	13.2	30.7	40.1	35.3	42.8
$j_i=14$	<1	<1	<1	<1	<1	<1	<1	<1	<1	7.6	<1	<1	7.0	9.5	15.4	15.3
$\sigma_{\text{rot,sum}}(\epsilon)$	12.92	2.52	0.83	0.36	0.23	0.19	0.13	0.09	0.06	0.04	0.03	0.05	0.11	0.24	0.34	0.58

data of Bailey and Healey<sup>101</sup> for the electron drift velocity and the characteristic energy for a 20%Cl<sub>2</sub>:80%He mixture by volume, and the ionization and attachment coefficients of Božin and Goodyear.<sup>102</sup> In Fig. 10 the Boltzmann-calculation results are compared with the close-coupling calculation result of Rescigno.<sup>100</sup> These cross sections differ substantially, especially at low energies, stressing the need for a direct measurement of  $\sigma_m(\epsilon)$ . They also indicate the need for measurements of electron transport coefficients that would allow a more reliable Boltzmann-code analysis. The need for such measurements is made more apparent because the cross sections of Rogoff *et al.*<sup>1</sup> have been used commonly in various discharge models. Of the available values for  $\sigma_m(\epsilon)$ , the *ab initio* calculations of Rescigno<sup>100</sup> are preferred because they are not model dependent and because of the agreement between Rescigno's calculations and measured values of  $\sigma_{\text{e},\text{t}}(\epsilon)$  and  $\sigma_{\text{diss,neut},\text{t}}(\epsilon)$  (see Secs. 3.3 and 5, respectively).

### 3.5. Inelastic Electron Scattering Cross Section, $\sigma_{\text{inel}}(\epsilon)$

#### 3.5.1. Rotational Excitation Cross Section, $\sigma_{\text{rot}}(\epsilon)$

Rotational excitation of Cl<sub>2</sub> by electron impact can be either direct or indirect via the formation of short-lived negative ion states. The experimental measurements of Gote and Ehrhardt<sup>94</sup> on the absolute differential cross sections for rotational excitation of Cl<sub>2</sub> by electron impact at energies between 2 and 200 eV and in the angular range 10°–160°, clearly show (Table 10) that rotational excitation of the Cl<sub>2</sub> molecule in its vibrational and electronic ground states by slow electrons is an efficient electron scattering process. Cross sections exceeding  $10^{-16} \text{ cm}^2$  have been measured. As discussed earlier in this section, Gote and Ehrhardt reported rotationally summed cross sections and partial rotational excitation cross sections (i.e., cross sections for excitation to various rotational levels) as the percentage of their relative

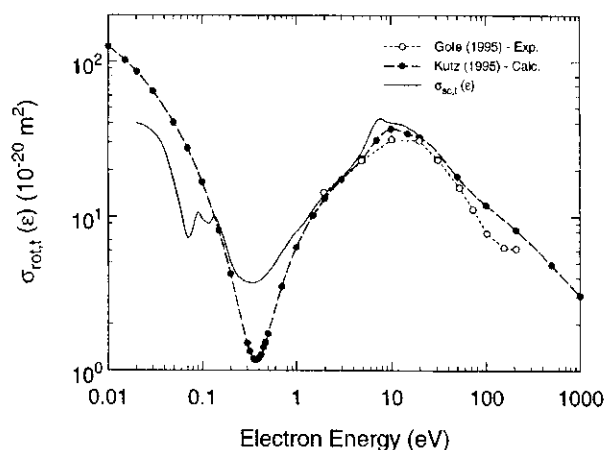


FIG. 7. Total cross section for rotational scattering,  $\sigma_{\text{rot,t}}(\epsilon)$ , for Cl<sub>2</sub> as reported by Kutz and Meyer (Ref. 98): (○) values calculated by Kutz and Meyer from the measurements of Gote and Ehrhardt (Ref. 94); (●) *ab initio* calculations (Ref. 98). For comparison the suggested  $\sigma_{\text{sc,t}}(\epsilon)$  from Table 9 (solid line in Fig. 6) is also plotted.

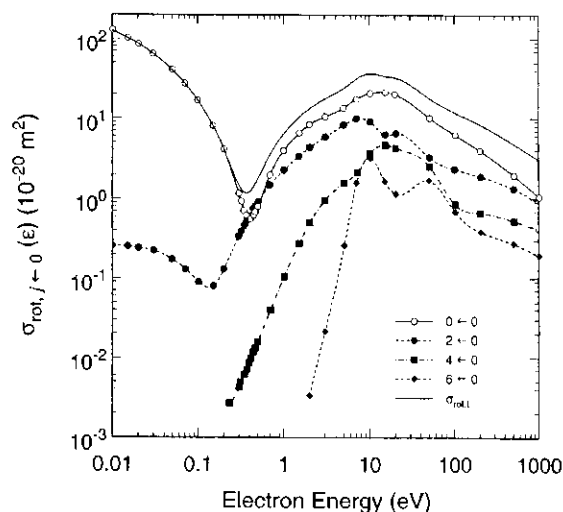


FIG. 8. Integrated (over angle) excitation cross sections,  $\sigma_{\text{rot},j \rightarrow 0}(\epsilon)$ , for Cl<sub>2</sub> from Ref. 98 for the rotational excitation channels (○) 0 ← 0, (●) 2 ← 0, (■) 4 ← 0, (◆) 6 ← 0 of Cl<sub>2</sub>. Also shown for comparison is  $\sigma_{\text{rot,t}}(\epsilon)$ .

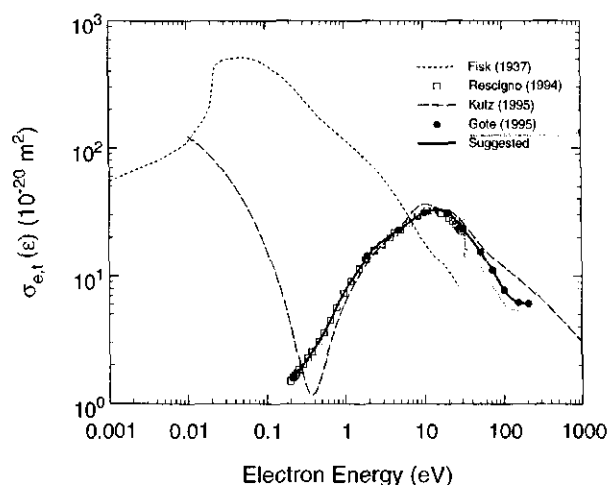


FIG. 9. Total elastic electron scattering cross section,  $\sigma_{el}(E)$ , for  $\text{Cl}_2$ : (---) calculated total elastic electron scattering cross section,  $\sigma_{el}(E)$  from Ref. 91; (●) measured  $\sigma_{rot}(E)$  [data of Ref. 98 based on measurements by Ref. 94]; (---) calculated total rotational electron scattering cross section,  $\sigma_{rot}(E)$  from Ref. 98; (□) calculated total elastic electron scattering cross section,  $\sigma_{el}(E)$  from Ref. 100; (—) suggested values.

contribution to the rotationally summed cross sections. The cross sections in the forward direction belong mostly to rotationally elastic scattering. Above a scattering angle of about  $30^\circ$ , the scattering is dominated by rotationally inelastic processes. Kutz and Meyer's<sup>98</sup> close-coupling calculation of the rotational excitation of  $\text{Cl}_2$  by electron impact over the energy range of 0.01–1000 eV, neglecting vibrational, resonant, and electronic excitation, shows two different excitation mechanisms, the importance of each depends on elec-

TABLE 11. Suggested total elastic electron scattering cross section,  $\sigma_{el}(E)$ , for  $\text{Cl}_2$

Electron energy (eV)	$\sigma_{el}(E)$ ( $10^{-20} \text{ m}^2$ )	Electron energy (eV)	$\sigma_{el}(E)$ ( $10^{-20} \text{ m}^2$ )
0.20	1.50	7.00	27.1
0.22	1.64	8.00	28.8
0.25	1.82	9.00	30.2
0.30	2.11	10.0	31.3
0.35	2.38	12.0	32.7
0.40	2.66	14.0	33.1
0.50	3.30	16.0	32.9
0.60	4.10	18.0	32.1
0.70	4.98	20.0	30.9
0.80	5.99	22.0	29.5
0.90	6.89	23.0	28.8
1.00	7.77	25.0	27.3
1.20	9.34	30.0	24.0
1.50	11.4	40.0	19.4
2.00	14.6	50.0	16.1
2.50	16.9	60.0	13.6
3.00	18.6	70.0	11.6
3.50	19.9	80.0	10.1
4.00	21.1	90.0	8.87
4.50	22.1	100.0	7.99
5.00	23.2	150.0	6.31
6.00	25.2	200.0	6.16

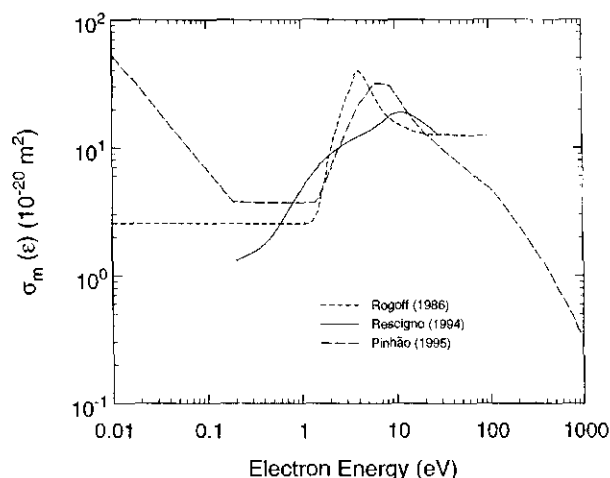


FIG. 10. Calculated momentum transfer cross sections,  $\sigma_m(E)$ , for  $\text{Cl}_2$ : (---) Ref. 1; (—) Ref. 100; (---) Ref. 40.

tron energy. At low electron energies only a few rotational quanta are exchanged and the differential cross section decreases exponentially with  $\Delta j$ . At high electron energies the excitation spectrum shows a rotational rainbow, i.e., the differential cross section has a maximum at a relatively high  $\Delta j$ . The location of the maximum depends on electron en-

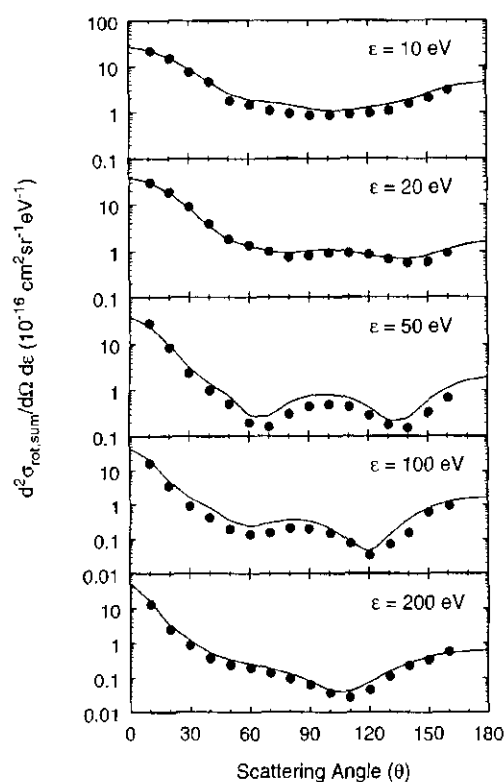


FIG. 11. Comparison of experimental and calculated rotationally summed differential electron scattering cross sections  $d^2\sigma_{rot,sum}/d\Omega dE$ , for  $\text{Cl}_2$  at incident electron energies of 10, 20, 50, 100, and 200 eV from Gote and Ehrhardt (Ref. 94): (●) experimental data from Ref. 94; (—) close-coupling calculation results from Ref. 98.



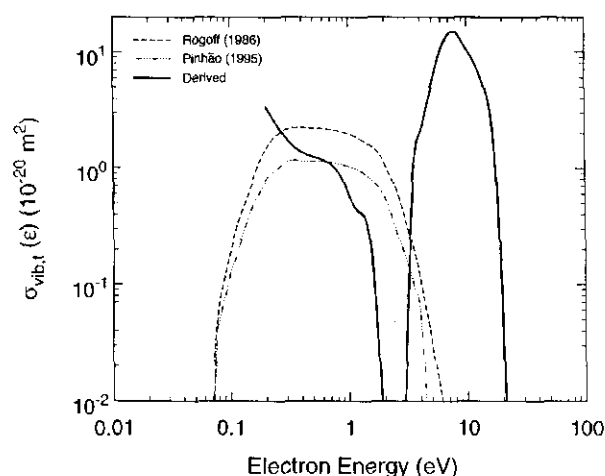


FIG. 12 Total vibrational excitation cross section,  $\sigma_{\text{vib},t}(\epsilon)$ , for Cl<sub>2</sub>. Results of Boltzmann-code analyses: (---) Ref. 1; (-·-·-) Ref. 40. Estimate of  $\sigma_{\text{vib},t}(\epsilon)$  derived from present analysis described in text (—).

ergy and scattering angle. For the observation of a rotational rainbow not only high electron energies, but also high scattering angles are needed. The scattering angle can only be large when, classically speaking, the impact parameter is small, i.e., when the impacting electron penetrates the electron cloud and comes near the core of the molecule. At low incident energy, the electron essentially interacts with the long-range parts of the potential of the target. For homonuclear molecules these are the quadrupole and polarization potentials.<sup>98</sup> In their calculation Kutz and Meyer<sup>98</sup> used the polarizabilities  $\alpha_0 = 24.42$  a.u. and  $\alpha_2 = 16.293$  a.u. (1 a.u. =  $0.1482 \times 10^{-24}$  cm<sup>3</sup>).

In Fig. 11 are compared the close-coupling rotationally summed differential electron scattering cross sections calculated by Kutz and Meyer<sup>98</sup> (solid line) with the experimental values of Gote and Ehrhardt<sup>94</sup> for various incident electron energies. The agreement is good adding credence to the calculation and the underlying assumptions.

The full-model potential calculation results of Kutz and Meyer for the integrated excitation cross section and for the first four rotational excitation channels are shown in Fig. 8. The total scattering cross section (for all scattering channels) has a minimum at about 0.5 eV which was found to be very sensitive to small changes of the potential. The integrated cross section decreases with the final rotational state  $j$ . At low scattering angles and electron energies only a few rotational quanta are transferred ("normal" excitation mechanism), whereas at high scattering angles and electron energies many rotational quanta can be exchanged (rotational rainbow mechanism).

Another calculation of rotational excitation of Cl<sub>2</sub> was performed by Ernesti *et al.*<sup>99</sup> within the two-center Coulomb-scattering approximation. This study predicted a rainbow scattering pattern which is consistent both with the close-coupling result and with the experimental data.

### 3.5.2. Total Vibrational Excitation Cross Section, $\sigma_{\text{vib},t}(\epsilon)$

There are no experimentally determined total vibrational excitation cross sections,  $\sigma_{\text{vib},t}(\epsilon)$ , for Cl<sub>2</sub>. There are only the results of two Boltzmann-code calculations,<sup>1,40</sup> based upon limited experimental data. These results are compared in Fig. 12. Their assumed energy dependence is similar (although there is no experimental evidence to support such a shape), and their magnitudes differ. Thus, there is a need for a direct measurement of the vibrational excitation cross section for this molecule and there is also a need for more and better electron transport data to enhance the usefulness of the  $\sigma_{\text{vib},t}(\epsilon)$  calculated from Boltzmann codes.

Vibrational excitation cross sections are important in efforts to model plasma reactors due to their large effect on the electron energy distribution function (see, for example, Refs. 103 and 104). For this reason, we have attempted to deduce a rough estimate of  $\sigma_{\text{vib},t}(\epsilon)$  from the available cross sections for other processes. We assumed the suggested values for  $\sigma_{\text{sc},t}(\epsilon)$  (Sec. 3.1, Fig. 6),  $\sigma_{\text{e},t}(\epsilon)$  (Sec. 3.3, Fig. 9),  $\sigma_{\text{i},t}(\epsilon)$  (to be discussed in Sec. 4.1, Fig. 14),  $\sigma_{\text{diss,neut},t}(\epsilon)$  (to be discussed in Sec. 5, Fig. 16), and  $\sigma_{\text{da},t}(\epsilon)$  (to be discussed in Sec. 6.1, Fig. 17), and took the difference

$$\sigma_{\text{sc},t}(\epsilon) - [\sigma_{\text{e},t}(\epsilon) + \sigma_{\text{i},t}(\epsilon) + \sigma_{\text{diss,neut},t}(\epsilon) + \sigma_{\text{da},t}(\epsilon)] \\ \approx \sigma_{\text{vib},t}(\epsilon) \approx \sigma_{\text{vib,indir}}(\epsilon) \quad (1)$$

to be a measure of  $\sigma_{\text{vib},t}(\epsilon)$ . Since direct vibrational excitation for a homopolar molecule such as Cl<sub>2</sub> is expected to be small,<sup>105,106</sup>  $\sigma_{\text{vib},t}(\epsilon)$  may be taken, in this case, to be the cross section for indirect (resonance enhanced) vibrational excitation,  $\sigma_{\text{vib,indir}}(\epsilon)$ , of the Cl<sub>2</sub> molecule via its temporary negative ion states. Values of  $\sigma_{\text{vib,indir}}(\epsilon)$  derived in this way are shown in Fig. 12 (solid line), where the two Boltzmann computed values of  $\sigma_{\text{vib},t}(\epsilon)$  are also shown. The  $\sigma_{\text{vib,indir}}(\epsilon)$  deduced in this study bears no similarity to the computed  $\sigma_{\text{vib},t}(\epsilon)$ . In spite of the large uncertainty involved in the derivation of  $\sigma_{\text{vib,indir}}(\epsilon)$ , this deduced cross section shows that the indirect vibrational excitation cross section of Cl<sub>2</sub> is very large. In the absence of any direct measurements of  $\sigma_{\text{vib},t}(\epsilon)$ , the present derived cross section  $\sigma_{\text{vib,indir}}(\epsilon)$  is preferred to those provided by the Boltzmann codes.

### 3.5.3. Electronic Excitation Cross Sections, $\sigma_{\text{elec}}(\epsilon)$

There have been no measurements of the cross sections for electron-impact excitation of any of the electronic states of Cl<sub>2</sub>. However, there have been three calculations of cross sections for some of the lowest excited electronic states of Cl<sub>2</sub>. Rogoff *et al.*<sup>1</sup> report cross sections for electron impact excitation of the electronic states  $^3\Pi_u$ ,  $^1\Pi_u$ , and the sum  $2\ ^1\Pi_u + 2\ ^1\Sigma_u^+$  that are derived from a Boltzmann-code analysis. Another Boltzmann-code calculation by Pinhão and Chouki<sup>40</sup> report cross sections for electronic excitation of  $^3\Pi_u + ^1\Pi_u$ ,  $^3\Sigma_u + ^3\Pi_g + ^1\Pi_g$ , and  $2\ ^1\Pi_u + 2\ ^1\Sigma_u^+$ . Also, Rescigno<sup>100</sup> performed close-coupling calculations using the complex Kohn variational method and reported excitation cross sections for  $^3\Pi_u$ ,  $^1\Pi_u$ ,  $^3\Pi_g$ ,  $^1\Pi_g$ , and  $^3\Sigma_u^+$ . Rescigno refers to the cross sections he calculated for these five states

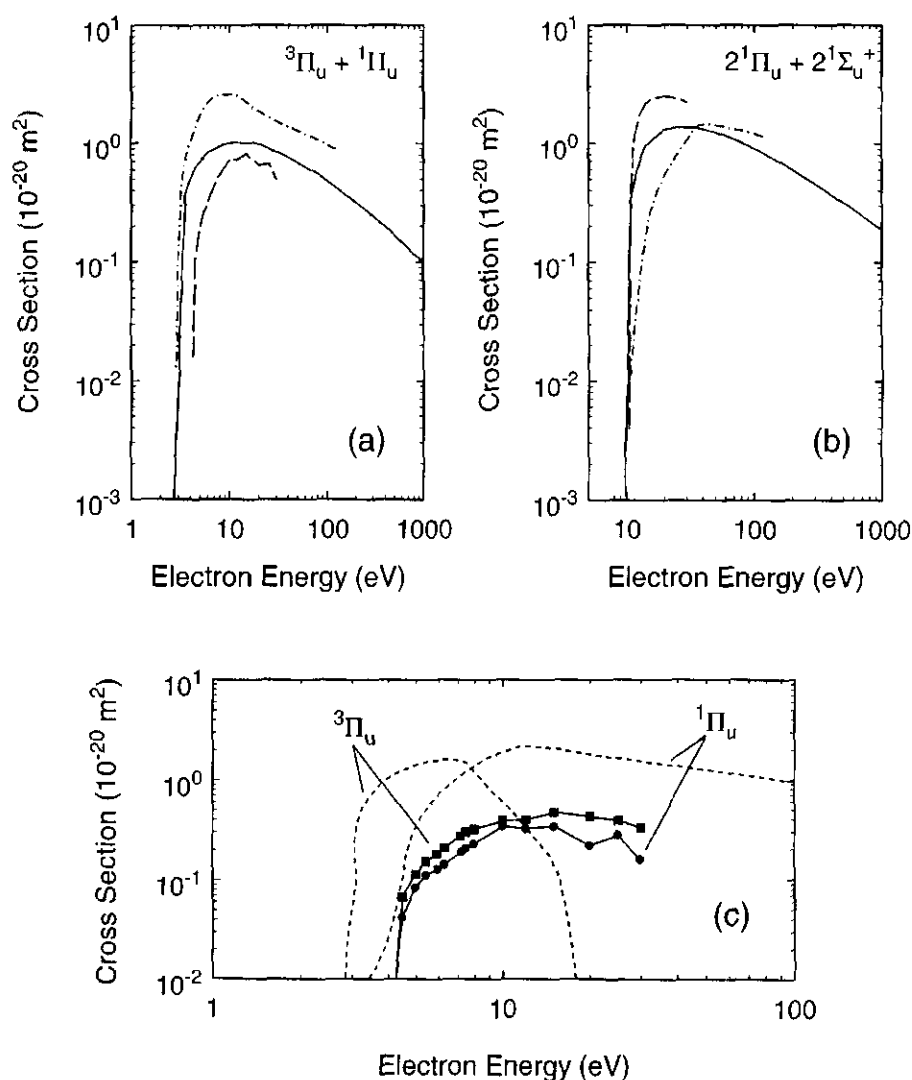


FIG. 13. Comparison of calculated cross sections for electronic excitation,  $\sigma_{\text{elec}}(\epsilon)$ , of Cl<sub>2</sub>. (a) Excitation of  $^3\Pi_u + ^1\Pi_u$ : (---) Ref. 1; (—) Ref. 40; (- -) Ref. 100. (b) Excitation of  $2\ ^1\Pi_u + 2\ ^1\Sigma_u^+$ : (---) Ref. 1; (—) Ref. 40; (- -) Ref. 100. (c) Excitation of  $^3\Pi_u$  and  $^1\Pi_u$ : (---) Ref. 1; (—) Ref. 100.

indiscriminately as cross sections for excitation or as cross sections for dissociation, the implication being that all excitations to these states lead to dissociation. This would be consistent with the potential energy curves for the excited states calculated by Peyerimhoff and Buenker<sup>46</sup> (Fig. 1). He also calculated the total cross sections for electron-impact excitation of the  $^1\Pi_u$  and  $^1\Sigma_u$  Rydberg states of Cl<sub>2</sub> using the Born-dipole approximation and found that the Born-dipole cross sections far exceeded those he calculated using the close-coupling method.

Since the excitation cross sections of Rogoff *et al.*<sup>1</sup> have been used in various plasma models, we compared them with the results of the other two calculations in the few cases where this is possible. Thus, in Fig. 13(a) the cross sections estimated by the three studies for  $^3\Pi_u + ^1\Pi_u$  are compared. In Fig. 13(b) a similar comparison is made for  $2\ ^1\Pi_u + 2\ ^1\Sigma_u^+$ . In Fig. 13(c) the cross sections of Rogoff *et al.*<sup>1</sup> and of Rescigno<sup>100</sup> for electron-impact excitation of the electronic

states  $^3\Pi_u$  and  $^1\Pi_u$  are compared. The vertical excitation energies of  $^3\Pi_u$  and  $^1\Pi_u$  are, respectively, 3.31 and ~4.05 eV (see Table 2). The agreement between the Boltzmann-code-deduced electronic excitation cross sections and those of Rescigno is poor. Clearly more work, both experimental and computational, is indicated.

## 4. Electron Impact Ionization for Cl<sub>2</sub>

### 4.1. Total Ionization Cross Section, $\sigma_{\text{it}}(\epsilon)$

In Fig. 14 are compared the available data on the electron-impact total ionization cross section,  $\sigma_{\text{it}}(\epsilon)$ , of Cl<sub>2</sub>. These include the measurements by Center and Mandl,<sup>107</sup> Kurepa and Belić,<sup>95</sup> Stevie and Vasile,<sup>108</sup> and Srivastava and Boivin.<sup>109</sup> The Center and Mandl cross section measurements were made using argon as the calibrant gas, and normalizing to the ionization cross section for Ar of Rapp and

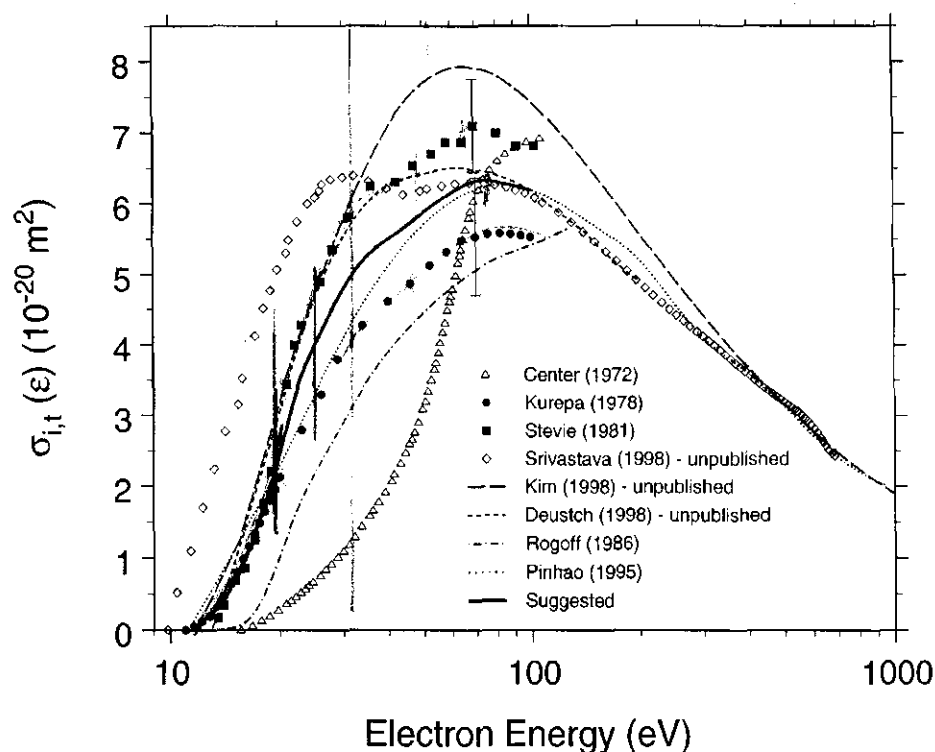


FIG. 14 Electron-impact total ionization cross section,  $\sigma_{i,t}(\epsilon)$ , for Cl<sub>2</sub>: ( $\Delta$ ) Ref. 107; ( $\bullet$ ) Ref. 95; ( $\blacksquare$ ) Ref. 108; ( $\diamond$ ) Ref. 109; (—) Ref. 110; (- - -) Ref. 111; (- · -) Ref. 1; (···) Ref. 40; (—) suggested.

Englander-Golden.<sup>112</sup> The stated uncertainty of these measurements is  $\pm 15\%$ . Kurepa and Belić's cross section measurements are absolute. They were made in the energy range of 10–100 eV and have a reported relative error of  $\pm 20\%$ . Below  $\sim 50$  eV they are higher than the values obtained by Center and Mandl. The third set of measurements were made by Stevie and Vasile<sup>108</sup> in the energy range 12–100 eV using a mass spectrometer and a modulated molecular beam. These determinations of  $\sigma_{i,t}(\epsilon)$  were made relative to those of the three calibrant gases Ar, O<sub>2</sub>, and Kr for which they used the respective data of Rapp and Englander-Golden.<sup>112</sup> The values plotted in the figure are the averages of the data using each of the three calibrant gases. The authors indicated an error bar in their data for 70 eV as shown in Fig. 14. Their uncertainties are approximately  $\pm 20\%$ . Their measurements agree with those of Kurepa and Belić<sup>95</sup> near the threshold, but they are considerably higher for energies greater than  $\sim 15$  eV. Clearly these three sets of data differ not only in magnitude, but also in the measured energy dependence of  $\sigma_{i,t}(\epsilon)$ . The more recent unpublished relative measurements of Srivastava<sup>109</sup> are also shown in Fig. 14. These cover a broader energy range, from threshold to 700 eV, and were arbitrarily normalized to the 70 eV point of the "suggested" curve discussed later and shown by the solid line in Fig. 14. Interestingly, the cross section of Srivastava shows structure

near 25 eV which, although not as evident, is nonetheless indicated by some of the other measurements, and might be due to autoionization.

In Fig. 14 are also shown the results of two recent unpublished calculations, one by Kim<sup>110</sup> and another by Deutsch *et al.*<sup>111</sup> The results of both of these calculations are in reasonable agreement with the measurements of Kurepa and

TABLE 12. Suggested total ionization cross section,  $\sigma_{i,t}(\epsilon)$ , for Cl<sub>2</sub>

Electron energy (eV)	$\sigma_{i,t}(\epsilon)$ ( $10^{-20}$ m <sup>2</sup> )	Electron energy (eV)	$\sigma_{i,t}(\epsilon)$ ( $10^{-20}$ m <sup>2</sup> )
11.5	0.03	35	5.26
12	0.11	40	5.49
13	0.25	45	5.68
14	0.43	50	5.87
15	0.69	55	6.03
16	0.99	60	6.15
17	1.32	65	6.25
18	1.67	70	6.32
19	2.06	75	6.33
20	2.47	80	6.31
22	3.25	85	6.28
24	3.79	90	6.25
26	4.17	95	6.22
28	4.51	100	6.19
30	4.80		

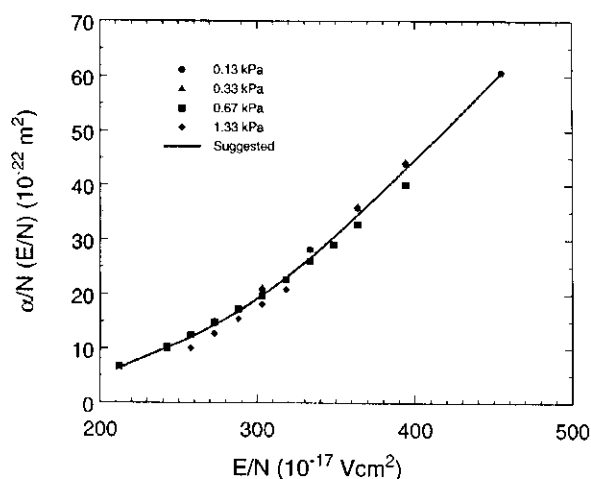


FIG. 15. Density-reduced electron-impact ionization coefficient,  $\alpha/N(E/N)$ , for  $\text{Cl}_2$  at various gas pressures. Data from Ref. 102. The solid line is a least-squares fit to all the data points and represents the suggested values for  $\alpha/N(E/N)$ .

Belic<sup>95</sup> and Stevie and Vasile.<sup>108</sup> The calculation of Kim includes multiple ionization but not autoionization.

At the present time we have averaged the measured values of Kurepa and Belic<sup>95</sup> and Stevie and Vasile,<sup>108</sup> even though the differences in their magnitudes exceed their combined uncertainties, and take this to be our suggested value for the  $\sigma_{\text{ion}}(\epsilon)$  of  $\text{Cl}_2$ . We have not included the values of Center and Mandl<sup>107</sup> due to the obviously inconsistent shape of their cross section when compared to the other<sup>95,108</sup> measured values. These average values are shown by the bold line in Fig. 14 (Table 12).

The model-dependent total ionization cross section of Rogoff *et al.*,<sup>1</sup> and Pinhao and Chouki<sup>40</sup> deduced from modeling of chlorine discharges are also plotted in Fig. 14. While the Pinhao and Chouki cross section is in general agreement with the most reliable measurements, that of Rogoff *et al.* is not. However, such a comparison is biased by the input cross section assumed by each calculation.

Threshold ionization energies leaving the  $\text{Cl}_2^+$  ion in various states of excitation have been given in Table 4. Also listed in Table 4 are the values for the threshold energy for

TABLE 13. Suggested density-reduced electron-impact ionization coefficient,  $\alpha/N(E/N)$ , for  $\text{Cl}_2$  (based on measurements of Božin and Goodyear from Ref. 102)

$E/N$ ( $10^{-17} \text{ V cm}^2$ )	$\alpha/N(E/N)$ ( $10^{-22} \text{ m}^2$ )	$E/N$ ( $10^{-17} \text{ V cm}^2$ )	$\alpha/N(E/N)$ ( $10^{-22} \text{ m}^2$ )
213	6.45	340	28.2
220	7.34	360	33.4
240	9.82	380	39.0
260	12.4	400	44.7
280	15.5	420	50.4
300	19.2	440	56.2
320	23.4	450	59.1

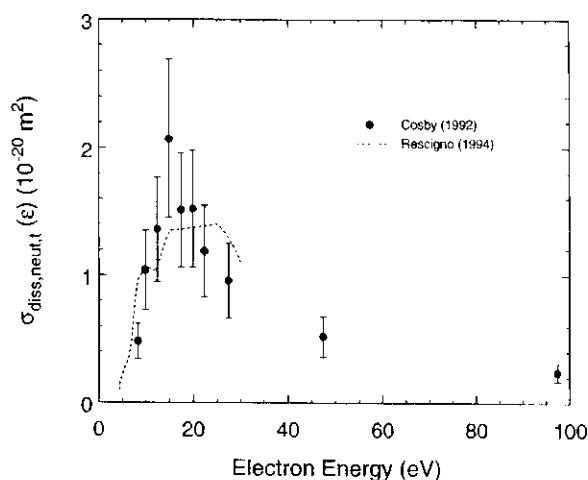


FIG. 16. Total cross section for electron-impact dissociation into neutral fragments,  $\sigma_{\text{diss,neut}}(\epsilon)$ , for  $\text{Cl}_2$ : (●) measurements by Cosby and Helm from Ref. 114; (---) calculations by Rescigno from Ref. 100 [sum of the cross sections for electronic excitation of the lowest five electronic states ( $^3\Pi_u$ ,  $^1\Pi_u$ ,  $^3\Pi_g$ ,  $^1\Pi_g$ ,  $^3\Sigma_u^+$ ) of  $\text{Cl}_2$ ].

dissociative ionization ( $\text{Cl}_2 + e \rightarrow \text{Cl}^+ + \text{Cl} + 2e$ ) and for double ionization.

There seem to be no cross section data on either the partial ionization, or the cross sections for multiple ionization of  $\text{Cl}_2$  by electron impact. Therefore, the relative production of  $\text{Cl}_2^+$  and  $\text{Cl}^+$  by electron impact is not known. Photoabsorption measurements, however, show that the production of  $\text{Cl}_2^+$  far exceeds the production of  $\text{Cl}^+$  for dissociative photoionization (see Fig. 3).

#### 4.2. Density-Reduced Electron-Impact Ionization Coefficient, $\alpha/N(E/N)$

The only measurement of the density-reduced electron-impact ionization coefficient,  $\alpha/N(E/N)$ , of  $\text{Cl}_2$  is that of Božin and Goodyear<sup>102</sup> shown in Fig. 15. These measurements were made at  $T=293 \text{ K}$  for  $\text{Cl}_2$  pressures of 0.13, 0.33, 0.67, and 1.33 kPa. From a least-square fit to the data in Fig. 15, we obtained the values listed in Table 13 which represent our suggested values for the  $\alpha/N(E/N)$  of  $\text{Cl}_2$ .

TABLE 14. Total cross section for electron-impact dissociation into neutral fragments,  $\sigma_{\text{diss,neut}}(\epsilon)$ , for  $\text{Cl}_2$  (data of Cosby and Helm from Ref. 114)

Electron energy (eV)	$\sigma_{\text{diss,neut}}(\epsilon)$ ( $10^{-20} \text{ m}^2$ )
8.4	$0.48 \pm 0.14$
9.9	$1.04 \pm 0.31$
12.4	$1.36 \pm 0.41$
14.9	$2.07 \pm 0.62$
17.4	$1.51 \pm 0.45$
19.9	$1.52 \pm 0.46$
22.4	$1.19 \pm 0.36$
27.4	$0.96 \pm 0.29$
47.4	$0.52 \pm 0.16$
97.4	$0.24 \pm 0.07$

TABLE 15. Negative ion states of Cl<sub>2</sub>

Energy (eV)	Assigned symmetry of corresponding negative ion state	Method/Reference
0.03 ± 0.03	$2\Pi_g^+$	Maxima in the dissociative electron attachment cross section measured in an electron-impact mass-spectrometric study (87)
2.5 ± 0.15	$2\Pi_u^+$	
5.5 ± 0.15	$2\Sigma_g^+$	
0.0	$2\Sigma_u^+$	Maxima in the dissociative electron attachment cross section measured in an electron-impact mass-spectrometric study (80, 95)
2.5 ± 0.05	$2\Pi_g^+$	
5.75 ± 0.05	$2\Pi_u^+$	
9.7 <sup>b</sup>	$2\Sigma_g^+$	
0	$2\Sigma_u^+$	Dissociative electron attachment using a crossed-beam electron impact spectrometer. Assignments based on angular distribution analysis of the Cl <sup>-</sup> ions (96) <sup>c</sup>
2.5	$2\Pi_g^+$	
5.5	$2\Pi_u^+$	
0.07	$2\Sigma_u^+$	Electron swarm (117)
2.4 ± 0.1		Electron-impact mass spectrometry (76)
7.46 ( $\nu=0$ ) and subsequent peaks separated by 0.08 eV corresponding to $\nu=1-5$	Electron-excited Feshbach resonances formed by addition of two $n\sigma$ electrons to the $X^2\Pi_g$ positive-ion core	Electron transmission (97)
~2 <sup>d</sup>	$2\Pi_g^+$	Studies of Cl <sup>-</sup> ions produced by dissociative electron attachment from condensed Cl <sub>2</sub> (118)
~5 <sup>d</sup>	$2\Pi_u^+$	

<sup>a</sup>These assignments are incorrect, see text.

<sup>b</sup>Azria *et al.* (Ref. 96) did not observe the 9.7 eV resonance indicated by the data of Kurepa and Belić (Ref. 95).

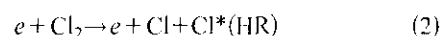
<sup>c</sup>According to Azria *et al.* (Ref. 96), there may be a small contribution of the  $2\Sigma_g^+$  state of Cl<sub>2</sub><sup>-</sup> to the Cl<sup>-</sup> formation at the low-energy side of the resonance at 5.5 eV.

<sup>d</sup>These values are about 0.5 eV lower than the corresponding gaseous data. This may be due to the effect of the polarization energy of condensed Cl<sub>2</sub> on the negative-ion states of the isolated Cl<sub>2</sub> molecule (Refs. 118 and 119).

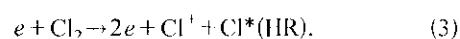
## 5. Total Cross Section for Electron-Impact Dissociation Into Neutral Fragments, $\sigma_{\text{diss,neut,t}}(\epsilon)$ for Cl<sub>2</sub>

There has been one measurement<sup>113,114</sup> of the total cross section for electron impact dissociation into neutrals,  $\sigma_{\text{diss,neut,t}}(\epsilon)$ , for Cl<sub>2</sub>, and these data of Cosby and Helm<sup>113,114</sup> are shown in Fig. 16. In Fig. 16 is also shown the sum of the cross sections calculated by Rescigno<sup>190</sup> for the lowest five excited electronic states ( $3\Pi_u$ ,  $1\Pi_u$ ,  $3\Pi_g$ ,  $1\Pi_g$ ,  $3\Sigma_u^+$ ) of Cl<sub>2</sub> which are reached by promoting an occupied valence electron into the antibonding ( $5\sigma_u$ ) orbital. The calculation by Rescigno showed that the total dissociation cross section is the largest for the  $3\Pi_u$  state up to the highest energy (30 eV) he investigated. The agreement between Rescigno's calculations and the experimental data is good, supporting the premise that all electronic excitations result in dissociation. The experimental data of Cosby and Helm<sup>113,114</sup> are listed in Table 14 as the presently suggested values for  $\sigma_{\text{diss,neut,t}}(\epsilon)$  for the Cl<sub>2</sub> molecule.

In an earlier study, Wells and Zipt<sup>115</sup> observed dissociative excitation of Cl<sub>2</sub> and identified the fragments as, in part, atomic chlorine in long-lived high-Rydberg excited states [Cl\* (IIR)] produced through



and



They associated an energy threshold for reactions (2) and (3), respectively, equal to  $14.8 \pm 1$  eV and  $29.2 \pm 5$  eV.

Another process for neutral fragment production is dissociative recombination ( $e + \text{Cl}_2^- \rightarrow \text{Cl} + \text{Cl}$ ). No data exist on this process (see Mitchel<sup>116</sup> for data on this process for other species).

## 6. Electron Attachment to Cl<sub>2</sub>

As we have discussed in Sec. 2.2, the Cl<sub>2</sub> negative ion consisting of Cl<sup>-</sup> ( $1S_0$ ) and Cl ( $2P_{3/2,1/2}$ ) has four electronic states whose order of increasing energy is:  $2\Sigma_u^+$ ,  $2\Pi_g$ ,  $2\Pi_u$ ,  $2\Sigma_g^+$  (Fig. 5). The participation of these states in dissociative electron attachment of Cl<sub>2</sub> depends on the way their potential-energy curves cross the ground-state potential energy curve  $X^1\Sigma_g^+$  of the neutral Cl<sub>2</sub> molecule. On the basis of the Cl<sub>2</sub> potential-energy curves in Fig. 5, one would expect formation of the parent anion Cl<sub>2</sub><sup>-</sup> at zero energy, and

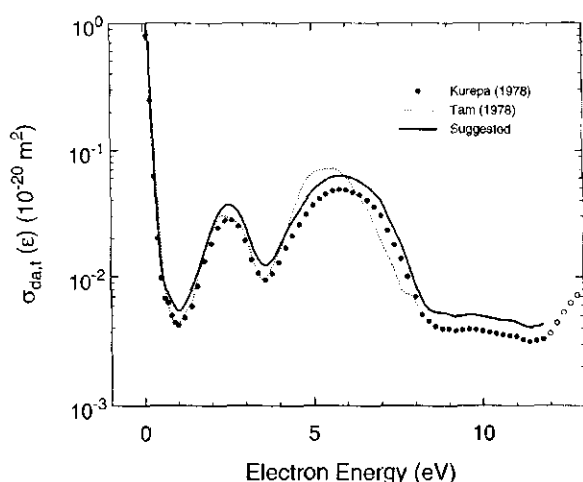
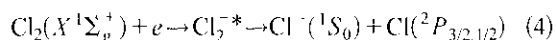


FIG. 17. Total dissociative electron attachment cross section,  $\sigma_{\text{d,a,t}}(e)$ , for  $\text{Cl}_2$ : (●) measurements of Kurepa and Belić from Ref. 95; (---) relative cross section for the production of  $\text{Cl}^-$  from  $\text{Cl}_2$  measured by Tam and Wong in Ref. 87 normalized to the Kurepa and Belić cross section at 2.5 eV; (—) cross section of Kurepa and Belić (Ref. 95) adjusted upwards by 30%. The open symbols represent the contribution to the measured cross section attributed to ion-pair production (see Sec. 6.5.).

the formation of  $\text{Cl}^-$  at near-zero energy and in three higher-energy ranges below 10 eV. For the fragment negative ion  $\text{Cl}^-$ , the dissociative attachment reactions



involve the ground state  $X^1\Sigma_g^+$  of  $\text{Cl}_2$  in the  $\nu=0$  and perhaps  $\nu=1$  state, and the four  $^2\Sigma_u^+$ ,  $^2\Pi_g$ ,  $^2\Pi_u$ ,  $^2\Sigma_g^+$  negative ion states of  $\text{Cl}_2$  which are correlated with the dissociation limit  $\text{Cl}^-(^1S_0) + \text{Cl}(^2P_{3/2,1/2})$ . This limit lies 1.10 eV [ $\text{Cl}(^2P_{1/2})$ ] and 1.21 eV [ $\text{Cl}(^2P_{3/2})$ ] below the minimum of the potential energy curve for the ground state of  $\text{Cl}_2$  [see Fig. 5(b)].

Three electron-beam experimental studies<sup>87,95,96</sup> have shown that the yield of  $\text{Cl}^-$  from  $\text{Cl}_2$  exhibits three peaks: at  $\sim 0$  eV, at 2.5 eV, and at 5.5 eV (Table 15). These were ascribed<sup>95,96</sup> to the  $^2\Sigma_u^+$ ,  $^2\Pi_g$ , and  $^2\Pi_u$  resonant states of  $\text{Cl}_2$ , respectively. The ground state,  $^2\Sigma_u^+$ , of  $\text{Cl}_2^-$  is formed by addition of an extra electron to the lowest unfilled ( $\sigma_u 3p$ )  $\text{Cl}_2$  orbital of the ground-state electron configuration of  $\text{Cl}_2$ :  $[(\dots)(\sigma_g 3p)^2(\pi_u 3p)^4(\pi_g 3p)^4]$ . The core-excited  $^2\Pi_g$  and  $^2\Pi_u$  states of  $\text{Cl}_2^-$  are formed by exciting one electron of the  $^2\Sigma_u^+$  shape resonance from the  $\pi_g 3p$  and  $\pi_u 3p$  to the  $\sigma_u 3p$  orbital, respectively. An electron-transmission study by Spence<sup>97</sup> located the lowest-lying electron-excited Feshbach resonance in  $\text{Cl}_2$  at 7.46 eV. He associated this resonance with Rydberg states having symmetry  $(X^2\Pi_g)(4s\sigma)^2[^2\Pi_{1/2,3/2}]$ . The derivative of the transmitted current in  $\text{Cl}_2$  between 7.0 and 9.0 eV showed a progression of six resonances starting at 7.46 eV, with an average spacing between adjacent resonances of 80 meV. A recent high resolution ( $\sim 60$  meV FWHM) electron beam study<sup>120</sup> of dissociative electron attachment to  $\text{Cl}_2$  between  $\sim 0.0$  and 0.7 eV showed two resonances at 0.03 and 0.250 eV. The former

peak has been attributed<sup>120</sup> to dissociative electron attachment via the  $^2\Sigma_u^+$  state of  $\text{Cl}_2^-$ . The latter may be due to dissociative electron attachment via one of the excited  $^2\Pi$  states of  $\text{Cl}_2^-$ .<sup>120</sup>

The parent negative ion  $\text{Cl}_2^-$  is not normally formed in the gas phase. The transient anion in the lowest negative ion state,  $\text{Cl}_2^*(^2\Sigma_u^+)$ , must be collisionally stabilized before it breaks up by dissociative electron attachment. Since, moreover, dissociative electron attachment occurs at subpicosecond times, collisional stabilization of  $\text{Cl}_2^*$  can only take place at high gas densities when the collisional stabilization time becomes comparable to, or shorter than, the dissociative electron attachment time, or in the condensed phase. No parent negative ions have been observed in electron attachment studies in the gas phase. They, however, have been observed in gas-phase negative-ion charge transfer reactions<sup>121,122</sup> and in the condensed phase.<sup>118</sup> With regard to the latter-type investigation, Azria *et al.*<sup>118</sup> studied the production of  $\text{Cl}^-$  by dissociative electron attachment in electron-stimulated desorption from  $\text{Cl}_2$  condensed on a platinum substrate. They found that the energy dependence of the  $\text{Cl}^-$  signal exhibits two peaks at about 2 and 5 eV which they attributed to the  $^2\Pi_g$  and  $^2\Pi_u$   $\text{Cl}_2^-$  resonant states. Thus, in the condensed phase (in the chlorine lattice on the surface of the substrate) the dissociation dynamics of  $\text{Cl}_2^-$  are similar to those in the gas phase except possibly with a 0.5 eV downward shift in the resonance energy positions. (See Christophorou<sup>119,123</sup> for a discussion of the effect of the medium and state of matter on the energetics of negative ion states.)

### 6.1. Total Dissociative Electron Attachment Cross Section, $\sigma_{\text{d,a,t}}(e)$

Dissociative electron attachment to  $\text{Cl}_2$  is rather simple in its products: only  $\text{Cl}^-$  is produced directly. Thus, electron beam experiments with mass analysis and total electron attachment experiments without mass analysis should yield the same results. In spite of this, it seems that the only absolute measurement of the total dissociative electron attachment cross section,  $\sigma_{\text{d,a,t}}(e)$ , of  $\text{Cl}_2$  is that of Kurepa and Belić.<sup>95</sup> Their data are shown in Fig. 17. They cover the energy range from 0 to 13.0 eV and have an uncertainty of  $\pm 20\%$ . They indicate that dissociative electron attachment to  $\text{Cl}_2$  principally proceeds via three negative-ion states located at  $\sim 0$  eV,  $(2.5 \pm 0.05)$  eV, and  $(5.75 \pm 0.05)$  eV. A weak process they observed between 9 and 11.5 eV was not observed by others<sup>96</sup> (see Table 15).

In Fig. 17 is also plotted, for comparison, the relative cross section for the production of  $\text{Cl}^-$  from  $\text{Cl}_2$  as determined in a higher-energy resolution study by Tam and Wong.<sup>87</sup> (Note that the energy scale for  $\text{Cl}^-/\text{Cl}_2$  in Fig. 2 of the paper of Tam and Wong is not that indicated on the energy axis of the figure in their paper.) Here the data of Tam and Wong have been normalized to the Kurepa and Belić cross section at 2.5 eV. Other than the small differences in the shape and energy position of the resonance at  $\sim 5$  eV, the overall shapes of the two cross sections are in reasonable agreement. The sharp peak at zero energy is worth noting as it is consistent with

TABLE 16. Suggested total dissociative electron attachment cross section,  $\sigma_{\text{da,t}}(\varepsilon)$ , for Cl<sub>2</sub>

Electron energy (eV)	$\sigma_{\text{da,t}}(\varepsilon)$ ( $10^{-20} \text{ m}^2$ )	Electron energy (eV)	$\sigma_{\text{da,t}}(\varepsilon)$ ( $10^{-20} \text{ m}^2$ )
0.05	1.83	5.2	0.053
0.10	1.04	5.6	0.062
0.20	0.32	6.0	0.062
0.30	0.081	6.2	0.060
0.40	0.026	6.6	0.052
0.50	0.013	7.0	0.039
0.60	0.0088	7.2	0.030
0.80	0.0065	7.6	0.018
1.0	0.0055	8.0	0.0091
1.2	0.0062	8.2	0.0066
1.6	0.011	8.6	0.0053
2.0	0.024	9.0	0.0051
2.2	0.032	9.2	0.0049
2.6	0.036	9.6	0.0051
3.0	0.025	10.	0.0049
3.2	0.018	10.2	0.0048
3.6	0.012	10.6	0.0046
4.0	0.017	11.0	0.0045
4.2	0.022	11.2	0.0042
4.6	0.033	11.6	0.0041
5.0	0.047	11.8	0.0043

the electron swarm data (Sec. 6.2). The energy positions of the negative ion resonances as determined in the study of Tam and Wong along with the Tam and Wong assignments are compared with other data in Table 15. Comparison with other studies indicates that the assignments of Tam and Wong are apparently incorrect. The sequence of their assignments is in error because their calculations show the potential energy curve for the  $^2\Sigma_u^-$  anionic state not crossing the potential energy curve for the  $X^1\Sigma_g^+$  ground state of the Cl<sub>2</sub> molecule.

Based on the analysis of the total electron attachment rate constant in Sec. 6.2.2, the values of  $\sigma_{\text{da,t}}(\varepsilon)$  given by Kurepa

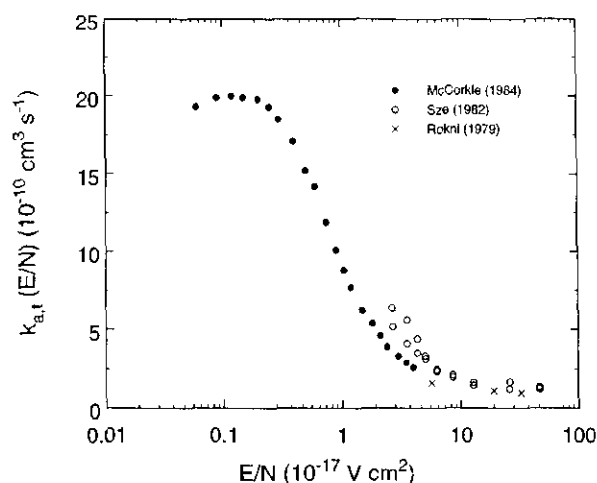


FIG. 18. Total electron attachment rate constant as a function of  $E/N$ ,  $k_{a,t}(E/N)$ , for Cl<sub>2</sub> ( $T \approx 298$ – $300$  K): (●) Ref. 117; (○) Ref. 124; (×) Ref. 88.

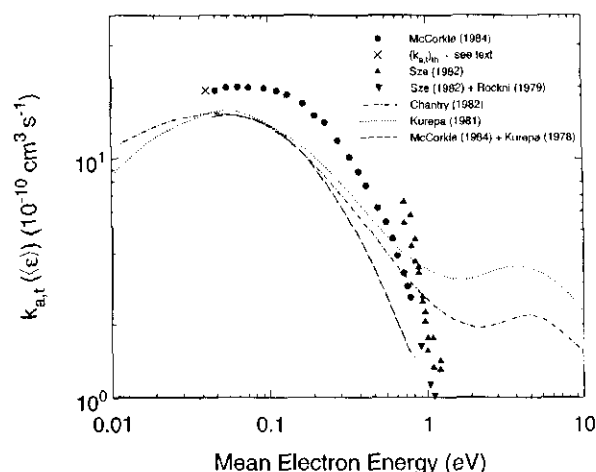


FIG. 19. Total electron attachment rate constant as a function of the mean electron energy  $\langle \varepsilon \rangle$ ,  $k_{a,t}(\langle \varepsilon \rangle)$ , for Cl<sub>2</sub> ( $T \approx 298$  K): (●) Ref. 117; (×)  $(k_{a,t})_{th}$  determined from the average of the two most recent values of the thermal ( $T \approx 300$  K) electron attachment rate, see Table 18; (▲) Ref. 124; (▼) Ref. 124 using the rate constants measured by Rockni *et al.* (Ref. 88); (---) Ref. 127 using the  $\sigma_{a,t}(\varepsilon)$  of Kurepa and Belić (Ref. 95) and a Maxwellian distribution function for the electron energies; (···) Ref. 128 using the  $\sigma_{a,t}(\varepsilon)$  of Kurepa and Belić (Ref. 95) and a Maxwellian distribution function for the electron energies; (- · -) Ref. 117 using the  $\sigma_{a,t}(\varepsilon)$  of Kurepa and Belić (Ref. 95) and the electron energy distribution functions they calculated for N<sub>2</sub>.

and Belić appear to be approximately 30% lower than indicated by the electron swarm measurements. We have, thus, adjusted their cross section upwards by this percentage for our suggested values for  $\sigma_{\text{da,t}}(\varepsilon)$ . This adjusted cross section is shown in the figure by the solid line, and values taken from this curve are listed in Table 16 as our suggested data for the  $\sigma_{\text{da,t}}(\varepsilon)$  of the Cl<sub>2</sub> molecule.

## 6.2. Total Electron Attachment Rate Constant as a Function of the Density-Reduced Electric Field $E/N$ , $k_{a,t}(E/N)$ , and the Mean Electron Energy $\langle \varepsilon \rangle$ , $k_{a,t}(\langle \varepsilon \rangle)$

### 6.2.1. $k_{a,t}(E/N)$ in N<sub>2</sub>

McCorkle *et al.*<sup>117</sup> measured the total electron attachment rate constant,  $k_{a,t}(E/N)$ , of Cl<sub>2</sub> using mixtures of Cl<sub>2</sub> with N<sub>2</sub>. Their measurements covered the  $E/N$  range of  $6 \times 10^{-19}$ – $4 \times 10^{-17} \text{ V cm}^2$ , with a probable uncertainty of  $\pm 10\%$ . The measurements were made at room temperature (298 K) and also at other temperatures above and below ambient (Sec. 6.2.4). The total gas number density in their experiments was  $6.48 \times 10^{19} \text{ molecules/cm}^3$  and the Cl<sub>2</sub> gas number density was in the range  $(0.2\text{--}2.3) \times 10^{15} \text{ molecules/cm}^3$ . The rate constant was found to be independent of both the total and the attaching gas pressures. The measurements at room temperature are plotted in Fig. 18.

Another measurement of  $k_{a,t}(E/N)$  was made by Sze *et al.*<sup>124</sup> using mixtures of Cl<sub>2</sub> with N<sub>2</sub>. These measurements were made at 300 K and for only one mixture composition [the Cl<sub>2</sub> gas number density in the mixture was 260 parts per

TABLE 17. Suggested total electron attachment rate constant,  $k_{a,t}(\langle \epsilon \rangle)$  ( $T = 298$  K), for  $\text{Cl}_2$  (data from Ref. 117)

$\langle \epsilon \rangle$ (eV)	$k_{a,t}(\langle \epsilon \rangle)$ ( $10^{-10} \text{ cm}^3 \text{ s}^{-1}$ )
0.046	19.3 (1.20) <sup>a</sup>
0.054	19.9 (0.9)
0.064	20.0 (0.9)
0.075	19.9 (1.1)
0.094	19.8 (1.2)
0.113	19.3 (1.3)
0.131	18.5 (1.3)
0.165	17.1 (1.5)
0.196	15.2 (1.4)
0.228	14.2 (1.5)
0.275	11.9 (1.5)
0.322	10.1 (1.2)
0.368	8.8 (1.2)
0.411	7.7 (1.4)
0.487	6.2 (1.1)
0.550	5.4 (0.9)
0.599	4.6 (0.7)
0.640	3.9 (0.5)
0.704	3.3 (0.5)
0.745	2.9 (0.5)
0.779	2.6 (0.5)

<sup>a</sup>Values in parentheses are standard deviations as given by the authors.

million (ppm)]. These measurements are also plotted in Fig. 18, along with the limited measurements made by Rokni *et al.*<sup>88</sup> at 300 K. With the exception of the measurements of Sze *et al.* below  $\sim 5 \times 10^{-17} \text{ V cm}^2$ , these data are not incompatible with those of McCorkle *et al.*

Besides their measurements in mixtures with  $\text{N}_2$ , Sze *et al.*<sup>124</sup> also reported  $k_{a,t}(E/N)$  for one mixture of  $\text{Cl}_2$  in Ar. These data are not included in the present paper since the measurements were made for only one mixture concentration (260 ppm) and the effect of  $\text{Cl}_2$  on the electron energy distribution function in pure Ar could not be assessed. For the same reason, early measurements by Bradbury<sup>125</sup> on the probability of electron attachment per collision in a  $\text{Cl}_2/\text{Ar}$  mixture are not included.

### 6.2.2. $k_{a,t}(\langle \epsilon \rangle)$

McCorkle *et al.*<sup>117</sup> used their measurements of  $k_{a,t}(E/N)$ , and the electron energy distribution functions for  $\text{N}_2$  they calculated at each  $E/N$  for which they measured  $k_{a,t}$  using a Boltzmann code, and determined the  $k_{a,t}(\langle \epsilon \rangle)$  for  $\text{Cl}_2$ . These derived data are shown in Fig. 19 for  $T = 298$  K. In this figure is plotted also the thermal value,  $(k_{a,t})_{\text{th}}$ , of  $k_{a,t}(\langle \epsilon \rangle)$  as given by the average of the two most recent measurements<sup>117,126</sup> of this quantity (Sec. 6.2.3). In addition, values of  $k_{a,t}(\langle \epsilon \rangle)$  reported by the following four groups of investigators are plotted in the figure:

- (1) Values reported by Sze *et al.*<sup>124</sup> determined from their  $k_{a,t}(E/N)$  measurements and also from the measurements of Rokni *et al.*<sup>88</sup> These are in fair agreement with the McCorkle *et al.*<sup>117</sup> data.

TABLE 18. Thermal values,  $(k_{a,t})_{\text{th}}$ , of the total electron attachment rate constant for  $\text{Cl}_2$  near room temperature

$(k_{a,t})_{\text{th}}$ ( $10^{-10} \text{ cm}^3 \text{ s}^{-1}$ )	Temperature (K)	Reference
$2.8 \pm 0.4$	300	129
3.1	293	130
11.0	300	131
$18.6 \pm 1.2$	298	117
$20.0 \pm 3.0$	300	126
$37 \pm 17$	350	132

- (2) Values estimated by McCorkle *et al.* using the electron energy distributions in  $\text{N}_2$  and the total electron attachment cross section of Kurepa and Belić<sup>95</sup> (Fig. 17). While the Kurepa and Belić-based  $k_{a,t}(\langle \epsilon \rangle)$  have a similar energy dependence to the directly measured rate constants, they are lower in magnitude (at a mean electron energy of 0.08 eV by  $\sim 30\%$ ) indicating that the Kurepa and Belić cross sections are lower than their true values.
- (3) Values of  $k_{a,t}(\langle \epsilon \rangle)$  determined by Chantry<sup>127</sup> and by Kurepa *et al.*<sup>128</sup> using the total electron attachment cross section of Kurepa and Belić<sup>95</sup> (Fig. 17) and a Maxwellian electron energy distribution function. Clearly the assumption of a Maxwellian distribution function for the electron energies is unrealistic at high  $E/N$ , as is shown by the large difference between the calculated  $k_{a,t}(\langle \epsilon \rangle)$  and the experimental measurements of  $k_{a,t}(\langle \epsilon \rangle)$ . The data of McCorkle *et al.*<sup>117</sup> are listed in Table 17 as our suggested values for the  $k_{a,t}(\langle \epsilon \rangle)$  of  $\text{Cl}_2$  at 298 K.

Values of  $k_{a,t}(\langle \epsilon \rangle)$  derived from limited measurements in mixtures of  $\text{Cl}_2$  with argon<sup>88,124</sup> are uncertain and are not included in this work.

### 6.2.3. Thermal Value, $(k_{a,t})_{\text{th}}$ , of the Total Electron Attachment Rate Constant

In Table 18 are listed the values of the electron attachment rate constant at thermal energies,  $(k_{a,t})_{\text{th}}$  ( $T = 300$  K). These are independent measurements by various groups<sup>117,126,129-132</sup> and they vary significantly. The two most recent measurements<sup>117,126</sup> are consistent with each other and we take their average,  $19.3 \times 10^{-10} \text{ cm}^3 \text{ s}^{-1}$ , as the best present estimate of  $(k_{a,t})_{\text{th}}$  for  $T = 300$  K (plotted on Fig. 19 as a  $\times$  symbol).

### 6.2.4. Effect of Temperature on the Electron Attachment Rate Constant, $k_{a,t}(\langle \epsilon \rangle, T)$

There have been two measurements<sup>117,126</sup> of the dependence of the total electron attachment rate constant  $k_{a,t}$  of  $\text{Cl}_2$  on gas temperature. The measurements of McCorkle *et al.*<sup>117</sup> were made at various mean electron energies from thermal to 0.78 eV, and the measurements of Smith *et al.*<sup>126</sup> were made at only thermal energies. The former results are reproduced in Fig. 20(a), and the latter are compared with the former in Fig. 20(b). All of the data for  $(k_{a,t})_{\text{th}}$  are tabulated in Table 19.



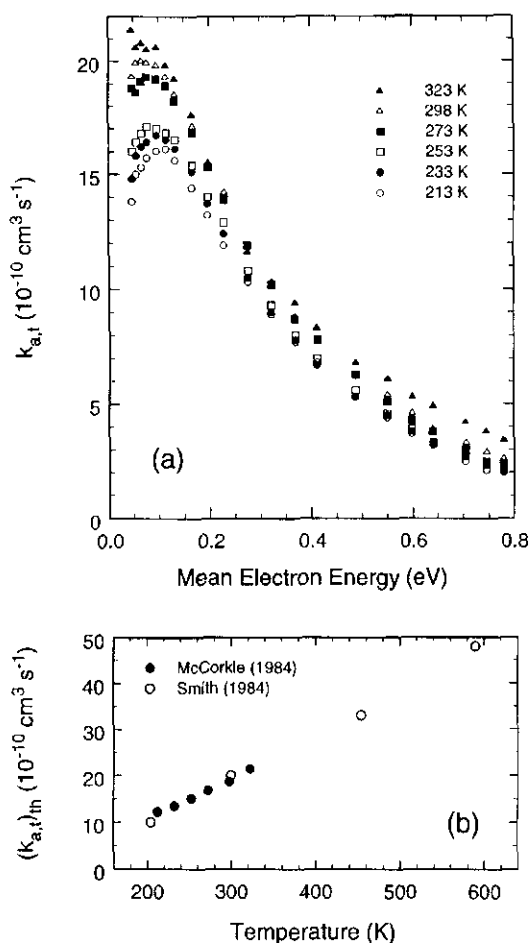


FIG. 20. (a) Variation of  $k_{a,1}(\epsilon)$  of Cl<sub>2</sub> with temperature from McCorkle *et al.* (Ref. 117). (b) Variation of  $(k_{a,1})_{th}$  of Cl<sub>2</sub> with temperature: (●) Ref. 117, (○) Ref. 126.

### 6.3. Density-Reduced Electron Attachment Coefficient, $\eta/N(E/N)$

The early measurements of  $\eta/N(E/N)$  by Bailey and Healey<sup>101</sup> in Cl<sub>2</sub> at 288 K are not in agreement with the more recent measurements of Božin and Goodyear<sup>102</sup> made at 293 K (Fig. 21). Božin and Goodyear indicated an uncertainty of

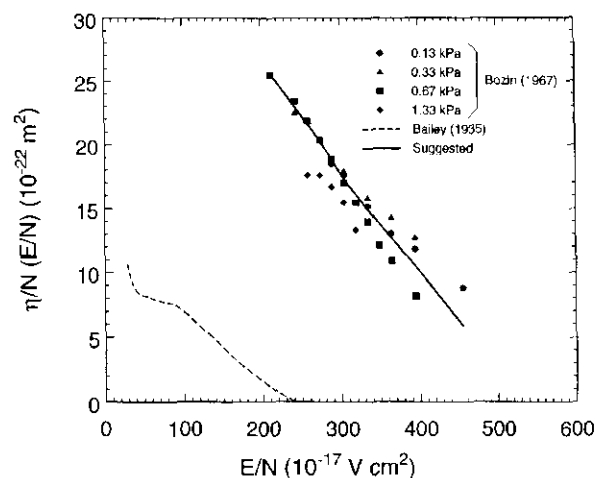


FIG. 21. Density-reduced electron attachment coefficient,  $\eta/N(E/N)$ , for Cl<sub>2</sub>: (●), (▲), (■), (◆) Ref. 102; (---) Ref. 101; (—) suggested values.

$\pm 10\%$ , but the average uncertainty of their data is more likely twice this value. They also indicated that their measurements for 1.33 kPa may be more uncertain than those at the other three pressures (see Fig. 21). Therefore, the solid line in Fig. 21 is a least-squares fit to the data of Božin and Goodyear at pressures of 0.13, 0.33, and 0.67 kPa, and data taken off this curve are listed in Table 20. In the absence of other measurements, these values are presently suggested for the  $\eta/N(E/N)$  of Cl<sub>2</sub>, but clearly there is a need for further measurements.

### 6.4. Density-Reduced Effective Ionization Coefficient, $(\alpha - \eta)/N(E/N)$

Božin and Goodyear<sup>102</sup> reported measurements of the density-reduced effective ionization coefficient  $(\alpha - \eta)/N(E/N)$  for pure Cl<sub>2</sub>. Their measurements were made at room temperature ( $T=293 \text{ K}$ ) for gas pressures of 0.13, 0.33, 0.67, and 1.33 kPa. Figure 22 shows their data which have a stated uncertainty of  $\pm 10\%$ . The solid curve is a least-squares fit to the data at all pressures, and values taken off this curve are listed in Table 21 as the presently suggested estimates of the  $(\alpha - \eta)/N(E/N)$  for pure chlorine.

TABLE 19. Variation of  $(k_{a,1})_{th}$  of Cl<sub>2</sub> with temperature

Temperature (K)	$(k_{a,1})_{th}$ ( $10^{-10} \text{ cm}^3 \text{ s}^{-1}$ )	Reference
213	12.2	117
233	13.5	
253	15.1	
273	16.7	
298	18.6	
323	21.4	
203	< 10	126
300	20	
455	33	
590	48	

TABLE 20. Suggested values for the density-reduced electron attachment coefficient,  $\eta/N(E/N)$ , for Cl<sub>2</sub> (data of Božin and Goodyear from Ref. 102)

$E/N$ ( $10^{-17} \text{ V cm}^2$ )	$\eta/N(E/N)$ ( $10^{-22} \text{ m}^2$ )	$E/N$ ( $10^{-17} \text{ V cm}^2$ )	$\eta/N(E/N)$ ( $10^{-22} \text{ m}^2$ )
215	25.3	350	13.7
225	24.4	375	11.9
250	22.3	400	10.0
275	20.0	425	8.14
300	17.6	450	6.26
325	15.6		

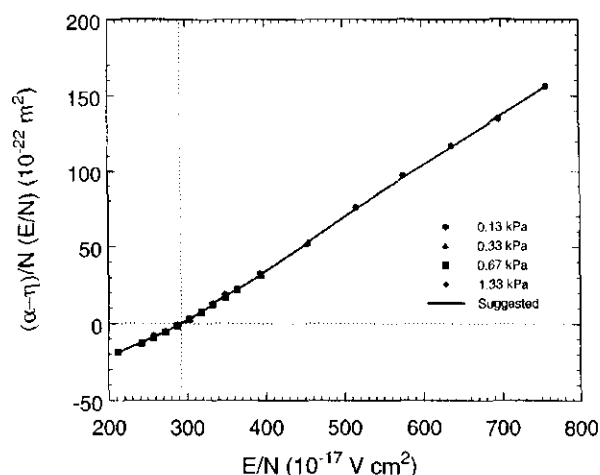
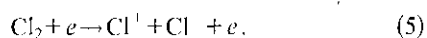


FIG. 22. Density-reduced effective ionization coefficient,  $(\alpha - \eta)/N(E/N)$ , for  $\text{Cl}_2$  from Božin and Goodyear (Ref. 102). The solid line represents the suggested values.

### 6.5. Cross Section for Ion-Pair Formation, $\sigma_{ip}(\epsilon)$

Besides the formation of negative ions via the resonant electron attachment processes discussed in the preceding sections, negative ions have been observed to form by electron impact on  $\text{Cl}_2$  via the direct process of polar dissociation, that is, via the ion-pair process



The energy onset for process (5) is 11.9 eV (Table 4). The absolute cross section measurements of Kurepa and Belić<sup>95</sup> for negative-ion formation above 11.9 eV (see Fig. 17) is due largely to the ion-pair process, Eq. (5), although in some energy regions contributions from indirect electron attachment processes are possible. The Kurepa and Belić data (quoted relative uncertainty  $\pm 20\%$ ) are plotted in Fig. 23. As discussed in Secs. 6.1 and 6.2, these data need to be adjusted upward by 30%, and the so-adjusted data are shown in Fig. 23 by the solid line. Data taken off this line are listed in Table 22 as our suggested values for the  $\sigma_{ip}(\epsilon)$  of  $\text{Cl}_2$ .

### 6.6. Negative Ions in $\text{Cl}_2$ Discharges

There have been a number of studies dealing with negative ions in  $\text{Cl}_2$  gas discharges. By way of example we refer in

TABLE 21. Suggested values of the density-reduced effective ionization coefficient,  $(\alpha - \eta)/N(E/N)$ , for  $\text{Cl}_2$  (data of Božin and Goodyear from Ref. 102)

$E/N$ ( $10^{-17} \text{ V cm}^2$ )	$(\alpha - \eta)/N(E/N)$ ( $10^{-22} \text{ m}^2$ )	$E/N$ ( $10^{-17} \text{ V cm}^2$ )	$(\alpha - \eta)/N(E/N)$ ( $10^{-22} \text{ m}^2$ )
215	-18.5	500	69.1
250	-10.7	550	86.8
300	2.13	600	103.7
350	18.0	650	120.3
400	33.7	700	136.9
450	50.9	750	153.4

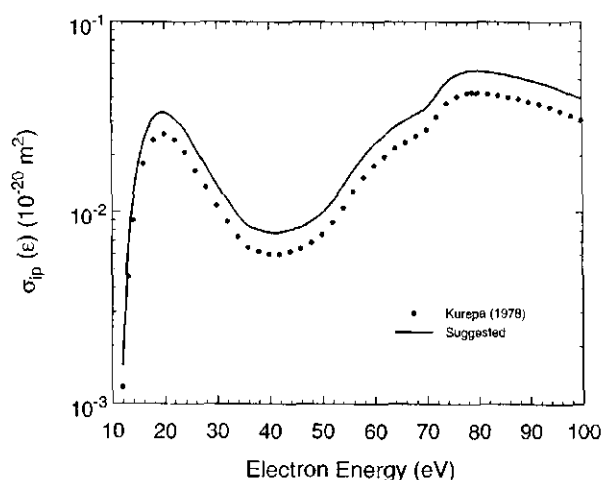


FIG. 23. Cross section for ion-pair formation,  $\sigma_{ip}(\epsilon)$ , for  $\text{Cl}_2$  of Kurepa and Belić from Ref. 95. The solid curve is the same data adjusted upward by 30% as discussed in Secs. 6.1 and 6.2.

this section to two such studies,<sup>133,134</sup> dealing with laser-induced photodetachment of negative ions and its use to infer the density of negative ions in the plasma. Han *et al.*<sup>133</sup> described a technique for sampling negative ions in the hollow cathode and hollow anode of  $\text{Cl}_2/\text{N}_2$  discharges. The photoelectron transient signals which were induced by laser photodetachment of the negative ions present in the discharge were employed to probe the ion concentration. The observed negative-ion transient signal allowed a study of the kinetics of the three negative ions ( $\text{Cl}^-$ ,  $\text{Cl}_2^-$ , and  $\text{Cl}_3^-$ ) they observed in the discharge. Interestingly, the authors concluded from their measurements that the  $\text{Cl}_3^-$  ion is likely to be due to the recombination of  $\text{Cl}^-$  and  $\text{Cl}_2$ , and the  $\text{Cl}_2^-$  ion is likely to be the result of three-body electron attachment to  $\text{Cl}_2$ . Hebner<sup>134</sup> also employed laser photodetachment spectro-

TABLE 22. Suggested cross section for negative ion-positive ion pair production,  $\sigma_{ip}(\epsilon)$ , in  $\text{Cl}_2$  between 12 and 100 eV (adjusted data of Kurepa and Belić from Ref. 95)

Electron energy (eV)	$\sigma_{ip}(\epsilon)$ ( $10^{-20} \text{ m}^2$ )	Electron energy (eV)	$\sigma_{ip}(\epsilon)$ ( $10^{-20} \text{ m}^2$ )
12	0.0016	52	0.0114
13	0.0060	56	0.0166
14	0.0117	60	0.0229
16	0.0234	62	0.0255
18	0.0312	66	0.0304
20	0.0335	70	0.0354
22	0.0312	72	0.0413
26	0.0216	76	0.0528
30	0.0140	80	0.0553
32	0.0116	82	0.0546
36	0.0085	86	0.0525
40	0.0078	90	0.0497
42	0.0078	92	0.0481
46	0.0083	96	0.0442
50	0.0099	100	0.0399

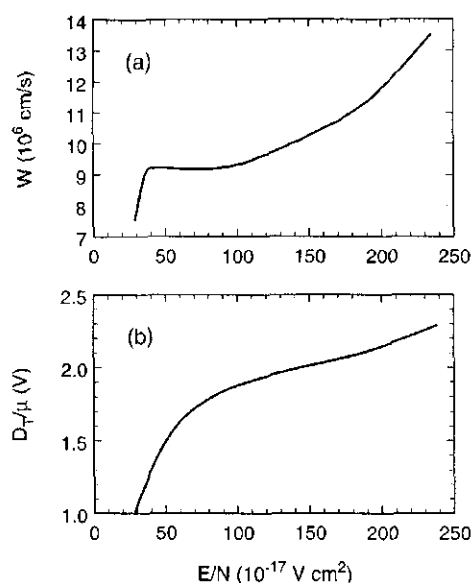


FIG. 24. (a) Electron drift velocity,  $w$ , for Cl<sub>2</sub> ( $T=288$  K), from data of Bailey and Healey (Ref. 101). (b) Ratio of the lateral electron diffusion coefficient to electron mobility,  $D_T/\mu$ , for Cl<sub>2</sub> ( $T=288$  K) derived from data given by Bailey and Healey (Ref. 101). Both data sets are uncertain.

copy to infer the density of chlorine negative ions in low pressure, inductively coupled chlorine plasmas.

## 7. Electron Transport for Cl<sub>2</sub>

### 7.1. Electron Drift Velocity, $w$

The only known measurements of electron drift velocity,  $w$ , for Cl<sub>2</sub> are those made in 1935 by Bailey and Healey<sup>101</sup>

using the volume mixtures 20%Cl<sub>2</sub>:80%He, 20%Cl<sub>2</sub>:80%CO<sub>2</sub>, and 40%Cl<sub>2</sub>:60%CO<sub>2</sub>. Bailey and Healey also showed a curve for  $w$  vs  $E/N$  which they identified as the  $w$  for Cl<sub>2</sub>. This curve is reproduced in Fig. 24(a), but it is considered uncertain because of its indirect determination from the drift velocities they measured in the mixtures just mentioned. Clearly, measurements of  $w(E/N)$  for Cl<sub>2</sub> are needed, and efforts are underway to measure this quantity in our laboratory for Cl<sub>2</sub> and its dilute mixtures in argon.<sup>135</sup>

### 7.2. Lateral Electron Diffusion Coefficient to Electron Mobility Ratio, $D_T/\mu$

There are no measurements of this quantity for Cl<sub>2</sub>. Bailey and Healey<sup>101</sup> reported measurements of the quantity  $k_M$  (mean energy of agitation of electrons in terms of the mean energy of agitation of the gas molecules at 288 K) which we used to determine the ratio of the lateral electron diffusion coefficient  $D_T$  to electron mobility  $\mu$ , via the relationship  $D_T/\mu = k_M(kT/e)$ . The values of  $D_T/\mu$  determined this way are shown in Fig. 24(b). They should be considered uncertain. Measurements of  $D_T/\mu$  over a wide range of  $E/N$  are needed.

## 8. Optical Emission from Cl<sub>2</sub> Gas Discharges

There have been a number of studies of light emission from chlorine excited in an electrical discharge (see, for instance, Refs. 136--142). It is clear from these investigations that the emission spectrum from a chlorine vapor discharge

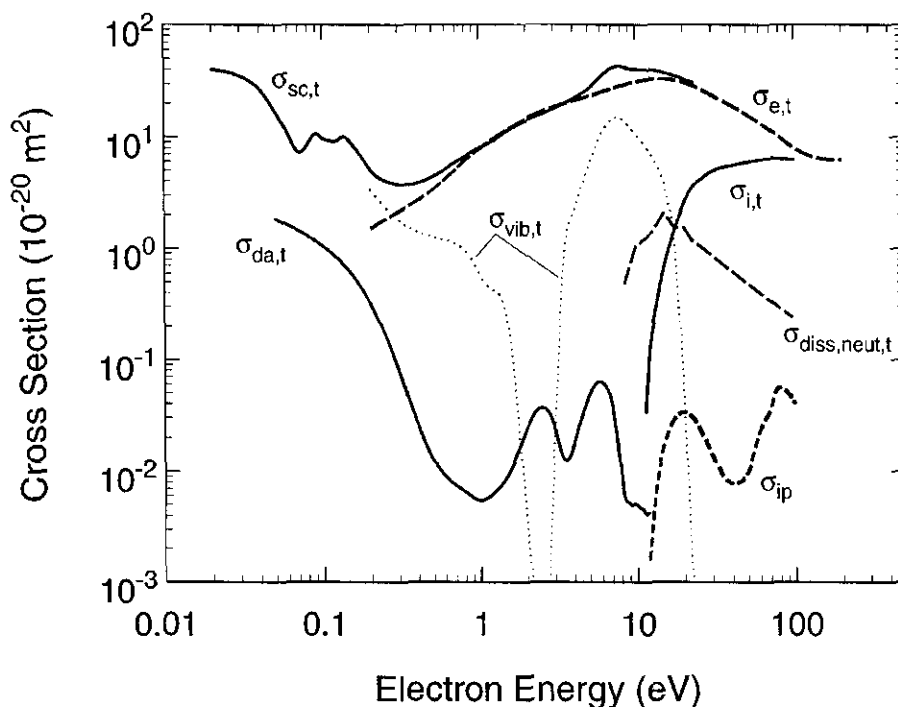


FIG. 25. Recommended and suggested cross sections for Cl<sub>2</sub>.

TABLE 23. Ionization energy of Cl ( $^2P_{3/2}$ ) for the production of  $\text{Cl}^+$  ( $^3P_{2,1,0}$ ),  $\text{Cl}^+$  ( $^1D_2$ ), and  $\text{Cl}^+$  ( $^1S_0$ )

Ionic state	Ionization energy (eV)	References
$^3P_2$	12.97	147 <sup>a</sup>
	$12.97 \pm 0.02$	146 <sup>a</sup>
	$12.967 \pm 0.001$	148, 149 <sup>b</sup>
$^3P_1$	13.06	147
	$13.06 \pm 0.02$	146
	13.053	148, 149
$^3P_0$	13.1	147
	13.090	148, 149
$^1D_2$	14.42	147
	$14.41 \pm 0.02$	146
	14.412	148, 149
$^1S_0$	16.42	147
	$16.42 \pm 0.02$	146
	16.423	148

<sup>a</sup>He I (584 Å) photoelectron spectra data.<sup>b</sup>Spectroscopic data.

consists, in addition to the atomic line spectrum, of a large number of red-degraded bands extending from about 640 to 340 nm which were generally assigned to  $\text{Cl}_2^+$ .

## 9. Suggested Cross Sections and Coefficients for $\text{Cl}_2$

Due to the paucity of confirmed data, only the cross section for total scattering,  $\sigma_{\text{sc},t}(\epsilon)$ , (Table 9, Fig. 6) is considered "recommended" at this time. However, a significant amount of data exist which are "suggested" as the best data presently available. These include:

- $\sigma_{e,t}(\epsilon)$  in Table 11 (Fig. 9);
- $\sigma_{i,t}(\epsilon)$  in Table 12 (Fig. 14);
- $\sigma_{\text{diss,neut},t}(\epsilon)$  in Table 14 (Fig. 16);
- $\sigma_{\text{da},t}(\epsilon)$  in Table 16 (Fig. 17); and
- $\sigma_{\text{ip},t}(\epsilon)$  in Table 22 (Fig. 23).

The cross sections that have been designated as "recommended" or "suggested" in this paper are plotted in Fig. 25. Also shown in Fig. 25 is the derived  $\sigma_{\text{vib,indir}}(\epsilon)$  (from Fig. 12) for which we do not provide tabulated data due to the potential for large uncertainties inherent in the derivation method used. It should be observed that the suggested values of  $\sigma_{e,t}(\epsilon)$  exceed those of  $\sigma_{\text{sc},t}(\epsilon)$  near 2 eV. While this is physically impossible, the amount that  $\sigma_{e,t}(\epsilon)$  exceeds  $\sigma_{\text{sc},t}(\epsilon)$  is less than the quoted uncertainties of the two measurements.

The cross section set shown in Fig. 25 is obviously not complete, and should not be used as such. Obvious deficiencies in the set are the lack of a momentum transfer cross section, and the limited energy range of the suggested values. The suggested data in the figure should serve as a basis for the formulation of any complete, self-consistent cross section set for use by modelers.

TABLE 24. Photoionization cross section,  $\sigma_{\text{pi},\text{Cl}}(\lambda)$ , of the Cl atom (measurements of Samson *et al.* from Ref. 151)

Wavelength (nm)	$\sigma_{\text{pi},\text{Cl}}(\lambda)$ ( $10^{-22} \text{ m}^2$ )	Wavelength (nm)	$\sigma_{\text{pi},\text{Cl}}(\lambda)$ ( $10^{-22} \text{ m}^2$ )
15.8	1.29	47.5	20.2
17.5	1.32	50.0	25.8
20.0	1.30	52.5	32.2
22.5	1.19	55.0	35.7
25.0	1.02	57.5	38.0
27.5	0.90	60.0	39.4
30.0	0.94	62.5	40.6
32.5	1.40	65.0	41.6
35.0	2.50	67.5	42.4
37.5	4.60	70.0	43.0
40.0	7.50	72.5	43.4
42.5	11.0	75.5	43.6
45.0	15.3		

Also suggested are the

- rate constant for electron attachment  $k_{a,t}(\epsilon)$  in Table 17 (Fig. 19);
- density-normalized ionization coefficient  $\alpha/N(E/N)$  in Table 13 (Fig. 15);
- density-reduced electron attachment coefficient  $\eta/N(E/N)$  in Table 20 (Fig. 21); and
- the effective ionization coefficient  $(\alpha - \eta)/N(E/N)$  in Table 21 (Fig. 22).

## 10. Data Needs for $\text{Cl}_2$

Although cross sections have been suggested for total elastic, vibrational excitation, ionization, dissociation into neutrals, dissociative electron attachment, and ion-pair formation, there is a need to improve the accuracy and reliability of all these cross sections. There is a need as well for measurements of the cross sections for momentum transfer, dissociative ionization, vibrational excitation, and electronic excitation, for which no data exist at this time.

With the possible exception of the rate constant for dissociative electron attachment, and the ionization and effective ionization coefficients, there is a need for measurement of all other coefficients (electron drift velocity in pure  $\text{Cl}_2$  and in mixtures with rare gases, electron attachment, and electron diffusion).

## 11. Electron Collision Data for Cl and $\text{Cl}^+$

### 11.1. Cl

Atomic chlorine is an open-shell atom with a ground-state configuration  $1s^2 2s^2 2p^6 3s^2 3p^5(^2P_{3/2})$ . Its electron affinity is well established. Of the 38 values listed by Christodoulides *et al.*,<sup>74</sup> those obtained using the photodetachment method are the most accurate. These are:  $3.613 \pm 0.003$  eV,<sup>143</sup>  $3.610 \pm 0.002$  eV,<sup>144</sup> and  $3.616 \pm 0.003$  eV.<sup>145</sup> A value of 3.613 eV is recommended. Studies of He I photoelectron

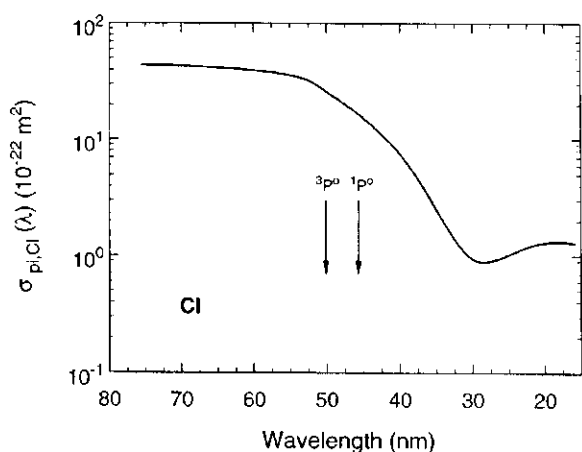


Fig. 26. Photoionization cross section as a function of wavelength,  $\sigma_{\text{pi,Cl}}(\lambda)$ , for atomic chlorine from the measurements of Samson *et al.* (Ref. 151). The vertical lines show the  $^3P^0$  and  $^1P^0$  limits.

spectra<sup>146,147</sup> of  $\text{Cl}(^2P_{3/2})$  gave the ionization threshold energies listed in Table 23 for the production of  $\text{Cl}^+$  in the ionic states  $^3P_{2,1,0}$ ,  $^1D_2$ , and  $^1S_0$ .

De Lange *et al.*<sup>150</sup> used electron modulation spectroscopy and measured the photoionization cross section of Cl at the He I wavelength (584 Å) normalized to that for HCl and HBr at this wavelength. The cross section for ionization of the Cl atom into the ionic states  $\text{Cl}^+ (^3P_{2,1,0})$ ,  $\text{Cl}^+ (^1D_2)$ , and  $\text{Cl}^+ (^1S_0)$  were measured to be  $(19.7 \pm 2.5) \times 10^{-18} \text{ cm}^2$ ,  $(11.4 \pm 1.5) \times 10^{-18} \text{ cm}^2$ , and  $(2.16 \pm 0.28) \times 10^{-18} \text{ cm}^2$ , respectively. The absolute photoionization cross section as a function of photon wavelength,  $\sigma_{\text{pi,Cl}}(\lambda)$ , of the Cl atom was measured by Samson *et al.*<sup>151</sup> from 755 to 158 Å (16.4–75 eV) with an overall estimated uncertainty of  $\pm 8\%$ . Their data are listed in Table 24 and are plotted in Fig. 26.

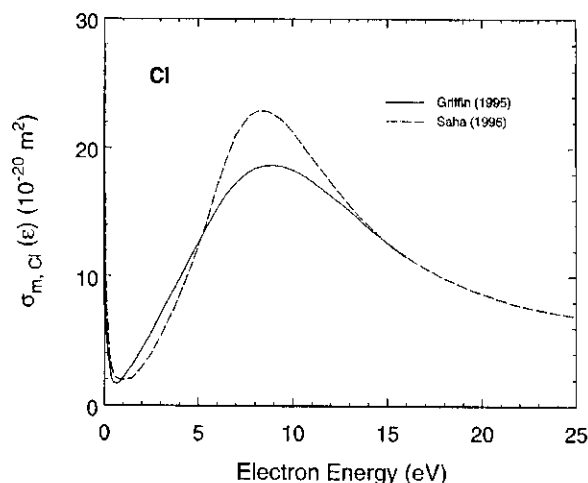


Fig. 27. Momentum transfer cross section,  $\sigma_{\text{m,Cl}}(\epsilon)$ , for atomic chlorine: (—) *R* matrix calculation from Ref. 152; (---) multiconfiguration Hartree-Fock calculation from Ref. 153.

### 11.1.1. Total Electron Scattering Cross Section, $\sigma_{\text{sc,t,Cl}}(\epsilon)$

There are no measurements or calculations of the total electron scattering cross section,  $\sigma_{\text{sc,t,Cl}}(\epsilon)$ , of atomic chlorine. However, since we are dealing with an atomic species, below the threshold for electronic excitation of the chlorine atom at 8.90 eV, the total scattering cross section  $\sigma_{\text{sc,t,Cl}}(\epsilon)$  is equal to the total elastic electron scattering cross section  $\sigma_{\text{e,t,Cl}}(\epsilon)$ . Above the ionization onset of the Cl atom at 12.97 eV,  $\sigma_{\text{sc,t,Cl}}(\epsilon) = \sigma_{\text{e,t,Cl}}(\epsilon) + \sigma_{\text{exc,t,Cl}}(\epsilon) + \sigma_{\text{i,t,Cl}}(\epsilon)$ , where  $\sigma_{\text{exc,t,Cl}}(\epsilon)$  and  $\sigma_{\text{i,t,Cl}}(\epsilon)$  are, respectively, the total cross sections for electronic excitation and electron-impact ionization of the Cl atom. Between 8.90 and 12.97 eV,  $\sigma_{\text{sc,t,Cl}}(\epsilon) = \sigma_{\text{e,t,Cl}}(\epsilon) + \sigma_{\text{exc,t,Cl}}(\epsilon)$ . Thus, in principle, the cross section  $\sigma_{\text{sc,t,Cl}}(\epsilon)$  for the chlorine atom for the three energy regions mentioned above can be constructed using the expressions indicated for each energy region and data on  $\sigma_{\text{e,t,Cl}}(\epsilon)$ ,  $\sigma_{\text{exc,t,Cl}}(\epsilon)$ , and  $\sigma_{\text{i,t,Cl}}(\epsilon)$ . Unfortunately, this exercise is not feasible at the present time since, as will be seen later in this section, only the cross section for single ionization  $\sigma_{\text{i,Cl}}(\epsilon)$  is known with reasonable accuracy.

### 11.1.2. Momentum Transfer Cross Section, $\sigma_{\text{m,Cl}}(\epsilon)$

There have been two calculations of the momentum transfer cross section,  $\sigma_{\text{m,Cl}}(\epsilon)$ , of the Cl atom, the *R* matrix calculation of Griffin *et al.*<sup>152</sup> and the multiconfiguration Hartree-Fock calculation of Saha.<sup>153</sup> Figure 27 compares the results of these two calculations. Both calculations show the presence of a Ramsauer-Townsend minimum in  $\sigma_{\text{m,Cl}}(\epsilon)$  (at 0.95 eV,<sup>153</sup> at  $\sim 0.7$  eV<sup>152</sup>). This minimum is similar to the well-known Ramsauer-Townsend minimum in the scattering cross section of the neighboring rare-gas Ar atom.

### 11.1.3. Total Elastic Electron Scattering Cross Section, $\sigma_{\text{e,t,Cl}}(\epsilon)$

There are four calculations of the total elastic electron scattering cross section,  $\sigma_{\text{e,t,Cl}}(\epsilon)$ , of the Cl atom,<sup>152–155</sup> but

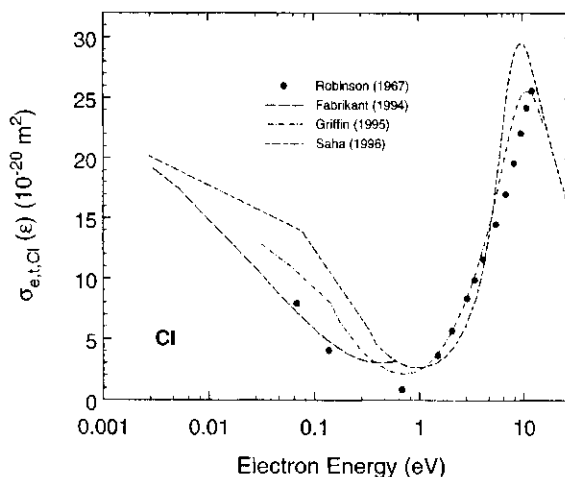


Fig. 28. Calculated total elastic electron scattering cross sections,  $\sigma_{\text{e,t,Cl}}(\epsilon)$ , for atomic chlorine: (●) Ref. 154; (---) Ref. 155; (- · -) Ref. 152; (····) Ref. 153.

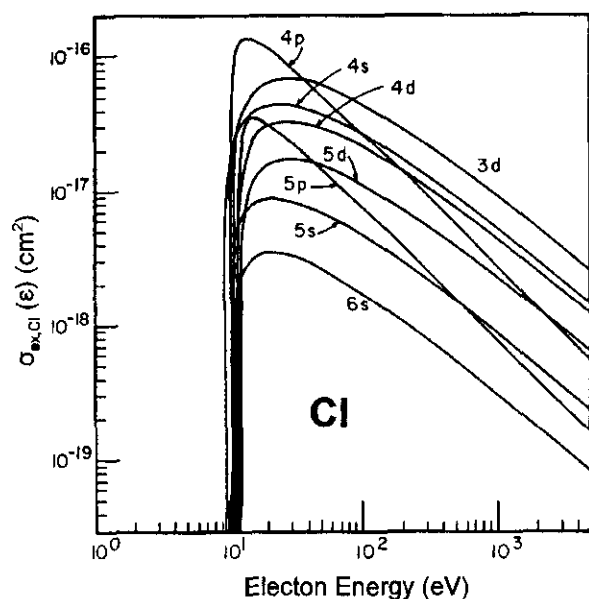


FIG. 29. Calculated cross sections for electron-impact excitation of the  $4s$ ,  $5s$ ,  $6s$ ,  $4p$ ,  $5p$ ,  $3d$ ,  $4d$ , and  $5d$  states of the chlorine atom from the ground state  $3p(^2P)$  from Ref. 156.

no measurements. These calculations are compared in Fig. 28. They all show the existence of a Ramsauer–Townsend minimum at  $\sim 0.7$  eV,<sup>154</sup> at  $\sim 0.4$  eV,<sup>155</sup> at  $0.75$  eV,<sup>152</sup> and at  $0.95$  eV.<sup>153</sup> Robinson and Geltman<sup>154</sup> performed a plane-wave calculation, Fabrikant<sup>155</sup> used the method of extrapolation of potential parameters along the isoelectronic sequence of positive ions to obtain scattering lengths for  $e$ -Cl scattering, Griffin *et al.*<sup>152</sup> used the  $R$  matrix method, and Saha<sup>153</sup> performed a multiconfiguration Hartree–Fock calculation. The agreement between these calculated cross sections is reasonable.

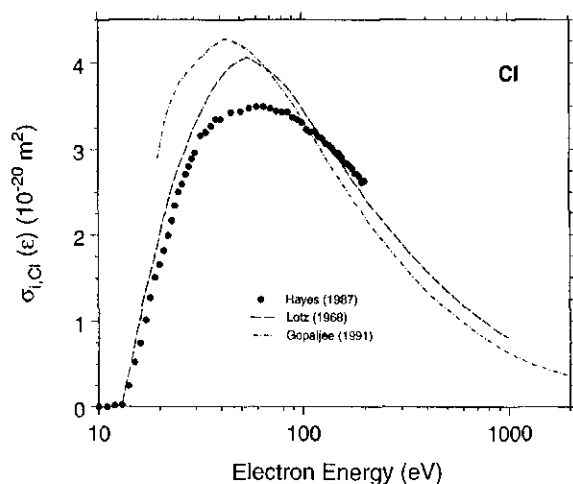


FIG. 30. Electron-impact single-ionization cross section,  $\sigma_{i,Cl}(\epsilon)$ , for the Cl atom. (●) measurements from Ref. 157; (---) calculations from Ref. 158; (- - -) calculations from Ref. 159.

TABLE 25. Cross section,  $\sigma_{i,Cl}(\epsilon)$ , for single ionization of Cl by electron impact (selected data of Hayes *et al.* from Ref. 157)

Electron energy (eV)	$\sigma_{i,Cl}(\epsilon)$ ( $10^{-20}$ m <sup>2</sup> )	Electron energy (eV)	$\sigma_{i,Cl}(\epsilon)$ ( $10^{-20}$ m <sup>2</sup> )
11	0.00	65	3.49
12	0.01	70	3.47
13	0.02	75	3.44
14	0.24	80	3.43
15	0.52	85	3.43
16	0.74	90	3.37
17	1.01	95	3.34
18	1.27	100	3.31
19	1.50	105	3.23
20	1.65	110	3.20
22	1.99	115	3.21
24	2.34	120	3.15
26	2.59	125	3.13
28	2.80	130	3.07
30	2.96	135	3.05
32	3.16	140	3.01
34	3.20	145	2.97
36	3.27	150	2.96
38	3.35	155	2.91
40	3.35	160	2.85
45	3.43	170	2.81
50	3.44	180	2.72
55	3.47	190	2.68
60	3.49	200	2.63

#### 11.1.4. Electron-Impact Excitation Cross Section, $\sigma_{exc,Cl}(\epsilon)$

Ganas<sup>156</sup> calculated cross sections,  $\sigma_{exc,Cl}(\epsilon)$ , for electron-impact excitation of the  $4s$ ,  $5s$ ,  $6s$ ,  $4p$ ,  $5p$ ,  $3d$ ,  $4d$ , and  $5d$  states of the chlorine atom from its ground state  $3p(^2P)$ . These are shown in Fig. 29. Similarly, Griffin *et al.*<sup>152</sup> calculated electron-impact excitation cross sections of Cl to the  $3p^4 4s^4 P_{5/2}$  level using the  $R$  matrix method, but the result of their calculation was found to depend on the number of states they considered. For this reason it is not considered here.

#### 11.1.5. Electron-Impact Single-Ionization Cross Section, $\sigma_{i,Cl}(\epsilon)$

Hayes *et al.*<sup>157</sup> measured the electron-impact single-ionization cross section,  $\sigma_{i,Cl}(\epsilon)$ , of the Cl atom from the ionization threshold to 200 eV with an absolute uncertainty of  $\pm 14\%$ . Their data are plotted in Fig. 30 and are listed in Table 25 as our suggested data since these are the only experimental measurements with a specified absolute uncertainty. Also shown in Fig. 30 are the  $\sigma_{i,Cl}(\epsilon)$  calculated by Lotz<sup>158</sup> and by Gopaljee *et al.*<sup>159</sup> Lotz calculated  $\sigma_{i,Cl}(\epsilon)$  using an empirical formula and estimated an error of  $+40\%/-30\%$ . Gopaljee *et al.*<sup>159</sup> used the binary encounter approximation. Not included in Fig. 30 are the distorted-wave calculation results of Griffin *et al.*<sup>152</sup> because they were found to vary considerably with the details of the calculation. Lennon *et al.*<sup>160</sup> also reviewed and recommended data for  $\sigma_{i,Cl}(\epsilon)$  and other positive ions of the Cl atom to  $16+$ .

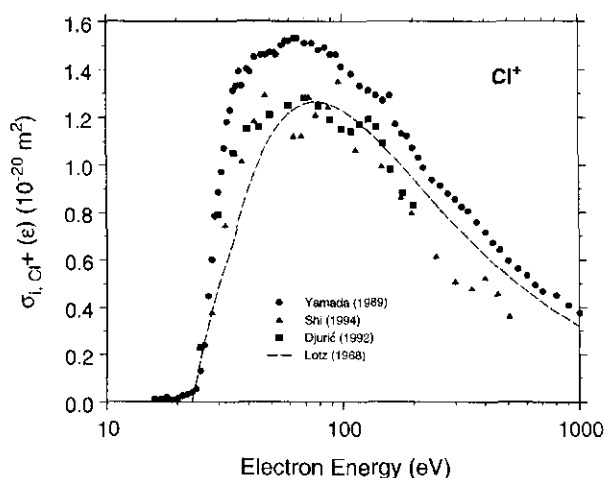
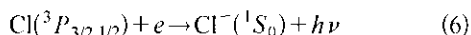


FIG. 31. Cross section,  $\sigma_{i,Cl^+}(\epsilon)$ , for single ionization of  $Cl^+$  by electron impact ( $Cl^+ + e \rightarrow Cl^{++} + 2e$ ): (●) measurements from Ref. 165; (▲) measurements from Ref. 166; (■) measurements from Ref. 167; (---) semiempirical results using the Lotz formula from Refs. 158 and 165.

#### 11.1.6. Radiative Attachment

Radiative attachment to the Cl atom, viz.,



and the resulting radiative attachment continuum  $h\nu$  (also known as the affinity spectrum) has long been investigated (e.g., see Refs. 144, 145, 161–163). The cross section for process (6) is expected to be very small.<sup>163,164</sup> In reaction (6) the photon energy consists of the electron affinity of the Cl atom and the kinetic energy of the attached electron. Because the kinetic energy of a free electron in, say, a plasma has a continuous range of values, the emission spectrum resulting from process (6) is continuous. From its long-wavelength limit (i.e., for the case where the kinetic energy of the captured electron is zero) the electron affinity (EA) of the Cl atom has been accurately determined. Thus, Pietsch and Rehder<sup>144</sup> obtained  $\lambda(P_{3/2}) = (343.4 \pm 0.2)$  nm, corresponding to an EA for Cl ( $P_{3/2}$ ) of  $(3.610 \pm 0.002)$  eV, and  $\lambda(P_{1/2}) = (333.1 \pm 0.4)$  nm, corresponding to an EA for Cl ( $P_{1/2}$ ) of  $(3.722 \pm 0.005)$  eV. Similarly, the radiative attachment continuum was found by Mück and Popp<sup>145</sup> to begin at 342.8 nm yielding an EA for Cl of 3.616 eV.

#### 11.2. Cl<sup>+</sup>

In Fig. 31 are shown the electron-impact ionization cross sections as a function of electron energy for  $Cl^+$ ,  $\sigma_{i,Cl^+}(\epsilon)$ , as measured in three crossed-beam experiments.<sup>165–167</sup> The results of Yamada *et al.*<sup>165</sup> extend from threshold to 1000 eV and have estimated total systematic errors of  $-8\%$  to  $+10\%$ . The measurements of Shi *et al.*<sup>166</sup> cover the electron-impact energy range from 30 to 500 eV and have a reported uncertainty of  $\pm 13\%$ . Similarly, the data of Djurić *et al.*<sup>167</sup> stretch from threshold to 200 eV and have a systematic uncertainty of  $\pm 10\%$ . The measurements of Yamada

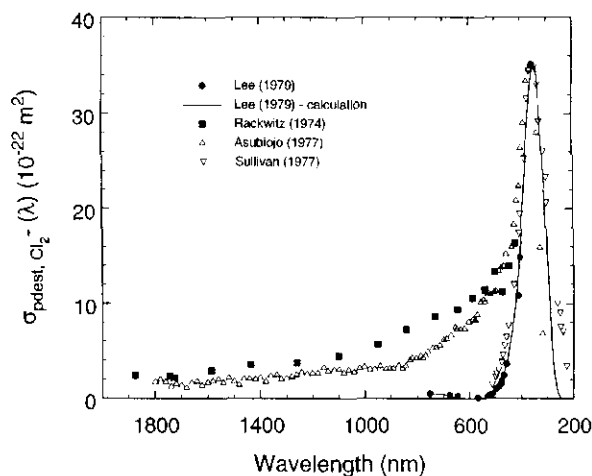


FIG. 32. Cross section for photodestruction of  $Cl_2$  as a function of photon wavelength,  $\sigma_{pd,Cl_2}(\lambda)$ : (●) measurements of Lee *et al.* (Ref. 89); (---) calculation by Lee *et al.* (Ref. 89); (■) measurements of Rackwitz *et al.* (Ref. 169); (Δ) relative measurements of Asubiojo *et al.* (Ref. 170) normalized to the data of Lee *et al.* at 354 nm; (▽) relative measurements of Sullivan *et al.* (Ref. 171) normalized to the data of Lee *et al.* at 354 nm.

*et al.* are consistently  $\sim 25\%$  higher than the other two sets of measurements, possibly because of detector efficiency problems.<sup>166,167</sup> Consistent with the measurements of Djurić *et al.* and Shi *et al.* is the prediction of the semiempirical formula of Lotz<sup>158</sup> (see Fig. 31).

For electron-impact ionization cross section data on  $Cl^{++}$  see Mueller *et al.*<sup>168</sup> See also, the review by Lennon *et al.*<sup>160</sup> for ionization cross sections and ionization rate coefficients for multiply charged positive ions of Cl.

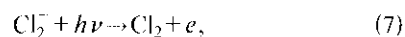
## 12. Electron Detachment, Electron Transfer, and Recombination and Diffusion Processes

### 12.1. Electron Detachment

The large cross section for dissociative electron attachment to the  $Cl_2$  molecule makes the dissociative electron attachment process for chlorine an efficient mechanism to remove slow electrons in chlorine-containing plasma gases. Due to the depletion of free electrons, a higher electric field strength is required to increase the source of ionization<sup>39</sup> and sustain the ionization balance. In the active discharge, although electron detachment processes involve both  $Cl_2^-$  and  $Cl^-$ , those involving  $Cl^-$  are by far more significant in view of the larger abundance of  $Cl^-$  (see Sec. 6).

#### 12.1.1. Photodestruction (Photodetachment and Photodissociation) of $Cl_2^-$

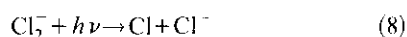
The interaction of light with  $Cl_2^-$  may result in either photodetachment



or photodissociation

TABLE 26. Photodestruction cross section,  $\sigma_{\text{pdest, Cl}_2^-}(\lambda)$ , for  $\text{Cl}_2^-$  (data of Lee *et al.* from Ref. 89)

Wavelength (nm)	$\sigma_{\text{pdest, Cl}_2^-}(\lambda)$ ( $10^{-22} \text{ m}^2$ )
350.7, 356.9	$35.1 \pm 3.0$
406.7	$14.9 \pm 1.1$
413.1	$10.8 \pm 0.4$
457.9	$3.55 \pm 0.42$
468.0	$2.41 \pm 0.28$
476.2	$1.64 \pm 0.19$
476.5	$1.85 \pm 0.20$
482.5	$1.46 \pm 0.18$
488.0	$1.19 \pm 0.13$
496.5	$0.99 \pm 0.12$
514.5	$0.43 \pm 0.06$
520.8	$0.39 \pm 0.05$
530.9	$0.28 \pm 0.03$
568.2	$0.11 \pm 0.05$
647.1	$0.25 \pm 0.03$
676.4	$0.37 \pm 0.04$
752.5	$0.51 \pm 0.06$



of the  $\text{Cl}_2^-$  ion. These processes can be discussed and understood with reference to the potential energy curves shown in Fig. 5 for the ground state of  $\text{Cl}_2$  ( $^1\Sigma_g^+$ ) and  $\text{Cl}_2^-$  ( $^2\Sigma_u^+$ ) and the excited states of  $\text{Cl}_2^-$  ( $^2\Sigma_g^+$  and  $^2\Pi_g$ ). Photodetachment from  $\text{Cl}_2^-$  ( $^2\Sigma_u^+$ ,  $\nu=0$ ) should be observed at a minimum energy corresponding to the EA of  $\text{Cl}_2$  (Table 4). The cross section for photodetachment depends on the threshold law for photodetachment and the Franck-Condon factors which describe the overlap of the  $\nu=0$  level of  $\text{Cl}_2^-$  ( $^2\Sigma_u^+$ ) with the vibrational levels of the  $\text{Cl}_2$  ( $^1\Sigma_g^+$ ) ground state. Vibrational excitation in the molecular ion will also have an effect on the probability of photodetachment. Because of the large difference in the bond length of  $\text{Cl}_2^-$  and  $\text{Cl}_2$  (Fig. 5, Tables 4 and 7), photodetachment will occur to high-lying vibrational levels of  $\text{Cl}_2$  with low probability. Photodissociation is expected to result from excitation of  $\text{Cl}_2^-$  ( $^2\Sigma_u^+$ ) into the repulsive excited states of  $\text{Cl}_2^-$ . The total photodestruction cross section is a combination of the two processes.

About 20 years ago processes (7) and (8) were the subject of a few investigations.<sup>89,169-171</sup> In Fig. 32 are shown the absolute measurements of Lee *et al.*<sup>89</sup> of the cross section,  $\sigma_{\text{pdest, Cl}_2^-}(\lambda)$ , for the photodestruction of the  $\text{Cl}_2^-$  ion. These were made over the wavelength range 350–760 nm using a drift-tube mass spectrometer–laser apparatus. The solid circles are their experimental measurements (listed in Table 26) and the solid curve is their calculated fit to their data. The strong peak in the photodestruction cross section was attributed<sup>89</sup> to the electronic transition  $^2\Sigma_u^+ \rightarrow ^2\Sigma_g^+$ . In the experiments of Lee *et al.*, the  $\text{Cl}_2^-$  ion was probably produced via a three-body electron attachment process to  $\text{Cl}_2$  and was converted to  $\text{Cl}_3^-$  in collisions with  $\text{Cl}_2$ . Also plotted in Fig.

32 are the absolute photodestruction cross section measurements of Rackwitz *et al.*<sup>169</sup> made in the photon energy range from 0.5 to 3.0 eV, and the relative photodestruction cross section of Asubiojo *et al.*<sup>170</sup> made between about 400 and 1800 nm and normalized to the data of Lee *et al.*<sup>89</sup> at 354 nm. The results of Rackwitz *et al.* suggest that the  $\text{Cl}_2^-$  ion formed by electron impact is vibrationally excited and this has a rather significant influence on the photodestruction cross section in the threshold region. This is supported by the work of Sullivan *et al.*<sup>171</sup> who examined photoinduced reactions of  $\text{Cl}_2^-$  in the gas phase using ion cyclotron resonance techniques. They found that the  $\text{Cl}_2^-$  ion undergoes photodissociation in preference to photodetachment and that the photodissociation spectrum of  $\text{Cl}_2^-$  exhibits one broad peak in the wavelength region from 220 to 700 nm with a maximum at  $(350 \pm 10)$  nm which they attributed to the  $^2\Sigma_u^+ \rightarrow ^2\Sigma_g^+$  transition. This cross section has also been plotted in Fig. 32 after it has been normalized to the Lee *et al.* data at 354 nm.

It can thus be concluded<sup>89</sup> from the results of these four investigations that the  $\text{Cl}_2^-$  ion photodissociates rather than photodetaches, that the cross section for photodestruction depends on the electronic excitation of  $\text{Cl}_2^-$  upon photon impact, that the cross section threshold shifts to energies lower than the dissociation energy limit (1.26 eV, Table 7) of  $\text{Cl}_2$  into  $\text{Cl}^- + \text{Cl}$  when the anion is vibrationally excited, and that the differences in the band widths between the four studies probably reflect differences in the vibrational temperature in the four experimental methods employed. The measurements of Lee *et al.*<sup>89</sup> with their quoted uncertainty are listed in Table 26 as our recommended values for  $\sigma_{\text{pdest, Cl}_2^-}(\lambda)$ .

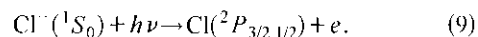
#### 12.1.2. Electron-Induced and Collisional Detachment of $\text{Cl}_2^-$

Apparently there are no data on electron-induced detachment, or collisional detachment involving the  $\text{Cl}_2^-$  ion.

#### 12.1.3. Photodetachment of $\text{Cl}^-$

For  $\text{Cl}^-$  the most significant reactions and parameters are those involving the removal of the attached electron. These processes have been discussed by many authors (see for instance, Refs. 172 and 173). In this section we discuss briefly data on photodetachment of the  $\text{Cl}^-$  ion and in Sec. 12.1.4 data on collisional detachment of the  $\text{Cl}^-$  ion.

The  $\text{Cl}^-$  has a complete  $3p^6$  subshell. Thus, the photodetachment process involves the removal of an electron from the  $p$  orbital and can be represented by



An early review of the experimental and theoretical data on the cross section,  $\sigma_{\text{pd, Cl}^-}(\lambda)$ , for reaction (9) was given by Popp.<sup>163</sup> In Fig. 33 are compared the experimental<sup>145,161,162,174-177</sup> and the calculated<sup>154,178-180</sup> data on  $\sigma_{\text{pd, Cl}^-}(\lambda)$  for process (9). Most of these results were obtained over 20 years ago. The uncertainties in the experimental measurements are as follows: the single measurement of Berry *et al.*<sup>174</sup> at 336 nm ( $15 \times 10^{-18} \text{ cm}^2$ ) has a quoted



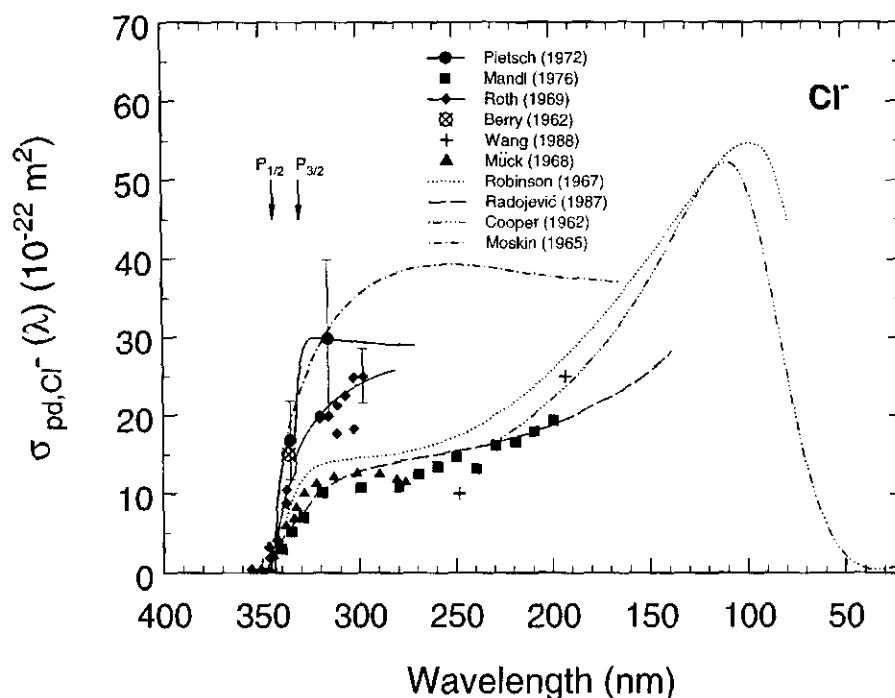


FIG. 33. Photodetachment cross section for Cl<sup>-</sup>,  $\sigma_{\text{pd,Cl}^-}(\lambda)$ , as a function of photon wavelength,  $\lambda$ . Measurements: (●) Ref. 162; (■) Ref. 175; (◆) Ref. 161; (⊗) Ref. 174; (+) Ref. 176; (▲) Ref. 145. Calculations: (···) Ref. 154; (—) Ref. 180; (---) Ref. 178; (---) Ref. 179. Typical error bars are shown in the figure for only the measurements of Refs. 161 and 162. See the text for the reported uncertainties of the other measurements. The energy positions of the  $P_{1/2}$  and  $P_{3/2}$  photodetachment thresholds are also shown.

uncertainty of  $+12 \times 10^{-18}$  and  $-5 \times 10^{-18} \text{ cm}^2$ ; Mück and Popp's,<sup>145</sup> and Mandl's<sup>175</sup> uncertainties were quoted as  $\pm 25\%$ ; Roth's<sup>161</sup> and Pietsch's<sup>162</sup> uncertainties are as shown by the typical error bars in Fig. 33; Wang and Lee<sup>176,177</sup> reported a photodetachment cross section value for Cl<sup>-</sup> equal to  $2.5 \times 10^{-17}$  and  $1.0 \times 10^{-17} \text{ cm}^2$  at 193 and 248 nm, respectively, but gave no uncertainty. On the calculation side, Robinson and Geltman<sup>154</sup> quoted an uncertainty of  $\pm 20\%$ . It should be noted that the relativistic random-phase approximation result of Radojević *et al.*<sup>180</sup> extends to 100 eV and that Radojević *et al.* shifted their calculated curve from the theoretical threshold to the experimental value. It is seen from Fig. 33 that the spread in the experimental data is outside of the quoted uncertainties. The limited recent measurements of Wang and Lee<sup>176</sup> are consistent with the earlier

measurements of Mandl,<sup>175</sup> and Mück and Popp,<sup>145</sup> but all three measurements are lower (often by a factor of 2 or more) than the data of Rothe,<sup>161</sup> Pietsch,<sup>162</sup> and Berry *et al.*<sup>174</sup> On the theoretical side, the calculated values of  $\sigma_{\text{pd,Cl}^-}(\lambda)$  by Moskin<sup>179</sup> differ substantially from the results of the other three calculations.<sup>154,178,180</sup>

#### 12.1.4. Collisional Detachment of Cl<sup>-</sup>

Collisional detachment reactions fall into three groups:<sup>172,173</sup> direct detachment, detachment with excitation (of autodetaching levels, or of a neutral product, or via charge transfer to a negative ion state of the target), and detachment with bonding (reactive collision with detachment, or associative detachment). The magnitude and the

TABLE 27. Associative detachment thermal rate constants involving Cl<sup>-</sup>

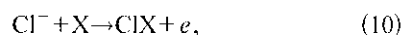
Reactants	Temperature (K)	Associative detachment thermal rate constant ( $\text{cm}^3 \text{ molecule}^{-1} \text{ s}^{-1}$ )	Reference
Cl <sup>-</sup> + H <sub>2</sub> → HCl + e	296	$9.6 \times 10^{-10}$	181
	296	$10.0 \times 10^{-10}$	182
	296	$9.0 \times 10^{-10}$	183
Cl <sup>-</sup> + O <sub>2</sub> → ClO + e	300	$< 1 \times 10^{-11}$	184
Cl <sup>-</sup> + N <sub>2</sub> → ClN + e	300	$< 1 \times 10^{-11}$	184
Cl + Cl <sub>2</sub> (+He) → Cl <sub>3</sub> <sup>-</sup>	ambient	$0.9 \times 10^{-29}$ ( $\text{cm}^6 \text{ molecule}^{-2} \text{ s}^{-1}$ )	185

TABLE 28. Energy threshold for the detachment of  $\text{Cl}^-$  in collisions with various target gases as reported by Doverspike *et al.* in Ref. 186

Reactants	Threshold energy (eV)
$\text{Cl}^- + \text{H}_2$	$5.5 \pm 0.1$
$\text{Cl}^- + \text{D}_2$	$5.5 \pm 0.1$
$\text{Cl}^- + \text{N}_2$	$7.6 \pm 0.1$
$\text{Cl}^- + \text{O}_2^a$	$4.4 \pm 0.2$
$\text{Cl}^- + \text{CO}$	$7.1 \pm 0.2$
$\text{Cl}^- + \text{CO}_2$	$7.3 \pm 0.2$
$\text{Cl}^- + \text{CH}_4$	$6.2 \pm 0.2$

<sup>a</sup>In addition to direct detachment there are several other processes which may contribute to the products of this reaction at energies below 4.4 eV, such as the charge-transfer reaction  $\text{Cl}^- + \text{O}_2 \rightarrow \text{Cl} + \text{O}_2^-$  which is endothermic by  $\sim 3.1$  eV and the associative detachment reaction  $\text{Cl}^- + \text{O}_2 \rightarrow \text{ClO}_2 + e$  which is endothermic by 3.4 eV (see Ref. 186).

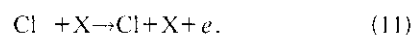
dependence of the collisional detachment cross section,  $\sigma_{\text{cd}}(\mathcal{E})$ , on the energy,  $\mathcal{E}$ , of the reactants varies with the type of the detachment process. (Note that  $\mathcal{E}$  refers to the energy of reactants, i.e., the projectile ion and the neutral target.) Thus, the rising parts of  $\sigma_{\text{cd}}(\mathcal{E})$  as the kinetic energy of the reactants increases are principally due to direct collisional detachment, while the rising parts of  $\sigma_{\text{cd}}(\mathcal{E})$  as the kinetic energy of the reactants decreases toward thermal energy are due to associative detachment. Generally, there is a threshold for the direct collisional detachment process which occurs (when the reactants are in their ground states) when their kinetic energy is equal to the EA of the species carrying the extra electron, although in certain cases such as for the reactions  $\text{Cl}^- + \text{M}$  (where M is a molecule), the  $\sigma_{\text{cd}}(\mathcal{E})$  increases rapidly from the threshold which itself is considerably greater than the EA of the Cl atom. The associative detachment process besides being responsible for the large cross sections at thermal and near-thermal energies also accounts for maxima often seen in the  $\sigma_{\text{cd}}(\mathcal{E})$  functions at higher energies due to negative ion resonances. In Table 27 are listed values of the thermal ( $T \approx 300$  K) rate constants for the associative detachment reactions



where  $\text{X} = \text{H}, \text{O}, \text{N}, \text{or } \text{Cl}_2$ .

The threshold for collisional detachment can be low, and the cross section for collisional detachment can be very large<sup>172,173</sup>—indeed, in many cases, much larger than the cross section for photodetachment. When the associative detachment reactions (10) are exothermic, that is, when the so-called energy defect (the energy difference between the dissociation energy of  $\text{ClX}$  and the EA of Cl) is positive, and the reactions are not hindered by geometric or other factors, the thermal values of the rate constants are large ( $\sim 10^{-9} \text{ cm}^3 \text{ s}^{-1}$ ) and close to the values of the orbiting Langevin collision rate constants. Collisional detachment, then, especially when it is field assisted, can be a dominant electron release mechanism in electrically stressed gases.

Doverspike *et al.*<sup>186</sup> measured absolute total electron detachment cross sections for collisions of  $\text{Cl}^-$  with a number of molecular targets X ( $\text{X} = \text{H}_2, \text{D}_2, \text{O}_2, \text{N}_2, \text{CO}, \text{CO}_2$ , and  $\text{CH}_4$ ) for collision energies below the threshold for detachment to several hundred eV. The reaction studied is



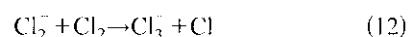
In all such collisions the detachment thresholds were found to exceed the electron affinity of the Cl atom. Table 28 lists the threshold values for collisional detachment as reported by Doverspike *et al.*<sup>186</sup> The results of Doverspike *et al.* are shown in Fig. 34(a) for energies near threshold and in Fig. 34(b) for higher energies.

Huq *et al.*<sup>188</sup> measured absolute total cross sections for charge transfer and electron detachment of  $\text{Cl}^-$  on  $\text{Cl}_2$ . In Fig. 35 are shown their measurements of the total cross sections for electron detachment and for “slow” ion production (via charge transfer). The quoted uncertainty is about  $\pm 10\%$ . In Fig. 35 are also shown the earlier measurements by Hasted and Smith<sup>189</sup> who reported cross sections for electron detachment in collisions of  $\text{Cl}^-$  with  $\text{Cl}_2$  in the energy range from 10 to 2500 eV. According to Huq *et al.*<sup>188</sup> it appears that, at the lowest energies, the Hasted and Smith study did not fully resolve ions from electrons.

Measurements of the translational energy thresholds for electron transfer reactions for various atomic negative ions to  $\text{Cl}_2$  at room temperature<sup>121,122</sup> allowed determination of the electron affinity of the  $\text{Cl}_2$  molecule. Thus, from measurements of the energy thresholds for the endothermic electron transfer reactions  $\text{I}^- + \text{Cl}_2$  and  $\text{Cl}^- + \text{Cl}_2$ , Hughes *et al.*<sup>122</sup> obtained a value of  $(2.62 \pm 0.2)$  eV for the EA of  $\text{Cl}_2$ . Similarly, from the room temperature relative cross sections for the reactions of  $\text{I}^-$ ,  $\text{Br}^-$ , and  $\text{Cl}^-$  with  $\text{Cl}_2$ , Chupka *et al.*<sup>121</sup> obtained for the EA of  $\text{Cl}_2$  the value of  $2.38 \pm 0.10$  eV.

## 12.2. Electron Transfer

While the reaction



is endoergic when the reactants are thermalized,<sup>89</sup> Hughes *et al.*<sup>122</sup> found that it becomes exoergic at energies in excess of 0.3 eV with a rate constant at this energy equal to  $0.0084 \times 10^{-10} \text{ cm}^3 \text{ molecule}^{-1} \text{ s}^{-1}$ . Similarly, the reaction



was found by Babcock and Streit<sup>185</sup> to have a three-body rate constant (with He as the third body) of  $0.9 \times 10^{-29} \text{ cm}^6 \text{ molecule}^{-2} \text{ s}^{-1}$ .

Measurements of the translational energy thresholds for electron-transfer reactions for various atomic negative ions (e.g.,  $\text{I}^-$  and  $\text{Cl}^-$ ) to  $\text{Cl}_2$  allowed determination of the electron affinity of the chlorine molecule. Thus, Hughes *et al.*<sup>122</sup>

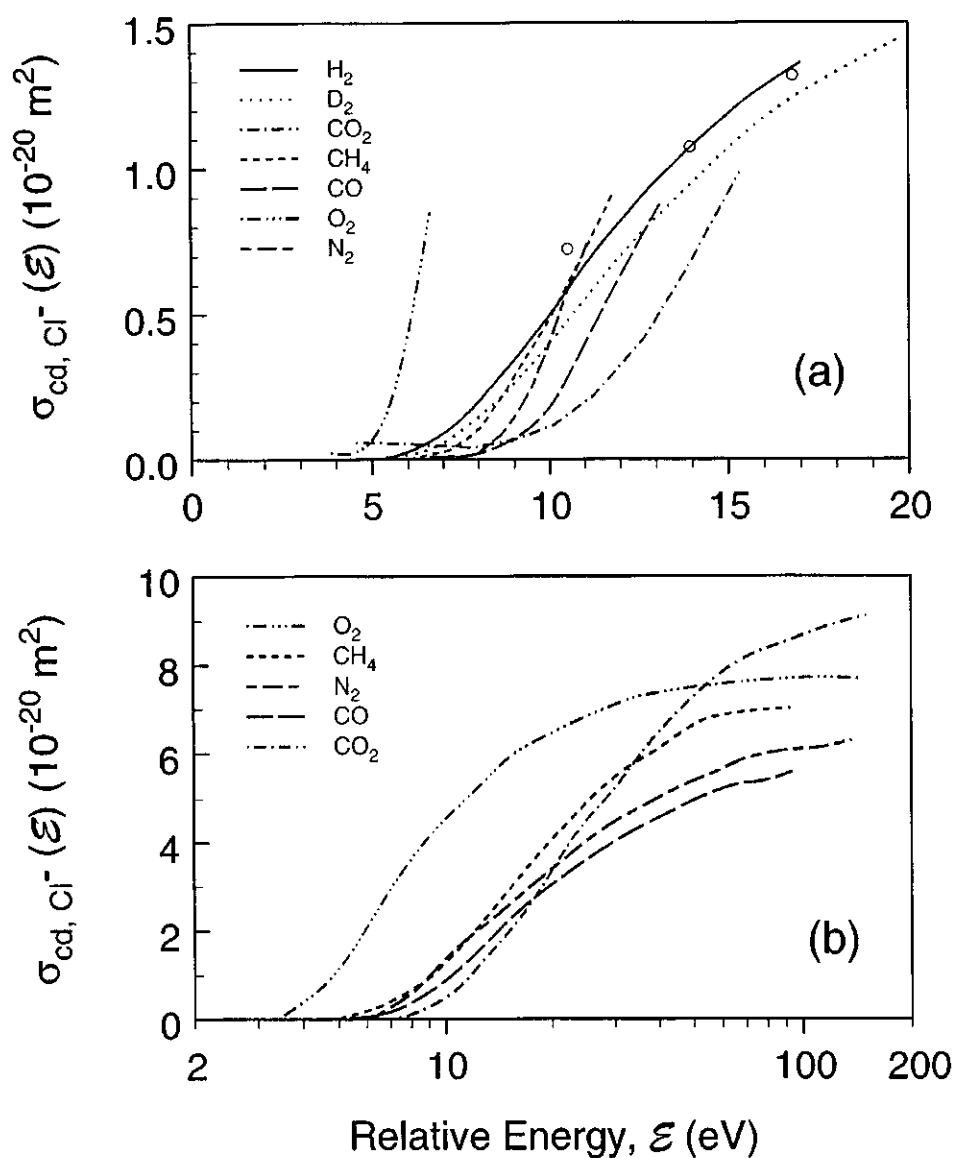


FIG. 34. Collisional detachment cross sections,  $\sigma_{cd, Cl^-}(\epsilon)$ , as a function of the relative energy of the reactants,  $\epsilon$ , involving Cl<sup>-</sup> and various molecular targets (a) near threshold energies (b) over a wider energy range. All data are from Dovespike *et al.* (Ref. 186) except for the three data points (O) for the Cl + H<sub>2</sub> reaction which are those of Bydin and Dukel'skii (Ref. 187).

and Chupka *et al.*<sup>121</sup> determined via such reactions the electron affinity of the Cl<sub>2</sub> molecule to be, respectively,  $(2.32 \pm 0.1)$  and  $(2.38 \pm 0.1)$  eV.

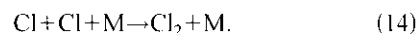
### 12.3. Recombination and Diffusion Processes

#### 12.3.1. Recombination of Cl<sub>2</sub><sup>+</sup> and Cl<sup>-</sup>

Positive ion-negative ion recombination measurements in flowing afterglow plasmas by Church and Smith<sup>190</sup> gave the value of  $5.0 \times 10^{-8} \text{ cm}^3 \text{ molecule}^{-1} \text{ s}^{-1}$  for the rate constant of the reaction  $\text{Cl}_2^+ + \text{Cl}^- \rightarrow \text{products}$ .

#### 12.3.2. Recombination of Cl

Boyd and Burns<sup>191</sup> compared recombination and dissociation rate constants for halogens obtained by a variety of experimental techniques. The Cl-Cl recombination is exothermic ( $\Delta H \sim -1.1$  eV) and requires a third body, M, i.e.,



Boyd and Burns observed that the three-body recombination rate constant for reaction (14) decreases with increasing temperature and that the Cl<sub>2</sub> molecules are not efficient third bodies at any temperature. Measurements of atomic chlorine concentration in Cl<sub>2</sub> plasmas using infrared absorption spectroscopy by Richards and Sawin<sup>2</sup> showed that gas-phase re-

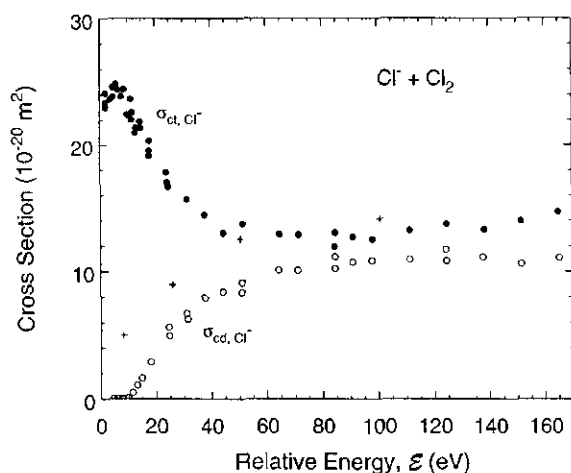


FIG. 35. Cross section,  $\sigma_{\text{et,Cl}}(E)$ , for charge transfer as a function of the relative energy of the reactants,  $E$ , in collisions of  $\text{Cl}^-$  with  $\text{Cl}_2$ : (●) data of Huq *et al.* from Ref. 188. For comparison the cross section  $\sigma_{\text{cd,Cl}}(E)$  is also shown: (○) data of Huq *et al.* from Ref. 188; (×) data of Hasted and Smith from Ref. 189.

combination is an insignificant Cl loss mechanism. For the temperature of their experiment (770 K), the rate constant for reaction (14) ( $M=\text{Cl}_2$ ) is  $\approx 2.8 \times 10^{-32} \text{ cm}^6 \text{ molecule}^{-2} \text{ s}^{-1}$ .<sup>191</sup> Richards and Sawin thus concluded that the major mechanism for Cl loss is likely to be a recombination on the electrode surfaces.

### 12.3.3. Diffusion of Cl and $\text{Cl}^-$ in Gases

Chang *et al.*<sup>192</sup> measured the diffusion coefficient of atomic chlorine in molecular chlorine. They reported a value for the diffusion coefficient of chlorine atoms in chlorine molecules of  $(0.149 \pm 0.025) \text{ cm}^2 \text{ s}^{-1}$  at 298 K and 1 atm. Similarly, Hwang *et al.*<sup>193</sup> measured the diffusion coefficients of atomic chlorine in rare gases via radiative recombination reactions. At 296 K and 101.33 kPa (1 atm) of rare-gas pressure, the values of the diffusion constant for Cl in He, Ne, Ar, Kr, and Xe were measured to be, respectively,  $(0.75 \pm 0.12) \text{ cm}^2 \text{ s}^{-1}$ ,  $(0.32 \pm 0.05) \text{ cm}^2 \text{ s}^{-1}$ ,  $(0.19 \pm 0.03) \text{ cm}^2 \text{ s}^{-1}$ ,  $(0.14 \pm 0.02) \text{ cm}^2 \text{ s}^{-1}$ , and  $(0.12 \pm 0.02) \text{ cm}^2 \text{ s}^{-1}$ .

Eisele *et al.*<sup>194</sup> measured the longitudinal diffusion coefficients for  $\text{Cl}^-$  ions in Ne, Ar, Kr, and Xe as a function of  $E/N$ . Measurements were made at about 300 K and at gas pressures below 0.067 kPa. They are shown in Fig. 36. As  $E/N \rightarrow 0$ , the ions are in thermal equilibrium with the gas molecules and the diffusion coefficient is isotropic, related to the ionic mobility  $K$  by the relation  $K = eD/kT$ , where  $e$  is the ionic charge,  $k$  is Boltzmann's constant, and  $T$  is the gas temperature. For larger values of  $E/N$ , this relation is not valid because the diffusion coefficient has components that refer to the directions parallel and perpendicular to the electric field (for computational techniques allowing the calculation of the diffusion coefficient at any value of  $E/N$  from knowledge of the ionic mobility at that  $E/N$  see Refs. 195–197).

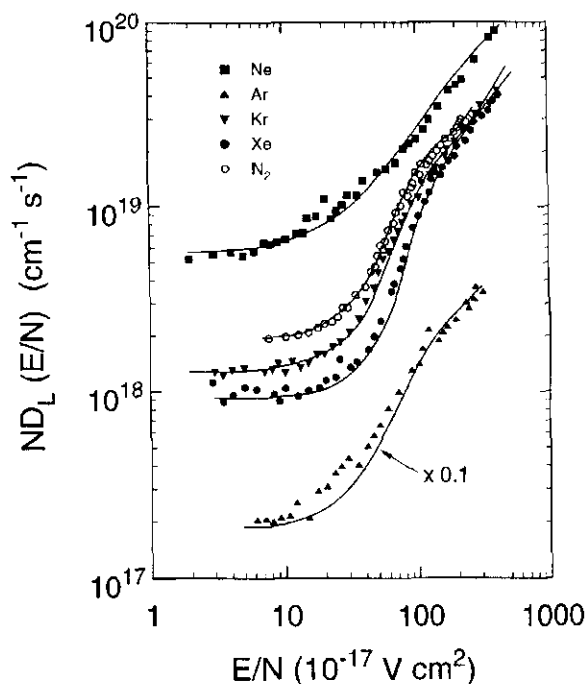


FIG. 36. The product,  $D_L N(E/N)$ , of the longitudinal diffusion coefficient  $D_L$  and the neutral gas number density  $N$  as a function of  $E/N$  for  $\text{Cl}^-$  in Ne, Ar, Kr, and Xe (data from Ref. 194). Also shown are measurements made in  $\text{N}_2$  from Ref. 198. The points are experimental data and the curves are calculated results using the generalized Einstein relation between  $D_L$  and  $K$  (see Refs. 194–197). Note that the Ar data have been multiplied by 0.1 for convenience of display.

Finally, Thackston *et al.*<sup>198</sup> reported measurements of the longitudinal diffusion coefficients for  $\text{Cl}^-$  in  $\text{N}_2$ . These are also shown in Fig. 36 with an uncertainty of  $\pm 7\%$  at all  $E/N$ .

## 13. Summary for Other Species and Processes

With the exception of the limited measurements on electron-impact ionization of Cl and  $\text{Cl}^+$ , no measurements are known to have been made for other electron collision processes for the species Cl,  $\text{Cl}^-$ ,  $\text{Cl}^+$ , and  $\text{Cl}_2$ . With regard to data on other important processes in  $\text{Cl}_2$  plasmas, data have been summarized in this paper on the photodetachment of  $\text{Cl}^-$ , charge transfer reactions involving  $\text{Cl}^-$  and various molecular partners, and diffusion coefficients for  $\text{Cl}^-$  in rare gases and  $\text{N}_2$ . Much work is needed on electron collision and other processes involving the main species in  $\text{Cl}_2$  plasmas.

## 14. Acknowledgments

The authors wish to thank Dr. Y.-K. Kim (NIST), Dr. T. D. Märk (Leopold-Franzens Universität), and Dr. S. K. Srivastava (JPL) for communication of their unpublished results, and Dr. P. C. Cosby and Dr. A. Garscadden for communication of the report in Ref. 114.

## 15. References

- <sup>1</sup>G. L. Rogoff, J. M. Kramer, and R. B. Piejak, *IEEE Trans. Plasma Sci.* **PS-14**, 103 (1986).
- <sup>2</sup>A. D. Richards and H. H. Sawin, *J. Appl. Phys.* **62**, 799 (1987).
- <sup>3</sup>D. S. Fischl and D. W. Hess, *J. Vac. Sci. Technol. B* **6**, 1577 (1988).
- <sup>4</sup>R. d'Agostino, F. Cramarossa, F. Fracassi, F. Illuzzi, and M. N. Armenise, *J. Vac. Sci. Technol. B* **6**, 1584 (1988).
- <sup>5</sup>*Plasma Etching*, edited by D. M. Manos and D. L. Flamm (Academic, Boston, 1989).
- <sup>6</sup>L. F. Kline and M. J. Kushner, *Crit. Rev. Solid State Mater. Sci.* **16**, 1 (1989).
- <sup>7</sup>T. Matsuura, H. Uetake, T. Ohmi, J. Murota, K. Fukuda, N. Mikoshiba, T. Kawashima, and Y. Yamashita, *Appl. Phys. Lett.* **56**, 1339 (1990).
- <sup>8</sup>V. V. Boiko, A. T. Rakhimov, and N. V. Suetin, *Sov. Phys. Tech. Phys.* **35**, 1268 (1990).
- <sup>9</sup>L. Peters, *Semicond. Int.*, May, 66 (1992).
- <sup>10</sup>E. S. Aydil and D. J. Economou, *J. Electrochem. Soc.* **139**, 1396 (1992).
- <sup>11</sup>N. L. Bassett and D. J. Economou, *J. Appl. Phys.* **75**, 1931 (1994).
- <sup>12</sup>S. C. Deshmukh and D. J. Economou, *J. Appl. Phys.* **72**, 4597 (1992).
- <sup>13</sup>P. L. G. Ventzek, M. Grapperhaus, and M. J. Kushner, *J. Vac. Sci. Technol. B* **12**, 3118 (1994).
- <sup>14</sup>C. C. Cheng, K. V. Guinn, V. M. Donnelly, and I. P. Herman, *J. Vac. Sci. Technol. A* **12**, 2630 (1994).
- <sup>15</sup>D. P. Lymberopoulos and D. J. Economou, *IEEE Trans. Plasma Science* **23**, 573 (1995).
- <sup>16</sup>C. Lee and M. A. Lieberman, *J. Vac. Sci. Technol. A* **13**, 368 (1995).
- <sup>17</sup>M. J. Kushner, *J. Appl. Phys.* **82**, 5312 (1997).
- <sup>18</sup>Y. T. Lee, M. A. Lieberman, A. J. Lichtenberg, F. Bose, H. Baltes, and R. Patrick, *J. Vac. Sci. Technol. A* **15**, 113 (1997).
- <sup>19</sup>G. I. Font and I. D. Boyd, *J. Vac. Sci. Technol. A* **15**, 313 (1997).
- <sup>20</sup>J. P. Chang, A. P. Mahorowala, and H. H. Sawin, *J. Vac. Sci. Technol. A* **16**, 217 (1998).
- <sup>21</sup>H. Doshita, K. Ohtani, and A. Namiki, *J. Vac. Sci. Technol. A* **16**, 265 (1998).
- <sup>22</sup>G. P. Kota, J. W. Coburn, and D. B. Graves, *J. Vac. Sci. Technol. A* **16**, 270 (1998).
- <sup>23</sup>M. V. Malyshev, V. M. Donnelly, A. Kornblit, and N. A. Ciampa, *J. Appl. Phys.* **84**, 137 (1998).
- <sup>24</sup>M. V. Malyshev, V. M. Donnelly, and S. Samukawa, *J. Appl. Phys.* **84**, 1222 (1998).
- <sup>25</sup>A. K. Hays, *Opt. Commun.* **28**, 209 (1979).
- <sup>26</sup>M. C. Castex, J. Le Calvé, D. Haaks, B. Jordan, and G. Zimmerer, *Chem. Phys. Lett.* **70**, 106 (1980).
- <sup>27</sup>M. Rokni and J. H. Jacob, in *Applied Atomic Collision Physics*, edited by H. S. W. Massey, E. W. McDaniel, and B. Bederson, *Gas Lasers*, Vol. 3 (Academic, New York, 1982), p. 273.
- <sup>28</sup>W. L. Nighan, in *Applied Atomic Collision Physics*, edited by H. S. W. Massey, E. W. McDaniel, and B. Bederson, *Gas Lasers*, Vol. 3 (Academic, New York, 1982), p. 319.
- <sup>29</sup>M. R. Flannery, in *Applied Atomic Collision Physics*, edited by H. S. W. Massey, E. W. McDaniel, and B. Bederson, *Gas Lasers*, Vol. 3 (Academic, New York, 1982), p. 141.
- <sup>30</sup>D. R. Bates, *Adv. At. Mol. Phys.* **20**, 1 (1985).
- <sup>31</sup>W. L. Morgan, *Plasma Chem. Plasma Process.* **12**, 449 (1992).
- <sup>32</sup>T. E. Graedel and P. J. Crutzen, *Chemie der Atmosphäre* (Spektrum Akademischer, Heidelberg, 1994).
- <sup>33</sup>D. Maric, J. P. Burrows, R. Meller, and G. K. Moortgat, *J. Photochem. Photobiol. A: Chem.* **70**, 205 (1993).
- <sup>34</sup>L. G. Christophorou, J. K. Olthoff, and M. V. V. S. Rao, *J. Phys. Chem. Ref. Data* **25**, 1341 (1996).
- <sup>35</sup>L. G. Christophorou, J. K. Olthoff, and M. V. V. S. Rao, *J. Phys. Chem. Ref. Data* **26**, 1 (1997).
- <sup>36</sup>L. G. Christophorou, J. K. Olthoff, and Y. Wang, *J. Phys. Chem. Ref. Data* **26**, 1205 (1997).
- <sup>37</sup>L. G. Christophorou and J. K. Olthoff, *J. Phys. Chem. Ref. Data* **27**, 1 (1998).
- <sup>38</sup>L. G. Christophorou and J. K. Olthoff, *J. Phys. Chem. Ref. Data* **27**, 889 (1998).
- <sup>39</sup>R. Nagpal and A. Garscadden, *Contrib. Plasma Phys.* **35**, 301 (1995).
- <sup>40</sup>N. Pinhão and A. Chouki, *Proceedings XXII International Conference on Phenomena in Ionized Gases*, Hoboken, NJ, July 31–August 4, 1995, edited by K. H. Becker, W. E. Carr, and E. E. Kunhardt, *Contributed Paper 2*, p. 5.
- <sup>41</sup>A. M. Efremov, V. I. Svetsov, and V. P. Mikhalkin, *High Energy Chem.* **29**, 433 (1995).
- <sup>42</sup>G. Herzberg, *Molecular Spectra and Molecular Structure I. Spectra of Diatomic Molecules*, 2nd ed. (Van Nostrand Reinhold, New York, 1950).
- <sup>43</sup>J. Jureta, S. Cvejanović, M. Kurepa, and D. Cvejanović, *Z. Phys. A* **304**, 143 (1982).
- <sup>44</sup>D. Spence, R. H. Huebner, H. Tanaka, M. A. Dillon, and R.-G. Wang, *J. Chem. Phys.* **80**, 2989 (1984).
- <sup>45</sup>K. P. Huber and G. Herzberg, *Molecular Spectra and Molecular Structure. IV. Constants of Diatomic Molecules* (Van Nostrand Reinhold, New York, 1979).
- <sup>46</sup>S. D. Peyerimhoff and R. J. Buenker, *Chem. Phys.* **57**, 279 (1981).
- <sup>47</sup>H. von Halban and K. Siedentopf, *Z. Phys. Chem.* **103**, 71 (1922a).
- <sup>48</sup>H. von Halban and K. Siedentopf, *Z. Electrochem.* **28**, 496 (1922b).
- <sup>49</sup>G. E. Gibson and N. S. Bayliss, *Phys. Rev.* **44**, 188 (1933).
- <sup>50</sup>F. W. Jones and W. Spooner, *Trans. Faraday Soc.* **31**, 811 (1935).
- <sup>51</sup>W. C. Fergusson, L. Slotkin, and W. G. Style, *Trans. Faraday Soc.* **32**, 956 (1936).
- <sup>52</sup>R. G. Aickin and N. S. Bayliss, *Trans. Faraday Soc.* **33**, 1333 (1937).
- <sup>53</sup>K. Watanabe, *J. Chem. Phys.* **26**, 542 (1957).
- <sup>54</sup>J. Lee and A. D. Walsh, *Trans. Faraday Soc.* **55**, 1281 (1959).
- <sup>55</sup>R. P. Iezkowski, J. L. Margrave, and J. W. Green, *J. Chem. Phys.* **33**, 1261 (1960).
- <sup>56</sup>A. E. Douglas, C. K. Moeller, and B. P. Stoicheff, *Can. J. Phys.* **41**, 1174 (1963).
- <sup>57</sup>D. J. Seery and D. Britton, *J. Phys. Chem.* **68**, 2263 (1964).
- <sup>58</sup>H. Okabe, *Photochemistry of Small Molecules* (Wiley-Interscience, New York, 1978).
- <sup>59</sup>C. Roxlo and A. Mandt, *J. Appl. Phys.* **51**, 2969 (1980).
- <sup>60</sup>J. A. Coxon, *J. Mol. Spectrosc.* **82**, 264 (1980).
- <sup>61</sup>A. E. Douglas, *Can. J. Phys.* **59**, 835 (1981).
- <sup>62</sup>J. B. Burkholder and E. J. Bair, *J. Phys. Chem.* **87**, 1859 (1983).
- <sup>63</sup>J. A. R. Samson and G. C. Angel, *J. Chem. Phys.* **86**, 1814 (1987).
- <sup>64</sup>J. W. Gallagher, C. E. Brion, J. A. R. Samson, and P. W. Langhoff, *J. Phys. Chem. Ref. Data* **17**, 9 (1988).
- <sup>65</sup>J. A. Ganske, H. N. Berko, and B. J. Finlayson-Pitts, *J. Geophys. Res.* **97**, 7651 (1992).
- <sup>66</sup>S. Hubinger and J. B. Nee, *J. Photochem. Photobiol., A* **86**, 1 (1995).
- <sup>67</sup>D. C. Frost, C. A. McDowell, and D. A. Vroom, *J. Chem. Phys.* **46**, 4255 (1967).
- <sup>68</sup>A. W. Potts and W. C. Price, *J. Chem. Soc. Faraday Trans. 2* **67**, 1242 (1971).
- <sup>69</sup>A. B. Cornford, D. C. Frost, C. A. McDowell, J. L. Ragle, and I. A. Stenhouse, *J. Chem. Phys.* **54**, 2651 (1971).
- <sup>70</sup>J. H. D. Eland, in *Electron Spectroscopy: Theory, Techniques, and Applications*, edited by C. R. Brundle and A. D. Baker (Academic, New York, 1979), Vol. 3, Chap. 5.
- <sup>71</sup>T. A. Carlson, M. O. Krause, F. A. Grimm, and T. A. Whitley, *J. Chem. Phys.* **78**, 638 (1983).
- <sup>72</sup>H. Van Lonkhuyzen and C. A. de Lange, *Chem. Phys.* **89**, 313 (1984).
- <sup>73</sup>A. G. McConkey, G. Dawber, L. Avaldi, M. A. MacDonald, G. C. King, and R. I. Hall, *J. Phys. B* **27**, 271 (1994).
- <sup>74</sup>A. A. Christodoulides, D. L. McCorkle, and I. G. Christophorou, in *Electron Molecule Interactions and Their Applications*, edited by I. G. Christophorou (Academic, New York, 1984), Vol. 2, Chap. 6.
- <sup>75</sup>S. G. Lias, J. E. Bartmess, J. F. Liebman, J. L. Holmes, R. D. Levin, and W. G. Mallard, *J. Phys. Chem. Ref. Data* **17**, 592 (1988).
- <sup>76</sup>D. C. Frost and C. A. McDowell, *Can. J. Chem.* **38**, 407 (1960).
- <sup>77</sup>L. Frost, A. M. Grisogono, I. E. McCarthy, E. Weigold, C. E. Brion, A. O. Bawagan, P. K. Mukherjee, W. Von Niessen, M. Rosi, and A. Sgamellotti, *Chem. Phys.* **113**, 1 (1987).
- <sup>78</sup>J. D. Morrison and A. J. C. Nicholson, *J. Chem. Phys.* **20**, 1021 (1952).
- <sup>79</sup>R. Thorburn, *Proc. Phys. Soc. (London)* **123**, 122 (1959).
- <sup>80</sup>M. V. Kurepa and D. S. Belić, *Chem. Phys. Lett.* **49**, 608 (1977).
- <sup>81</sup>V. E. Bondybey and C. Fletcher, *J. Chem. Phys.* **64**, 3615 (1976).
- <sup>82</sup>T. Moeller, B. Jordan, P. Gürtler, G. Zimmerer, D. Haaks, J. Le Calvé, and M.-C. Castex, *Chem. Phys.* **76**, 295 (1983).
- <sup>83</sup>R. G. McLoughlin, J. D. Morrison, and D. L. Smith, *Int. J. Mass Spectrom. Ion Proc.* **58**, 201 (1984).

- <sup>84</sup>R. J. Stubbs, T. A. York, and J. Comer, *J. Phys. B* **18**, 3229 (1985).
- <sup>85</sup>T. L. Gilbert and A. C. Wahl, *J. Chem. Phys.* **55**, 5247 (1971).
- <sup>86</sup>P. W. Tasker, G. G. Balint-Kurti, and R. N. Dixon, *Mol. Phys.* **32**, 1651 (1976).
- <sup>87</sup>W.-C. Tam and S. F. Wong, *J. Chem. Phys.* **68**, 5626 (1978).
- <sup>88</sup>M. Rokni, J. H. Jacob, and J. A. Mangano, *Appl. Phys. Lett.* **34**, 187 (1979).
- <sup>89</sup>I. C. Lee, G. P. Smith, J. T. Moseley, P. C. Cosby, and J. A. Guest, *J. Chem. Phys.* **70**, 3237 (1979).
- <sup>90</sup>J. G. Dojahn, E. C. M. Chen, and W. E. Wentworth, *J. Phys. Chem.* **100**, 9649 (1996).
- <sup>91</sup>J. B. Fisk, *Phys. Rev.* **51**, 25 (1937).
- <sup>92</sup>R. J. Gulley, T. A. Field, W. A. Steer, N. J. Mason, S. L. Lunt, J.-P. Ziesel, and D. Field, *J. Phys. B* **31**, 2971 (1998).
- <sup>93</sup>G. D. Cooper, J. E. Sanabia, J. H. Moore, J. K. Olthoff, and L. G. Christophorou, *J. Chem. Phys.* **110**, 682 (1999).
- <sup>94</sup>M. Gote and H. Ehrhardt, *J. Phys. B* **28**, 3957 (1995).
- <sup>95</sup>M. V. Kurepa and D. S. Bilić, *J. Phys. B* **11**, 3719 (1978).
- <sup>96</sup>R. Azria, R. Abouaf, and D. Teillet-Billy, *J. Phys. B* **15**, L569 (1982).
- <sup>97</sup>D. Spence, *Phys. Rev. A* **10**, 1045 (1974).
- <sup>98</sup>H. Kutz and H.-D. Meyer, *Phys. Rev. A* **51**, 3819 (1995).
- <sup>99</sup>A. Ernesti, M. Gote, and H. J. Kotsch, *Phys. Rev. A* **52**, 1266 (1995).
- <sup>100</sup>T. N. Rescigno, *Phys. Rev. A* **50**, 1382 (1994).
- <sup>101</sup>V. A. Bailey and R. H. Healey, *Philos. Mag.* **19**, 725 (1935).
- <sup>102</sup>S. E. Božin and C. C. Goodyear, *Br. J. Appl. Phys.* **18**, 49 (1967).
- <sup>103</sup>M.-C. Bordage, P. Ségur, and A. Chouki, *J. Appl. Phys.* **80**, 1325 (1996).
- <sup>104</sup>M.-C. Bordage, P. Ségur, L. G. Christophorou, and J. K. Olthoff, *J. Appl. Phys.* (submitted).
- <sup>105</sup>L. G. Christophorou, *Atomic and Molecular Radiation Physics* (Wiley-Interscience, New York, 1971), p. 328.
- <sup>106</sup>H. Ehrhardt, L. Langhans, F. Linder, and H. S. Taylor, *Phys. Rev.* **173**, 222 (1968).
- <sup>107</sup>R. E. Center and A. Mandl, *J. Chem. Phys.* **57**, 4104 (1972).
- <sup>108</sup>F. A. Stevie and M. J. Vasile, *J. Chem. Phys.* **74**, 5106 (1981).
- <sup>109</sup>S. K. Srivastava and R. Boivin, *Bull. Am. Phys. Soc.* **42**, 1738 (1997); S. K. Srivastava (private communication, January 1998).
- <sup>110</sup>Y.-K. Kim (private communication, January 1998).
- <sup>111</sup>H. Deutsch, K. Becker, and T. D. Märk (private communication, February 1998).
- <sup>112</sup>D. Rapp and P. Englander-Golden, *J. Chem. Phys.* **43**, 1464 (1965).
- <sup>113</sup>P. C. Cosby, *Bull. Am. Phys. Soc.* **35**, 1822 (1990).
- <sup>114</sup>P. C. Cosby and H. Helm, Wright Laboratory Report No. WL-TR-93-2004, Wright Patterson AFB, OH 45433-7650 (1992); (private communication, June 1998).
- <sup>115</sup>W. C. Wells and E. C. Zipf, *J. Chem. Phys.* **66**, 5828 (1977).
- <sup>116</sup>J. B. A. Mitchell, *Phys. Rep.* **186**, 216 (1990).
- <sup>117</sup>D. L. McCorkle, A. A. Christodoulides, and L. G. Christophorou, *Chem. Phys. Lett.* **109**, 276 (1984).
- <sup>118</sup>R. Azria, L. Parenteau, and L. Sanche, *J. Chem. Phys.* **87**, 2292 (1987).
- <sup>119</sup>L. G. Christophorou, in *Linking the Gaseous and the Condensed Phases of Matter, the Behavior of Slow Electrons*, edited by L. G. Christophorou, E. Illenberger, and W. F. Schmidt (Plenum, New York, 1994), p. 3.
- <sup>120</sup>D. Muigg, G. Denifl, A. Stamatović, E. Illenberger, I. Walker, and T. D. Märk, *Chem. Phys. Lett.* (submitted); (private communication, October 1998).
- <sup>121</sup>W. A. Chupka, J. Berkowitz, and D. Gutman, *J. Chem. Phys.* **55**, 2724 (1971).
- <sup>122</sup>B. M. Hughes, C. Lifshitz, and T. O. Tiernan, *J. Chem. Phys.* **59**, 3162 (1973).
- <sup>123</sup>L. G. Christophorou, *Z. Phys. Chem. (Munich)* **195**, 195 (1996).
- <sup>124</sup>R. C. Sze, A. E. Greene, and C. A. Brau, *J. Appl. Phys.* **53**, 1312 (1982).
- <sup>125</sup>N. E. Bradbury, *J. Chem. Phys.* **2**, 827 (1934).
- <sup>126</sup>D. Smith, N. G. Adams, and E. Alge, *J. Phys. B* **17**, 461 (1984).
- <sup>127</sup>P. J. Chantry, in *Applied Atomic Collision Physics*, edited by H. S. W. Massey, E. W. McDaniel, and B. Bederson, *Gas Lasers*, Vol. 3 (Academic, New York, 1982), p. 35.
- <sup>128</sup>M. V. Kurepa, D. S. Bilić, and D. S. Bilić, *Chem. Phys.* **59**, 125 (1981).
- <sup>129</sup>J. A. Ayala, W. E. Wentworth, and E. C. M. Chen, *J. Phys. Chem.* **85**, 768 (1981).
- <sup>130</sup>A. A. Christodoulides, R. Schumacher, and R. N. Schindler, *J. Phys. Chem.* **79**, 1904 (1975).
- <sup>131</sup>E. Schultes, A. A. Christodoulides, and R. N. Schindler, *Chem. Phys.* **8**, 354 (1975).
- <sup>132</sup>G. D. Sides, T. O. Tiernan, and R. J. Hanrahan, *J. Chem. Phys.* **65**, 1966 (1976).
- <sup>133</sup>J. C. Han, M. Suto, J. C. Lee, and Z. Lj. Petrović, *J. Appl. Phys.* **68**, 2649 (1990).
- <sup>134</sup>G. A. Heibner, *J. Vac. Sci. Technol. A* **14**, 2158 (1996).
- <sup>135</sup>R. Siegel, Y. Wang, L. G. Christophorou, and J. K. Olthoff (to be published).
- <sup>136</sup>Y. Ota and Y. Uchida, *Jpn. J. Phys.* **5**, 53 (1928).
- <sup>137</sup>A. Elliott and W. H. B. Cameron, *Proc. R. Soc. London, Ser. A* **158**, 681 (1937).
- <sup>138</sup>A. Elliott and W. H. B. Cameron, *Proc. R. Soc. London, Ser. A* **164**, 531 (1938).
- <sup>139</sup>H. G. Howell, *Proc. Phys. Soc. London, Ser. A* **66**, 759 (1953).
- <sup>140</sup>V. V. Rao and P. T. Rao, *Can. J. Phys.* **36**, 1557 (1958).
- <sup>141</sup>P. B. V. Haranath and P. T. Rao, *Indian J. Phys.* **32**, 401 (1958).
- <sup>142</sup>F. P. Huberman, *J. Mol. Spectrosc.* **20**, 29 (1966).
- <sup>143</sup>R. S. Berry and C. W. Reimann, *J. Chem. Phys.* **38**, 1540 (1963).
- <sup>144</sup>G. Pietsch and L. Rehder, *Z. Naturforsch. A* **22a**, 2127 (1967).
- <sup>145</sup>G. Mück and H.-P. Popp, *Z. Naturforsch. A* **23a**, 1213 (1968).
- <sup>146</sup>D. M. de Leeuw, R. Mooyman, and C. A. de Lange, *Chem. Phys. Lett.* **54**, 231 (1978).
- <sup>147</sup>K. Kimura, T. Yamazaki, and Y. Achiba, *Chem. Phys. Lett.* **58**, 104 (1978).
- <sup>148</sup>R. E. Huffman, J. C. Larrabee, and Y. Tanaka, *J. Chem. Phys.* **47**, 856 (1967).
- <sup>149</sup>R. E. Huffman, J. C. Larrabee, and Y. Tanaka, *J. Chem. Phys.* **48**, 3835 (1968).
- <sup>150</sup>C. A. de Lange, P. Van der Meulen, and W. J. Van der Meer, *J. Mol. Struct.* **173**, 215 (1988).
- <sup>151</sup>J. A. R. Samson, Y. Shefer, and G. C. Angel, *Phys. Rev. Lett.* **56**, 2020 (1986).
- <sup>152</sup>D. C. Griffin, M. S. Pindzola, T. W. Gorczyca, and N. R. Badnell, *Phys. Rev. A* **51**, 2265 (1995).
- <sup>153</sup>H. P. Saha, *Phys. Rev. A* **53**, 1553 (1996).
- <sup>154</sup>E. J. Robinson and S. Geltman, *Phys. Rev.* **153**, 4 (1967).
- <sup>155</sup>I. I. Fabrikant, *J. Phys. B* **27**, 4545 (1994).
- <sup>156</sup>P. S. Ganas, *J. Appl. Phys.* **63**, 277 (1988).
- <sup>157</sup>T. R. Hayes, R. C. Wetzel, and R. S. Freund, *Phys. Rev. A* **35**, 578 (1987).
- <sup>158</sup>W. Lotz, *Z. Phys.* **216**, 241 (1968).
- <sup>159</sup>Gopaljee, S. N. Chatterjee, and B. N. Roy, *Pramana, J. Phys.* **36**, 325 (1991).
- <sup>160</sup>M. A. Lennon, K. L. Bell, H. B. Gilbody, J. G. Hughes, A. E. Kingston, M. J. Murray, and F. J. Smith, *J. Phys. Chem. Ref. Data* **17**, 1285 (1988).
- <sup>161</sup>D. E. Rothe, *Phys. Rev.* **177**, 93 (1969).
- <sup>162</sup>G. Pietsch, *Z. Naturforsch. A* **27a**, 989 (1972).
- <sup>163</sup>H.-P. Popp, *Phys. Rep.* **16**, 169 (1975).
- <sup>164</sup>L. G. Christophorou, *Atomic and Molecular Radiation Physics* (Wiley-Interscience, New York, 1971), Chap. 7.
- <sup>165</sup>I. Yamada, A. Danjo, T. Hirayama, A. Matsumoto, S. Ohtani, H. Suzuki, T. Takayanagi, H. Tawara, K. Wakiya, and M. Yoshino, *J. Phys. Soc. Jpn.* **58**, 3151 (1989).
- <sup>166</sup>W. Shi, D. Fang, F. Lu, H. Gao, J. Gu, S. Wu, W. Wu, J. Tang, and F. Yang, *Chin. Phys. Lett.* **11**, 73 (1994).
- <sup>167</sup>N. Djurić, E. W. Bell, E. Daniel, and G. H. Dunn, *Phys. Rev. A* **46**, 270 (1992).
- <sup>168</sup>D. W. Mueller, T. J. Morgan, G. H. Dunn, D. C. Gregory, and D. H. Crandall, *Phys. Rev.* **31**, 2905 (1985).
- <sup>169</sup>R. Rackwitz, D. Feldmann, E. Heinicke, and H. J. Kaiser, *Z. Naturforsch. A* **29a**, 1797 (1974).
- <sup>170</sup>O. I. Asubiojo, H. L. McPeters, W. N. Olmstead, and J. I. Brauman, *Chem. Phys. Lett.* **48**, 127 (1977).
- <sup>171</sup>S. A. Sullivan, B. S. Freiser, and J. L. Beauchamp, *Chem. Phys. Lett.* **48**, 294 (1977).
- <sup>172</sup>R. L. Champion and L. D. Doverspike, in *Electron-Molecule Interactions and Their Applications*, edited by L. G. Christophorou (Academic, New York, 1984), Vol. 1, p. 619.
- <sup>173</sup>L. G. Christophorou, *Contrib. Plasma Phys.* **27**, 237 (1987).
- <sup>174</sup>R. S. Berry, C. W. Reimann, and G. N. Spokes, *J. Chem. Phys.* **37**, 2278 (1962).

- <sup>175</sup>A. Mandl, Phys. Rev. A **14**, 345 (1976).  
<sup>176</sup>W. C. Wang and L. C. Lee, J. Phys. D **21**, 675 (1988).  
<sup>177</sup>W. C. Wang and L. C. Lee, IEEE Trans. Plasma Science **PS-15**, 460 (1987).  
<sup>178</sup>J. W. Cooper and J. B. Martin, Phys. Rev. **126**, 1482 (1962).  
<sup>179</sup>Yu. V. Moskvina, High Temp. **3**, 765 (1965).  
<sup>180</sup>V. Radojević, H. P. Kelly, and W. R. Johnson, Phys. Rev. A **35**, 2117 (1987).  
<sup>181</sup>C. J. Howard, F. C. Fehsenfeld, and M. McFarland, J. Chem. Phys. **60**, 5086 (1974).  
<sup>182</sup>F. C. Fehsenfeld, C. J. Howard, and E. E. Ferguson, J. Chem. Phys. **58**, 5841 (1973).  
<sup>183</sup>F. C. Fehsenfeld, J. Chem. Phys. **54**, 438 (1971).  
<sup>184</sup>F. C. Fehsenfeld, E. E. Ferguson, and A. L. Schmeltekopf, J. Chem. Phys. **45**, 1844 (1966).  
<sup>185</sup>L. M. Babcock and G. E. Streit, J. Chem. Phys. **76**, 2407 (1982).  
<sup>186</sup>L. D. Doverspike, B. T. Smith, and R. L. Champion, Phys. Rev. A **22**, 393 (1980).  
<sup>187</sup>Iu. F. Bydin and V. M. Dukel'skii, Sov. Phys.-JETP **4**, 474 (1957).  
<sup>188</sup>M. S. Huq, D. Scott, N. R. White, R. L. Champion, and L. D. Doverspike, J. Chem. Phys. **80**, 3651 (1984).  
<sup>189</sup>J. B. Hasted and R. A. Smith, Proc. R. Soc. London Ser. A **235**, 349 (1956).  
<sup>190</sup>M. J. Church and D. Smith, J. Phys. D **11**, 2199 (1978).  
<sup>191</sup>R. K. Boyd and G. Burns, J. Phys. Chem. **83**, 88 (1979).  
<sup>192</sup>Y.-T. Chang, C.-J. Hwang, and T.-M. Su, Chem. Phys. Lett. **114**, 92 (1985).  
<sup>193</sup>C.-J. Hwang, R.-C. Jiang, and T.-M. Su, J. Chem. Phys. **84**, 5095 (1986).  
<sup>194</sup>F. L. Eisele, M. G. Thackston, W. M. Pope, H. W. Ellis, and E. W. McDaniel, J. Chem. Phys. **70**, 5918 (1979).  
<sup>195</sup>L. A. Vieland and E. A. Mason, J. Chem. Phys. **63**, 2913 (1975).  
<sup>196</sup>H. R. Skullerud, J. Phys. B **9**, 535 (1976).  
<sup>197</sup>E. A. Mason and E. W. McDaniel, *Transport Properties of Ions in Gases* (Wiley, New York, 1988).  
<sup>198</sup>M. G. Thackston, M. S. Byers, F. B. Holleman, R. D. Chelf, J. R. Twist, and E. W. McDaniel, J. Chem. Phys. **78**, 4781 (1983).